JPL Publication 16-9

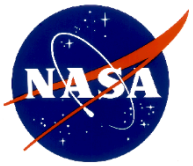

A Method for Estimating the Probability of Floating Gate Prompt Charge Loss in a Radiation Environment

L. D. Edmonds
Jet Propulsion Laboratory

National Aeronautics and Space Administration

Jet Propulsion Laboratory
California Institute of Technology
Pasadena, California

March 2016

This research was carried out at the Jet Propulsion Laboratory, California Institute of Technology, under a contract with the National Aeronautics and Space Administration.

Abstract:

Since advancing technology has been producing smaller structures in electronic circuits, the floating gates in modern flash memories are becoming susceptible to prompt charge loss from ionizing radiation environments found in space. A method for estimating the risk of a charge-loss event is given.

Table of Contents

I. Introduction

The floating gates (FGs) in flash memory devices are subject to two known effects produced by radiation environments, such as the ion environments found in space. One, which is not the topic of this report, is a radiation-induced leakage current (RILC) [1]. This effect reduces the data retention time of the floating gates. For applications in which data refreshes are possible, this effect can be mitigated by sufficiently frequent refreshes.

The topic of this report is the other effect, which is a prompt (i.e., occurs immediately after an ion hit) effective charge loss of the floating gate. The term "effective" is used here because there are at least two physical mechanisms that contribute to this. One is an actual charge loss discussed by Cellere *et al*. [2]. The other is a partial compensation of the FG charge by charge created in a nearby oxide which was discussed by Guertin *et al.* [3]. The charge state of an FG is experimentally determined by the threshold voltage of a field-effect transistor (FET) surrounding the FG, but a voltage shift cannot distinguish an actual charge loss from charge compensation[1], so an effective charge loss refers in this report to any combination of actual loss and compensation that produces a shift in the threshold voltage. Until recently, a prompt FG charge loss was less of a concern compared to single event effects in the control circuitry. However, the FG charge loss is a major concern in some of the more recent technologies that rely on smaller amounts of charge stored in the FG.

The goal of this report is to construct a model for this charge loss that is simple enough to be analytically tractable but still close enough to reality to serve as a data-fitting tool that, when fitted to laboratory test data, predicts the risk of an FG becoming deprogram by a given radiation environment. It is important to note that either kind of charge loss (actual or partial compensation) can be restored by erasing and then reprogramming the memory [2, 3. Therefore, excluding RILC and total ionizing dose (TID) effects in other circuit elements, the irradiation history prior to the most recent erase and program operation is not relevant.

An important issue that must be addressed is that FG charge loss ("effective" will be tacitly assumed whenever no clarification is explicitly given) is cumulative. Test data in [3] were obtained by exposing a flash memory device to a variety of test ions characterized by linear energy transfer (LET), and a variety of fluences. Prior to exposure, the FGs were programmed (charged). After each exposure, the FGs were monitored to determine which ones lost enough charge to be sensed by the circuity as being deprogrammed (uncharged).[2] Plots in [3] of the number of deprogrammed FGs versus fluence indicate that a single ion hit is enough to deprogram an FG at the largest tested LETs, but multiple hits are needed at the smaller LETs. Since multiple hits are sometimes required, this situation is not the classic single-event effect (SEE). For SEE, cross sections are experimentally defined to be the number of counts divided by fluence and can be measured in a laboratory, then used to predict SEE rates in a given space environment. The concept of an interaction cross section will be used in this analysis (as explained in the next section) but, as pointed out in [3], a cross section for charge-loss events is not well defined. Specifically, an event cross section cannot be calculated by simply dividing the number of deprogrammed FGs by the tested fluence because this ratio is not a constant but, instead, increases with increasing fluence. The reason is that irradiation effects are additive so

[1] Sometimes a distinction can be made by investigating the time profile of the voltage shift [3], but the analysis given here will not require such measurements.

[2] We are discussing single-level cells having only two possible logic states. For multi-level cells there are several kinds of events that can occur. An example is a cell initially in the most highly-charged logic state that loses enough charge to be in any one of the lower-charged logic states.

the probability of an FG becoming deprogrammed by the next ion hit depends on whether it was already exposed to prior irradiation (unlike the classic SEE problem in which past history is quickly forgotten so the present environment is the only concern). On the other hand, this situation is also not the classic TID effect. While TID is cumulative, the classic situation involves such large numbers of particle hits that these numbers are close enough to statistical averages to be deterministic instead of stochastic. That is not the situation for an FG that can be deprogrammed by one or a few ion hits. This is a micro-dose problem that requires a custom-made statistical analysis to interpret laboratory test data in such a way that mission risk estimates can be made. Such an analysis is given in this report.

Definitions and explanations of symbols and acronyms are included in the main text but can also be found in Appendix F. This appendix also explains the significance of various quantities and can serve as a summary of this work.

II. Interaction Cross Sections

Until Section XII, all ion hits are tacitly assumed to be at normal incidence and the hit location is described by two coordinates: x and y. Directional effects will be discussed in Section XII. The concept of a cross section begins with the concept that the FG charge loss produced by a given ion species and energy depends on where the ion hits the physical structure. In this context, the physical structure consists of the FG itself together with any oxide (or other) materials that are close enough to the FG to be relevant. To be more specific, we assume that, for the selected ion species and energy, there is some function $W(x,y)$ satisfying

$$\delta q = W(x, y),$$

where δq is the charge loss produced by one hit to the selected location. The symbol δ is used to emphasize a single hit, while Δ will be used in later sections for cumulative charge loss. Note that the function W is unique to the selected ion species and energy. To make the above equation more general we include another argument in the W function, call it L, that completely characterizes the ion species and energy in such a way that the function W is completely determined by this one parameter. The equation then becomes

$$\delta q = W(L, x, y). \tag{1}$$

The charge loss from one hit is then determined by specifying the L-value and hit location of the ion. The most obvious convenient choice for L is the ion LET, although this choice has some limitations. The limitations are due to the fact that different ions with the same LET can produce different track structures. The radial track structure is significant in two ways. The first is its effect on the yield function that determines the number of electron-hole pairs liberated in an oxide that survive the prompt recombination [4]. It was argued in [2] that this is not important when considering an actual charge loss of an FG, but it might still be relevant when the charge loss is an affective charge loss produced from the charging of a nearby oxide. A second significance occurs in devices small enough for the ion-track width to be comparable to or larger than the geometric sizes of the ultra-small physical structures associated with some of the more modern FGs. Note that the (x,y) in (1) is a point; the hit location of the ion. It does not include a track width. The track width is implicitly contained in the function W. Ions that produce wider tracks can have hit locations further from a physical structure and still affect that structure, so the W function is more spread out for wider tracks. If different ions with the same LET produce different track widths, then LET is not enough information to specify the W function. However, until future work finds a better choice for L that is as (or almost as) convenient to work with as LET, we will take L to be the LET.

A simplifying assumption that is essential to this analysis is that the function W does not depend on whether there were previous ion hits. This assumption is clearly wrong because it does not predict any saturation. If the same function W applies to all hits and the charge loss is cumulative, the total charge loss would increase without bound as the number of hits increases without bound. In reality, the total charge loss will not exceed the charge initially stored in the FG. This will be a large error for an overkill exposure, i.e., an exposure that produces more than enough hits needed to deprogram the FG. However, conservatism in the model representation of an overkill exposure is not relevant to the ability of the model to predict the probability of the FG becoming deprogrammed. If the existence of a well-defined function W satisfying (1) is an

adequate approximation up to the point that the cumulative charge loss is enough to deprogram the FG, the model can still serve its intended purpose. The approximation of treating the W function as independent of irradiation history might be called a small perturbation approximation because it is expected to be accurate for a selected ion hit if the accumulated charge loss from all prior hits (prior to the selected hit, but after the most recent erase-and-program operation) is small compared to the initial charge stored in the FG.

The W function is used to define a cross section. We now interpret δq as an independent variable and define the corresponding sensitive region, a set of points denoted $S(L,\delta q)$, to be those points (x,y) satisfying $W(L,x,y) > \delta q$. In other words, an ion with LET L will produce a charge loss that exceeds δq if, and only if, it hits the region $S(L,\delta q)$. The cross section denoted $\sigma(L,\delta q)$ is defined to be the area of $S(L,\delta q)$.

Recall that the W function accounts for track width, so the cross section $\sigma(L,\delta q)$ can exceed the geometric area of a physical structure by an amount that accounts for track width. However, hits that are sufficiently far from the FG will have no effect on the selected FG, so the cross section $\sigma(L,\delta q)$ (which increases with decreasing δq) has a finite value in the limit as $\delta q \rightarrow 0^+$, where the "+" superscript means that the approach to zero is from above. However, there is a complication. It is conceivable that the saturation value could be different for different LETs, or even for different ions having the same LET. For example, there might be a hit location (x,y) such that a hit at this point by an ion that produces a narrow track has no effect, while an ion that produces a wider track results in a nonzero charge loss. The saturation cross section would then be larger for the wide-track ions than for the narrow-track ions. An analysis that allows for different ions to have different saturation cross sections would lead to a discontinuity in a probability function discussed in the next section, and this is a mathematical nuisance. It is an avoidable nuisance because there is a simple way to work around this. Referring to the two-ion comparison just given, all we have to do is assign to the narrow-track ion a charge loss that is too small to have any physical significance, but still greater than zero to avoid a mathematical nuisance. In this model, if there is any LET such that a hit at a point (x,y) produces a greater-than-zero charge loss, then any ion that hits this point will produce some greater-than-zero charge loss, although it might be too small to have any physical significance. In other words, in this model, the set of points (x,y) satisfying $W(L,x,y) > 0$ is the same set for all L. The saturation sensitive region, denoted S_{sat}, is defined to be this set of points, and the saturation cross section, denoted σ_{sat}, is defined to be the area of S_{sat}. Using this model and these definitions, an ion hit produces a nonzero charge loss if, and only if, it hits the region S_{sat}, regardless of LET. We also have

$$\lim_{\delta q \rightarrow 0^+} \sigma(L,\delta q) = \sigma_{sat} \quad \text{for all } L > 0 \,. \tag{2}$$

The above discussions refer to a single isolated FG; isolated except for the presence of oxide structures close enough to the FG for charge trapping in the oxide to affect the effective charge loss of the FG. We now consider a device containing a collection of FGs. Each FG has its own set of points $S(L,\delta q)$, call the set $S_1(L,\delta q)$ for FG #1 and $S_2(L,\delta q)$ for FG #2. It is possible that a single ion hit can affect both FGs so the two sets have some points in common; i.e., the

sets overlap.[3] The set $S_1(L,\delta q)$ is defined to be the set of hit locations that produce a charge loss exceeding δq in FG #1 regardless of whether this ion hit does or does not affect any other FGs. The expected number of these events in FG #1 is the expected number of hits to the set $S_1(L,\delta q)$, which is the area of $S_1(L,\delta q)$ (the cross section) multiplied by fluence. Similarly, the expected number of these events in FG #2 is the area of $S_2(L,\delta q)$ (the cross section) multiplied by fluence. The sum of these expected numbers is obtained by multiplying the sum of the cross sections by fluence. This is true regardless of whether the two sets, $S_1(L,\delta q)$ and $S_2(L,\delta q)$, have any overlap, but this counting convention counts the number of events, not the number of ion hits. For example, if one ion hit produces an event in both FG #1 and FG #2, the count is 2 (for two events), not 1 (for one ion hit). This counting convention is convenient, and will be mentioned again in Section XII when ion trajectories at angles are discussed, because the number of counts summed over a collection of FGs is obtained from the sum of cross sections regardless of whether there is or is not overlap. If there is overlap, the sum of cross sections will be larger than the area of the union of the point sets.

[3] A distinction will be made later (Section VI) between weak and strong interactions. We do not expect overlapping sets for strong interactions from normal incident ion hits when FGs are laterally separated (i.e., not one above another), but there might be overlap for weak interactions.

III. The Single-Hit Sample Space

Consider two geometric regions, S_{sat} and S_A, with respective areas σ_{sat} and A. The region S_A contains all points that are contained in S_{sat}. Let $H(L)$ denote the integral irradiation fluence; the fluence that includes all ions in the environment having an LET that exceeds L. The fluence at each L is assumed to be spatially homogeneous over the region S_A, which is defined to mean that any portion of S_A has the same probability of being hit by an ion of a given LET as any other portion having the same area. We take A to be large enough so that the number of hits to this area is large enough so that the number of hits can accurately (in terms of fractional or percent error, we are not concerned with absolute error here) be represented by the statistical average number of hits, which is the total fluence $H(0)$ times the area A. Note that A is an artificial parameter in the sense that it will not appear in the final results, but it provides a convenient way to derive those results. We now consider a set of randomly selected ions where random refers to both hit location (within the region S_A) and LET (with probability determined by relative abundances of different ions in the environment). The expected (statistical average) number of ions that individually produce a charge loss exceeding δq is denoted $N_1(\delta Q>\delta q)$. The upper case δQ denotes a statistical variable while the lower case δq denotes a value of a variable. The subscript 1 emphasizes that these are single particle events. This expected number is given by

$$N_1(\delta Q > \delta q) = \int_0^\infty h(L)\,\sigma(L,\delta q)\,dL\,,$$

where $h(L)$ is the differential fluence and is the negative of the L derivative of $H(L)$ (the negative sign is needed to produce a positive differential fluence). Similarly, the expected number of hits (including all LETs) to the region S_{sat} is given by

$$N_1(\textit{hits to } S_{sat}) = H(0)\,\sigma_{sat}\,,$$

while the exact (in terms of fractional error in the large-A limit) number of hits to S_A is

$$N_{total} = H(0)\,A\,.$$

Note that whether or not $\delta Q > \delta q$ is a "yes or no" condition so the binomial distribution, which gives the probability of N_1 successes in N_{total} tries, applies. For this distribution, the probability for a single hit to produce a success (i.e., the probability of a success from a single try) is the expected number of successes divided by N_{total}. Therefore, the probability that a single, randomly selected ion (from the population that hits the region S_A and has the LET distribution implied by h(L)), produces a charge loss that exceeds δq is given by

$$P_1'(\delta Q > \delta q) = \frac{1}{H(0)\,A}\int_0^\infty h(L)\,\sigma(L,\delta q)\,dL\,, \qquad (3)$$

where the prime distinguishes P_1' from another probability that refers to another sample space discussed later. Similarly,

$$P_1'(\text{hit to } S_{sat}) = \frac{\sigma_{sat}}{A} \ . \tag{4}$$

Note that a single randomly selected ion that produces a charge shift must also hit the region S_{sat}, so

$$P_1'(\delta Q > \delta q) = P_1'(\delta Q > \delta q \ \textit{and} \ \text{hit to } S_{sat}) \ .$$

Using the definition of conditional probability to rewrite the right side gives

$$P_1'(\delta Q > \delta q) = P_1'(\delta Q > \delta q \mid \text{hit to } S_{sat}) \ P_1'(\text{hit to } S_{sat}) \ , \tag{5}$$

where $P_1'(\delta Q > \delta q \mid \text{hit to } S_{sat})$ is a conditional probability; the probability that the ion hit will produce a charge loss that exceeds δq, *given that* this ion hit the region S_{sat}. Combining (3) and (4) with the above gives

$$P_1'(\delta Q > \delta q \mid \text{hit to } S_{sat}) = \frac{1}{H(0)\,\sigma_{sat}} \int_0^\infty h(L)\,\sigma(L,\delta q)\,dL \ . \tag{6}$$

Note that the area A does not explicitly appear on the right side of (6). This area still has an implicit role in that it defines fluence, which is actually a macroscopic quantity. By letting A be large enough so that N_{total} is large enough to have a definite (instead of stochastic) value, the fluence can be defined by dividing N_{total} by A. The fluence is homogeneous when any portion of S_A has the same probability of being hit by an ion of a given LET as any other portion having the same area. By combining these equal probabilities with a definite value of N_{total}, we have calculated the probability that a small portion of S_A will be hit, even if that portion is too small for a large number of hits, and this makes a connection between a macroscopic fluence and microscopic statistics. However, when the meaning of fluence is understood, the area A has no further role in this analysis.

Having calculated the conditional probability in (6), we can use this to assign probabilities to events in a different sample space. This sample space is the set of all possible outcomes allowed by the condition that there is exactly one ion hit to the region S_{sat}. The ion can have any LET with probability determined by relative abundances of different ions in the environment. This sample space is a subset of the larger sample space (in which there were N_{total} hits to a macroscopic region S_A) that the conditional probability in (6) applies to. Therefore, the probability, denoted $P_1(\delta Q > \delta q)$, that a randomly selected hit will produce a charge loss exceeding δq in this sample space is given by

$$P_1(\delta Q > \delta q) = \frac{1}{H(0)\,\sigma_{sat}} \int_0^\infty h(L)\,\sigma(L,\delta q)\,dL \ . \tag{7}$$

To shorten the notation, we define F by

$$F(\delta q) \equiv P_1(\delta Q \le \delta q) \ . \tag{8}$$

The direction of the inequality was selected to satisfy the usual convention for a cumulative probability distribution, that $F(\delta q)$ increases with increasing δq. Note that the condition $\delta Q > 0$ is implied for this sample space because, as discussed in the previous section, any ion hit to the region S_{sat} produces a greater-than-zero charge loss. Using this fact with (8), we conclude that $F(0)$ is defined and equal to zero, as is the limit of $F(\delta q)$ as $\delta q \to 0^+$, so $F(\delta q)$ is continuous at $\delta q = 0$. Note that the conditions $\delta Q > \delta q$ and $\delta Q \le \delta q$ are mutually exclusive and all-inclusive, so (8) can be written as

$$F(\delta q) = 1 - P_1(\delta Q > \delta q) = 1 - \frac{1}{H(0)\,\sigma_{sat}} \int_0^\infty h(L)\,\sigma(L, \delta q)\,dL\,, \tag{9}$$

where the second equality used (7). As a consistency check, note that (2) and (9) produce agreement with the earlier statement that $F(\delta q) \to 0$ as $\delta q \to 0^+$.

The probability density function associated with F, denoted f, is given by

$$f(\delta q) \equiv \frac{d}{d\,\delta q} F(\delta q) = -\frac{1}{H(0)\,\sigma_{sat}} \frac{d}{d\,\delta q} \int_0^\infty h(L)\,\sigma(L, \delta q)\,dL\,. \tag{10a}$$

Integrating (10a) while using $F(0) = 0$ gives

$$\int_0^{\delta q} f(x)\,dx = F(\delta q)\,. \tag{10b}$$

In particular, because $F(\delta q) \to 1$ as $\delta q \to \infty$, we have the normalization condition

$$\int_0^\infty f(x)\,dx = 1\,. \tag{10c}$$

The cumulative probability function and the probability density for the single-hit sample space given by (9) and (10a) are the essential results derived in this section.

IV. The Sample Space for *n* Hits

This sample space considered in this section is the set of all possible outcomes allowed by the condition that there is exactly n ion hits to the region S_{sat}. As with the single-hit sample space, any of the n ions can have any LET, independently of each other, with the probability distribution for an LET assignment determined by the relative abundances of different ions in the environment. The probability function for this sample space is denoted P_n, where the n subscript denotes the sample size. The quantity of interest here is the sum of charge losses summed over the particle hits. To shorten the notation, the cumulative probability function for this sum is denoted F_n defined by

$$F_n(\Delta q) \equiv P_n(\Delta_n Q \le \Delta q), \tag{11a}$$

where Δq is an arbitrarily selected number, and the random variable $\Delta_n Q$ is defined to be the sum of random variables given by

$$\Delta_n Q \equiv \sum_{k=1}^{n} \delta Q_k \ , \tag{11b}$$

where δQ_k is the charge loss from the k^{th} hit. Note that, when n =1, F_n is the function F in the previous section and $\Delta_n Q$ is δQ.

The cumulative probability function F_n can be calculated from a recurrence relation that contains the single-hit probability density f that was already calculated in the previous section. The recurrence relation derived in [5], expressed in the notation used here, is

$$F_{n+1}(\Delta q) = \int_0^\infty f(x)\, F_n(\Delta q - x)\, dx \quad \text{for } n = 1, 2, \ldots . \tag{12}$$

Having listed (12), we have no further need to conform to the convention in (6) in which a cumulative probability function is increasing. It will be more convenient in the next section to work with the function G_n defined by

$$G_n(\Delta q) \equiv P_n(\Delta_n Q > \Delta q) = 1 - F_n(\Delta q) \quad \text{for } n = 1, 2, \ldots . \tag{13}$$

Using (13) to substitute for F_n in (12) and using the fact that f is a normalized probability density shows that G_n satisfies the recurrence relation

$$G_{n+1}(\Delta q) = \int_0^\infty f(x)\, G_n(\Delta q - x)\, dx \quad \text{for } n = 1, 2, \ldots . \tag{14}$$

The infinite integration limit in (14) is often convenient for analytical investigations (e.g., in Sections VI and VII) but a finite integration limit is more convenient when the goal is to evaluate the integrals numerically. A finite integration limit is obtained by noting from (13) that $G_n(x) = 1$ if $x \le 0$, so $G_n(x - \xi) = 1$ if $\xi \ge x$. This property allows (14) to be written as

$$G_{n+1}(x) = G_1(x) + \int_0^x f(\xi)\, G_n(x-\xi)\, d\xi$$

$$= G_1(x) + \int_0^x f(x-\xi)\, G_n(\xi)\, d\xi \quad \text{for } n = 1, 2, \ldots, \tag{15a}$$

where the second equality was obtained by changing integration variables, and G_1 is given, via (9), by

$$G_1(x) = 1 - F_1(x) = 1 - F(x) = \frac{1}{H(0)\,\sigma_{sat}} \int_0^\infty h(L)\, \sigma(L,x)\, dL\,. \tag{15b}$$

As a reminder, f is given by

$$f(x) = -\frac{d}{d\,x} G_1(x) = -\frac{1}{H(0)\,\sigma_{sat}} \frac{d}{d\,x} \int_0^\infty h(L)\, \sigma(L,x)\, dL \tag{15c}$$

and satisfies

$$\int_0^x f(\xi)\, d\xi = 1 - G_1(x)\,. \tag{15d}$$

From the probability interpretation of G_n given by (13), it is evident that the following conditions apply:

$$0 \le G_n(x) \le G_{n+1}(x) \le 1 \quad \text{for all } x \ge 0 \text{ and all } n = 1, 2, \ldots \tag{16a}$$

$$\lim_{x \to 0} G_n(x) = G_n(0) = 1 \quad \text{for all } n = 1, 2, \ldots \tag{16b}$$

$$\lim_{x \to \infty} G_n(x) = 0 \quad \text{for all } n = 1, 2, \ldots \tag{16c}$$

$$\lim_{n \to \infty} G_n(x) = 1 \quad \text{for all } x \ge 0\,. \tag{16d}$$

$$G_n(x) = 1 \quad \text{for all } x \le 0 \text{ and all } n = 1, 2, \ldots \tag{16e}$$

$$\text{If } -\infty < x_1 \le x_2 < \infty \text{ then } G_n(x_1) \ge G_n(x_2) \quad \text{for all } n = 1, 2, \ldots\,. \tag{16f}$$

All of the properties listed in (16) can be shown to be consistent with (15). Each inequality in (16a) is most easily proven from (15) by mathematical induction while recognizing that a larger integrand on the right side of (15a) produces a larger left side. The property (16b) is evident from inspection of (15a) while recognizing that $G_1(0) = 1$. Verification of the property (16c) is postponed to the next paragraph because some discussion is needed. The property (16d) is seen to be consistent with (15) by using (15d) to conclude that (15a) is satisfied when $G_{n+1}(x)$ and $G_n(\xi)$ are both replaced by 1. Property (16e) is seen to be consistent with (15a) by noting that a negative x produces an integration interval in (15a) on which $f = 0$, so (15a) gives $G_{n+1}(x) =$

$G_1(x) = 1$. Because of this property, numerical integrations utilizing the recurrence relation (15a) are needed only when $x > 0$. To show that property (16f) is consistent with (15a) we must first show that (16f) applies when $n = 1$. Recall from Section II that the cross section $\sigma(L,\delta q)$ is the area of $S(L,\delta q)$, which is the set of points (x,y) satisfying $W(L,x,y) > \delta q$. This implies that $\sigma(L, \delta q_1) \geq \sigma(L, \delta q_2)$ when $\delta q_1 \leq \delta q_2$. This fact, together with (15b), while noting that $h(L) \geq 0$, implies (16f) when $n = 1$. To establish (16f) for $n = 2, 3, \ldots$, we use (15a) to get

$$G_{n+1}(x_1) = G_1(x_1) + \int_0^{x_1} f(\xi)\, G_n(x_1 - \xi)\, d\xi =$$

$$G_1(x_1) + \int_0^{x_2} f(\xi)\, G_n(x_1 - \xi)\, d\xi - \int_{x_1}^{x_2} f(\xi)\, G_n(x_1 - \xi)\, d\xi .$$

When $x_1 \leq x_2$ we can use (16e) in the integral on the far right and then use (15d) to get

$$G_{n+1}(x_1) = G_1(x_1) + \int_0^{x_2} f(\xi)\, G_n(x_1 - \xi)\, d\xi - \int_{x_1}^{x_2} f(\xi)\, d\xi = G_1(x_2) + \int_0^{x_2} f(\xi)\, G_n(x_1 - \xi)\, d\xi .$$

The last step uses the above equation in a simple proof by mathematical induction to establish (16f) for $n = 2, 3, \ldots$.

Property (16c) requires some discussion because its validity requires the function G_1 to have this property. This was already tacitly assumed in the statement above (10c) (note that $F = F_1 = 1 - G_1$, so the statement that $F \rightarrow 1$ is equivalent to $G_1 \rightarrow 0$). This is clearly correct for any real case because the ion LETs in any real environment are limited to a finite range (the upper integration limit in (3) can still be infinite because the flux is zero at LETs larger than contained in the environment), and any finite LET can only produce a finite charge loss even at the worst possible hit location, so there is some maximum charge loss, call it δq_{max}, satisfying $G_1(\delta q) = 0$ when $\delta q > \delta q_{max}$. However, models sometimes use simplifying approximations that might not agree with all aspects of reality. We assume that any approximation that might be used for the function f will satisfy (10c), which implies that G_1 satisfies (16c). It is shown in Appendix A that (15) then implies (16c) for each n.

It is interesting to consider expected values for the sample spaces. For the single-hit sample space, the expected value of δq, denoted $< \delta Q >$, is defined by

$$\langle \delta Q \rangle \equiv \int_0^{\infty} x\, f(x)\, dx . \tag{17a}$$

For the sample space consisting of n hits, the expected value of the accumulated charge loss is denoted $E_n[\Delta Q]$ and defined by

$$E_n[\Delta Q] \equiv \int_0^{\infty} x\, f_n(x)\, dx , \tag{17b}$$

where the probability density f_n is defined by

$$f_n(x) \equiv -\frac{d}{dx} G_n(x) . \tag{18}$$

It is well known from statistics that

$$E_n[\Delta Q] = n\langle \delta Q \rangle . \tag{19}$$

As a check for consistency, note that (19) can be derived from (15). This is shown in Appendix A.

Note the competing limits in (16c) and (16d). Because of this, a value of Δq that is large enough to satisfy $G_n(\Delta q) \approx 0$ depends on how large n is. A larger n requires a larger Δq for the approximation to apply. Similarly, a value of n that is large enough to satisfy $G_n(\Delta q) \approx 1$ depends on how large Δq is. A larger Δq requires a larger n for the approximation to apply. We can get some additional information by taking the limit as n and Δq increase together. It can be shown from (15) that

$$\lim_{n\to\infty} G_n(n\,\delta q) = \begin{cases} 1 & \text{if} \quad \delta q < \langle \delta q \rangle \\ 0 & \text{if} \quad \delta q > \langle \delta q \rangle \end{cases} . \tag{20}$$

V. A Generic Micro-Dose Model

This section presents an analysis applicable to any micro-dose problem that can be adequately modeled from the assumptions stated in previous sections when δQ is given some appropriate physical interpretation (e.g., a transistor threshold voltage shift) for a single-ion hit, and the quantity of interest is the sum over hits denoted ΔQ. Assumptions that are more specific to the case in which ΔQ is the sum of effective charge losses of an FG will be used in the next section. We will continue to use "charge loss" terminology in this section, but the results derived here can also be applied to other physical interpretations of ΔQ.

The analysis begins in the same way as the analysis in Section III began, but the macroscopic area A, which receives a large enough number of hits for this number to be certain to be close to the statistical average, is replaced by the microscopic area σ_{sat}. The sample space considered in this section is defined by a specified homogeneous fluence $h(L)$, but the area σ_{sat} is allowed to be small enough so that the number of hits to the region S_{sat} must be treated as a random variable. The equation that replaces (5) when the number of hits is a random variable is

$$P(\Delta Q > \Delta q) = \sum_{n=1}^{\infty} P(\Delta Q > \Delta q \,|\, n)\; P(n)\,, \tag{21}$$

where $P(\Delta Q > \Delta q \;|\; n)$ is the probability that the accumulated charge loss exceeds an arbitrary value Δq, given that S_{sat} received exactly n hits, and $P(n)$ is the probability that S_{sat} received exactly n hits. The conditional probability $P(\Delta Q > \Delta q \;|\; n)$ is the function $G_n(\Delta q)$ defined by (13) for the sample space in which S_{sat} received exactly n hits. Also, the probability $P(n)$ is related to the expected number of hits, which is $H(0)\sigma_{sat}$, by the Poisson distribution given by

$$P(n) = \frac{1}{n!}\big[H(0)\,\sigma_{sat}\big]^n \exp\big[-H(0)\,\sigma_{sat}\big]. \tag{22}$$

Making these substitutions into (21) gives

$$P(\Delta Q > \Delta q) = \exp\big[-H(0)\,\sigma_{sat}\big]\sum_{n=1}^{\infty}\frac{1}{n!}G_n(\Delta q)\,\big[H(0)\,\sigma_{sat}\big]^n \;\;, \tag{23}$$

where $G_n(\Delta q)$ is calculated from either (14) or (15a), with f and G_1 obtained from (15b) and (15c). If an event is defined by the condition that the accumulated charge loss exceeds some critical value, call it Δq_C, then the probability for an event is $P(\Delta Q > \Delta q_C)$.

An interesting limiting case is when Δq approaches zero. Using (16b), the sum becomes a series expansion for $\exp[H(0)\sigma_{sat}] - 1$, so the probability becomes $1 - \exp[-H(0)\sigma_{sat}]$. This is recognized (via the Poisson distribution) to be the probability of one or more ion hits to the region S_{sat}, which is the expected result.

VI. Specializing to Floating Gate Prompt Charge Loss

In order to continue with the results derived in the previous section, we must put some information into the cross section $\sigma(L,\delta q)$ that reflects the specific case of interest. The case considered here is the prompt effective charge loss of an FG.

The first approximation used here is the assumption that, for any given hit location, the charge loss from an ion hit is proportional to the ion LET.[4] This approximation clearly fails when the charge loss is sufficiently large because the approximation does not predict any saturation; i.e., the predicted charge loss increases without bound as the LET increases without bound. In reality, the charge loss cannot exceed the charge initially stored in the FG. Therefore, this approximation is in the category of a small-perturbation approximation discussed in Section II. However, as pointed out in that discussion, if the approximation is adequate up to the point at which the charge loss becomes overkill, then the approximation is useful for this analysis. This approximation implies that the cross section for a given LET to produce a given charge loss is the same as the cross section for twice that LET to produce twice that charge loss. More generally, the quantities L and δq should appear in the function $\sigma(L,\delta q)$ only in the combination $L/\delta q$.

An important observation from Cellere *et al.* in [6] is that there are at least two distinct physical mechanisms contributing to charge loss. One, called the strong interaction here, produces a relatively large charge loss from a single ion hit but has a small enough cross section so that a relatively small number of hits are expected. Data in [6] indicate that the cross section for this event is equal to the geometric area of the FG, which is consistent with the assertion in [6] that this event occurs when an ion strikes the FG and the effective charge loss is an actual charge loss. A characteristic of this interaction is that each ion hit (when all ions have the same LET) to this region produces nearly the same charge loss. The other interaction, called the weak interaction here, generally produces a smaller effective charge loss from a single-ion hit but can still be important because of a larger number of interactions due to a larger cross section. This weak interaction produces the secondary effects discussed in [6] and might be the same as the partial compensation (via the charging of a nearby oxide) discussed by Guertin *et al.* in [3].

The model used here regards the region S_{sat} as being made up of two non-overlapping portions. One, denoted $S_{S,sat}$, is the region at which ion hits to this region produce strong interactions. This region is assumed to be the FG. The other region, denoted $S_{W,sat}$, is the region at which ion hits to this region produce weak interactions. The area of $S_{S,sat}$ is denoted $\sigma_{S,sat}$ and is assumed to be the FG area. The area of $S_{W,sat}$ is denoted $\sigma_{W,sat}$ and satisfies $\sigma_{W,sat} + \sigma_{S,sat} = \sigma_{sat}$. The region $S_S(L,\delta q)$ is that portion of $S_{S,sat}$ at which a hit by an ion with LET L produces a charge loss exceeding δq via a strong interaction (the only possible interaction for this region) and the area of this region is the cross section denoted $\sigma_S(L,\delta q)$. The region $S_W(L,\delta q)$ is that portion of $S_{W,sat}$ at which a hit by an ion with LET L produces a charge loss exceeding δq via a weak interaction (the only possible interaction for this region) and the area of this region is the cross section denoted $\sigma_W(L,\delta q)$.

The strong interaction cross section is approximated by assuming that all ion hits, at a given LET, to the region $S_S(L,\delta q)$ produce the same charge loss. With the charge loss assumed to be proportional to the LET, the charge loss divided by LET is a constant, denoted $1/a_1$,[5] for all

[4] Recall that the cross section refers to normal incident hits so a dependence on the angle of the ion track is not discussed here. It will be discussed later in Section XII.

[5] Stated another way, the charge loss from a strong interaction is the LET divided by a_1. A small value of a_1 implies that a small LET is enough to produce a given charge loss.

hits to this region. This constant is an adjustable fitting parameter if there is not enough available information for it to be known. No hit to the region $S_S(L,\delta q)$ will produce a charge loss greater than δq if δq is greater than L/a_1, but a hit anywhere to the region $S_S(L,\delta q)$ will produce a charge loss greater than δq if δq is less than L/a_1. Therefore, the strong interaction cross section is the step function given by

$$\sigma_S(L,\delta q) = \begin{cases} \sigma_{S,sat} & \text{if} \quad \delta q < L/a_1 \\ 0 & \text{if} \quad \delta q > L/a_1 \end{cases}. \tag{24a}$$

Since the model is intended to be only a data fitting tool, analytical simplicity is given a higher priority than physical accuracy so we treat the weak interactions in the same way as the strong interactions. Specifically, the cross section for weak interactions is approximated by another step function, given by

$$\sigma_W(L,\delta q) = \begin{cases} \sigma_{W,sat} & \text{if} \quad \delta q < L/a_2 \\ 0 & \text{if} \quad \delta q > L/a_2 \end{cases}, \tag{24b}$$

where $\sigma_{W,sat}$ and a_2 are two more adjustable fitting parameters, having the same interpretations for weak interactions that the parameters $\sigma_{S,sat}$ and a_1 have for strong interactions. It should be noted that the use of a step function is not a new idea for curve-fitting applications. Specifically, for SEE rate calculations, the RPP model explained in [7] is not physically correct (because charge collection is not as simple as predicted by a sensitive volume model [8]), but the integrated RPP model (the IRPP model) constructed from the RPP model by including a statistical distribution of critical charges has been successful enough to be the most commonly used model for SEE rate calculations. The reason is that a suitably selected statistical distribution of critical charges (usually a Weibull function with some adjustable parameters) is able to compensate for error in the physical model. Similarly, error in the simplifying assumption (24b) can be at least partially compensated by a suitably selected statistical distribution of critical charge losses. The inclusion of a statistical distribution of critical charge loss will be done for the general case later in Section VIII, while data discussed later in Section X indicate that a Weibull function is the best choice, but for the present discussion, it is enough to know that errors in the physical model used in this section can be at least partially compensated by introducing some adjustable fitting parameters in later sections. With this simplified model, the total cross section is the sum given by

$$\sigma(L,\delta q) = \sigma_S(L,\delta q) + \sigma_W(L,\delta q), \qquad \sigma_{sat} = \sigma_{S,sat} + \sigma_{W,sat}. \tag{24c}$$

To calculate the probability in (23), we must calculate the functions G_n. We start with G_1 by using (15b) with (24) to get

$$G_1(x) = \frac{H(a_1 x)\sigma_{S,sat} + H(a_2 x)\sigma_{W,sat}}{H(0)\,\sigma_{sat}} \tag{25a}$$

and (15c) gives

$$f(x) = \frac{a_1\, h(a_1\, x)\sigma_{S,sat} + a_2\, h(a_2\, x)\sigma_{W,sat}}{H(0)\,\sigma_{sat}}. \tag{25b}$$

The remaining functions G_2, G_3, …, are calculated from (25) together with either (14) or (15a). These calculations require that the four parameters a_1, a_2, $\sigma_{S,sat}$, and $\sigma_{W,sat}$ be known. When known, numerical values can be assigned to Δq and then the probability $P(\Delta Q > \Delta q)$ can be calculated from (23).

A "charge loss event" (CLE) is defined by the condition that the accumulated effective charge loss exceeds some critical value, call it Δq_C. For example, the critical value might be the value at which the device circuitry signals that the FG has become deprogrammed. Or, the critical value might be the value at which the threshold voltage shift in a surrounding FET exceeds one volt (or some other amount selected by an experimenter measuring threshold voltage shifts). The probability of a CLE, denoted P(CLE), is the probability given by (23) evaluated at $\Delta q = \Delta q_C$ when $\Delta q_C \geq 0$. However, a modification needed to treat the case of a negative-critical-charge loss is needed and can be understood after explaining the meaning of a negative-critical-charge loss. A critical-charge loss that is negative is interpreted to mean that prior to any irradiation the FG charge was already too small for the FG to be sensed as being in the charged (programmed) state. A charge-loss event is experimentally recognized by the charge state, so this FG will be experimentally identified as having undergone a CLE prior to any irradiation. In other words, any FG with a negative ΔQ_C (i.e., any FG that was insufficiently charged prior to irradiation) is regarded as having already undergone a CLE prior to any irradiation. The probability of a CLE in this FG is 1, regardless of the amount of irradiation. The modification of (23) evaluated at $\Delta q = \Delta q_C$ needed to produce this result is

$$P(CLE) = \exp\left[-H(0)\,\sigma_{sat}\right]\left\{U(-\Delta q_C) + \sum_{n=1}^{\infty}\frac{1}{n!}G_n(\Delta q_C)\left[H(0)\,\sigma_{sat}\right]^n\right\}, \tag{26}$$

where U is the unit step function defined by $U(x) = 1$ when $x > 0$ and $U(x) = 0$ when $x \leq 0$. This produces the desired result because, if we take the limit as Δq_C approaches zero from above and use (16b), we find that the curly bracket becomes a series expansion for $\exp[H(0)\sigma_{sat}] - 1$, so the probability becomes $1 - \exp[-H(0)\sigma_{sat}]$. This can be recognized (via the Poisson distribution) to be the probability of one or more ion hits to the region S_{sat}, which is the expected result. However, if Δq_C is negative, the step function contributes and this, together with (16e), implies that the curly bracket is a series expansion for $\exp[H(0)\sigma_{sat}]$, so the probability becomes 1, which is the required result.

Eq. (26) can be used as is for numerical calculations if the numerical routine starts with (25) and then numerically evaluates one of the integrals in (15a) to obtain G_2, G_3, etc. Numerical integrations are needed only when $x > 0$ because of (16e). But (26) has a disadvantage from the point of view of analysis because the dependence of $P(CLE)$ on $\sigma_{S,sat}$ or $\sigma_{W,sat}$ is obscured by an implicit dependence contained in G_n. An equation that is more useful for analysis is one that explicitly shows the dependence on $\sigma_{S,sat}$ and $\sigma_{W,sat}$. Such an equation can be obtained by first defining $C_{m,n}(x)$, $D_{m,n}(x)$, and $E_{m,n}(x)$ by

$$C_{0,0}(x) \equiv H(a_1\, x) \tag{27a}$$

$$C_{0,n}(x) \equiv \int_0^\infty \ldots \int_0^\infty h(\gamma_1)..h(\gamma_n) H\left(a_1 \left[x - \frac{\gamma_1 + \ldots + \gamma_n}{a_2} \right] \right) d\gamma_1 \ldots d\gamma_n \quad \text{for all } n = 1, 2, \ldots \tag{27b}$$

$$C_{m,0}(x) \equiv \int_0^\infty \ldots \int_0^\infty h(\xi_1)..h(\xi_m) H\left(a_1 \left[x - \frac{\xi_1 + \ldots + \xi_m}{a_1} \right] \right) d\xi_1 \ldots d\xi_m \quad \text{for all } m = 1, 2, \ldots \tag{27c}$$

$$C_{m,n}(x) \equiv$$
$$\int_0^\infty \ldots \int_0^\infty h(\xi_1)..h(\xi_m) h(\gamma_1)...h(\gamma_n) H\left(a_1 \left[x - \frac{\xi_1 + \ldots + \xi_m}{a_1} - \frac{\gamma_1 + \ldots + \gamma_n}{a_2} \right] \right) d\xi_1 \ldots d\xi_m d\gamma_1 \ldots d\gamma_n$$
$$\text{for all } m = 1, 2, \ldots \text{ and all } n = 1, 2, \ldots \tag{27d}$$

$$D_{0,0}(x) \equiv H(a_2\, x) \tag{27e}$$

$$D_{0,n}(x) \equiv \int_0^\infty \ldots \int_0^\infty h(\gamma_1)..h(\gamma_n) H\left(a_2 \left[x - \frac{\gamma_1 + \ldots + \gamma_n}{a_2} \right] \right) d\gamma_1 \ldots d\gamma_n \quad \text{for all } n = 1, 2, \ldots \tag{27f}$$

$$D_{m,0}(x) \equiv \int_0^\infty \ldots \int_0^\infty h(\xi_1)..h(\xi_m) H\left(a_2 \left[x - \frac{\xi_1 + \ldots + \xi_m}{a_1} \right] \right) d\xi_1 \ldots d\xi_m \quad \text{for all } m = 1, 2, \ldots \tag{27g}$$

$$D_{m,n}(x) \equiv$$
$$\int_0^\infty \ldots \int_0^\infty h(\xi_1)..h(\xi_m) h(\gamma_1)...h(\gamma_n) H\left(a_2 \left[x - \frac{\xi_1 + \ldots + \xi_m}{a_1} - \frac{\gamma_1 + \ldots + \gamma_n}{a_2} \right] \right) d\xi_1 \ldots d\xi_m d\gamma_1 \ldots d\gamma_n$$
$$\text{for all } m = 1, 2, \ldots \text{ and all } n = 1, 2, \ldots \tag{27h}$$

$$E_{0,0}(x) \equiv U(-x) \tag{27i}$$

$$E_{0,n}(x) \equiv D_{0,n-1}(x) \quad \text{for all } n = 1, 2, \ldots \tag{27j}$$

$$E_{m,0}(x) \equiv C_{m-1,0}(x) \quad \text{for all } m = 1, 2, \ldots \tag{27k}$$

$$E_{m,n}(x) \equiv \frac{m}{m+n} C_{m-1,n}(x) + \frac{n}{m+n} D_{m,n-1}(x) \quad \text{for all } m = 1, 2, \ldots \text{ and all } n = 1, 2, \ldots \tag{27L}$$

The parameters defined by (27) are constructed from the environmental fluence, evaluated at arguments that depend on a_1 and a_2 which describe FG sensitivities, but do not depend on the cross sections $\sigma_{S,sat}$ or $\sigma_{W,sat}$. It is shown in Appendix B that (26) can be written as

$$P(CLE) = \exp\left[- H(0)\, \sigma_{sat} \right] \sum_{m,n=0}^{\infty} \frac{1}{m!\, n!} E_{m,n}(\Delta q_C)\, {\sigma_{S,sat}}^m\, {\sigma_{W,sat}}^n . \tag{28}$$

VII. An FG in a Pure Spectrum

An advantage of testing a device with heavy ions at a particle accelerator is that a single-ion species and energy can be selected so that all particles that hit the device during a beam run have the same LET. This is classified here as a pure spectrum. Two derivations of $P(CLE)$ produced by a pure spectrum are considered here. The first does not start with (28) because the simplifications provided by a pure spectrum provide a fairly simple derivation when starting from first principles. This derivation has the advantage of being easy to follow, but a disadvantage is that it does not easily generalize to more complex spectra (e.g., a superposition of two pure spectrums). The second derivation uses (28) to derive the same conclusion that was produced by the first derivation.

A derivation from first principles goes back to (21) and replaces it with

$$P(\Delta Q > \Delta q) = \sum_{m,n=0}^{\infty} P(\Delta Q > \Delta q \mid m,n)\, P_S(m)\, P_W(n), \tag{29}$$

where $P(\Delta Q > \Delta q \mid m,n)$ is the probability that the accumulated charge loss exceeds Δq, given that $S_{S,sat}$ received exactly m hits and $S_{W,sat}$ received exactly n hits, $P_S(m)$ is the probability that $S_{S,sat}$ received exactly m hits, and $P_W(n)$ is the probability that $S_{W,sat}$ received exactly n hits. The latter probabilities are obtained by changing (22) into

$$P_S(m) = \frac{1}{m!}\left[H\,\sigma_{S,sat}\right]^m \exp\left[-H\,\sigma_{S,sat}\right], \qquad P_W(n) = \frac{1}{n!}\left[H\,\sigma_{W,sat}\right]^n \exp\left[-H\,\sigma_{W,sat}\right], \tag{30a}$$

where H is the beam fluence. To evaluate the conditional probability in (29), let L_T denote the LET of the test ion. From the definitions of a_1 and a_2 given in the previous section, m hits to $S_{S,sat}$ and n hits to $S_{W,sat}$ produce a definite value for the accumulated charge loss given by

$$\Delta Q = \left(\frac{m}{a_1} + \frac{n}{a_2}\right) L_T,$$

so the conditional probability is given by

$$P(\Delta Q > \Delta q \mid m,n) = \begin{cases} 1 & \text{if} \quad \Delta q < \left(\dfrac{m}{a_1} + \dfrac{n}{a_2}\right) L_T \\ 0 & \text{if} \quad \Delta q \geq \left(\dfrac{m}{a_1} + \dfrac{n}{a_2}\right) L_T \end{cases} = U\left(\left(\frac{m}{a_1} + \frac{n}{a_2}\right) L_T - \Delta q\right), \tag{30b}$$

where U is the unit step function defined by

$$U(x) \equiv \begin{cases} 1 & \text{if} \quad x > 0 \\ 0 & \text{if} \quad x \leq 0 \end{cases}. \tag{31a}$$

We also define *U*-bar, the compliment of the unit step function, for later use by

$$\overline{U}(x) \equiv 1 - U(x) = \begin{cases} 0 & \text{if} \quad x > 0 \\ 1 & \text{if} \quad x \le 0 \end{cases} . \tag{31b}$$

We often (e.g., when evaluating integrals containing continuous functions) do not have to make a distinction between *U*-bar(x) and $U(-x)$, but a distinction is needed when the discontinuous point at $x = 0$ has some significance. Substituting (30) into (29) gives

$$P(\Delta Q > \Delta q) = \exp\left[-H\,\sigma_{sat}\right] \sum_{m,n=0}^{\infty} \frac{1}{m!\,n!} U\left(\left(\frac{m}{a_1} + \frac{n}{a_2}\right) L_T - \Delta q\right) \left[H\,\sigma_{S,sat}\right]^m \left[H\,\sigma_{W,sat}\right]^n . \tag{32a}$$

A CLE occurs when $\Delta q = \Delta q_C$. Evaluating the above probability at this point gives

$$P(\text{CLE}) = \exp\left[-H\,\sigma_{sat}\right] \sum_{m,n=0}^{\infty} \frac{1}{m!\,n!} U\left(\left(\frac{m}{a_1} + \frac{n}{a_2}\right) L_T - \Delta q_C\right) \left[H\,\sigma_{S,sat}\right]^m \left[H\,\sigma_{W,sat}\right]^n . \tag{32b}$$

The results in (32) are useful for revealing some properties, such as the behavior of P(CLE) when $H\sigma_{sat}$ is small enough for the infinite series to be approximated by the first few non-vanishing terms, but the infinite series is not convenient for most numerical calculations. For the purpose of numerical calculations, it is convenient to replace the infinite series by an expression containing a finite sum. This is done by expressing the exponential function as a power series to get

$$1 = \exp\left[-H\,\sigma_{sat}\right] \exp\left[H\,\sigma_{S,sat}\right] \exp\left[H\,\sigma_{W,sat}\right] =$$

$$\exp\left[-H\,\sigma_{sat}\right] \sum_{m,n=0}^{\infty} \frac{1}{m!\,n!} \left[H\,\sigma_{S,sat}\right]^m \left[H\,\sigma_{W,sat}\right]^n \tag{33}$$

and combine this with (32) to get

$$P(\Delta Q > \Delta q) =$$

$$1 - \exp\left[-H\,\sigma_{sat}\right] \sum_{m,n=0}^{\infty} \frac{1}{m!\,n!} \overline{U}\left(\left(\frac{m}{a_1} + \frac{n}{a_2}\right) L_T - \Delta q\right) \left[H\,\sigma_{S,sat}\right]^m \left[H\,\sigma_{W,sat}\right]^n , \tag{34a}$$

$$P(\text{CLE}) =$$

$$1 - \exp\left[-H\,\sigma_{sat}\right] \sum_{m,n=0}^{\infty} \frac{1}{m!\,n!} \overline{U}\left(\left(\frac{m}{a_1} + \frac{n}{a_2}\right) L_T - \Delta q_C\right) \left[H\,\sigma_{S,sat}\right]^m \left[H\,\sigma_{W,sat}\right]^n . \tag{34b}$$

U-bar is zero when m and/or n are sufficiently large, so only a finite number of terms contribute to the sums on the right sides of (34). Note that *U*-bar can be omitted from the right sides of (34) by imposing suitable restrictions on the summation indices. But including *U*-bar with an unrestricted sum, instead of omitting *U*-bar and using a restricted sum, is more convenient for the

analysis in the next section. As a check for consistency, note that a positive Δq that is sufficiently close to zero results in only the $m = n = 0$ term contributing to the double sum in (34a), so the probability becomes $1–\exp[–H\sigma_{sat}]$. This can be recognized (via the Poisson distribution) to be the probability of one or more ion hits to the region S_{sat}, which is the expected result.

The second derivation of (32b), which implies (34b), requires only two steps because this derivation utilizes (28). The first step uses $h(\xi) = H(0)\delta(\xi - L_T)$ (where δ is the Dirac δ-function) and $H(\xi) = H(0)U(L_T - \xi)$ with (27) to get

$$E_{m,n}(x) = H(0)^{m+n}\, U\left(\frac{m\,L_T}{a_1} + \frac{n\,L_T}{a_2} - x\right) \quad \text{for all } m = 0,1,2,\ldots \text{ and all } n = 0,1,2,\ldots .$$

The second step substitutes this result into (28) to obtain (32b).

VIII. FG-to-FG Variations

The previous sections considered an FG characterized by well-defined values for each of the parameters a_1, a_2, $\sigma_{S,sat}$, $\sigma_{W,sat}$, and Δq_C. These parameters may or may not be known, but they are still well defined in the sense that they are not random variables. The only random variables previously considered were the numbers of ion hits to various regions. However, data in [6] show that, even without any irradiation, there is a significant spread in the threshold voltages associated with different FGs in a flash memory. The model used here attributes this spread to variations of Δq_C among different FGs. The interpretation of a probability is now extended to include randomness in the selection of an FG, so the critical-charge loss becomes another random variable and is denoted ΔQ_C. The probability calculated from (26) is now interpreted as a conditional probability. The notation that will now be used for this probability is $P(\text{CLE} \mid \Delta Q_C = \Delta q_C)$ and is the probability of a charge-loss event, *given that* the critical-charge loss is equal to Δq_C. The probability of a CLE is constructed from this conditional probability from

$$P(\text{CLE}) = \int_{-\infty}^{\infty} P(\text{CLE} \mid \Delta Q_C = \xi)\, \rho(\xi)\, d\xi\,, \tag{35}$$

where $\rho(\xi)$ is the probability density for the critical charge loss to equal ξ. This probability density is presently unspecified because any one of a number of distributions might be considered. A definite choice (a Weibull function) will be made for an example in Section X and we will use this choice in later sections, but the analysis in this section will be versatile enough to allow other choices to be made. The integration limits in (35) include negative values of the critical charge loss so that we will be allowed (though not required) to consider critical-charge-loss distributions that include negative values of the critical-charge loss. The meaning of a negative value was explained in Section VI. As a reminder, a negative-critical-charge loss means that the initial FG charge was not sufficient for the FG to be sensed as being in the programmed (charged) state. Such an FG will satisfy the experimental definition of having undergone a CLE, regardless of the amount of irradiation it was exposed to.

One expression for $P(\text{CLE} \mid \Delta Q_C = \Delta q_C)$ is the right side of (26). Using this expression with (35) gives

$$\begin{aligned} P(\text{CLE}) = {} & \exp\left[-H(0)\,\sigma_{sat}\right] \mathcal{F}(0) + \\ & \exp\left[-H(0)\,\sigma_{sat}\right] \sum_{n=1}^{\infty} \frac{1}{n!} \left[\int_{-\infty}^{\infty} G_n(\xi)\, \rho(\xi)\, d\xi \right] \left[H(0)\,\sigma_{sat}\right]^n, \end{aligned} \tag{36}$$

where $\mathcal{F}$ is the cumulative distribution function for the critical-charge loss and satisfies

$$\mathcal{F}(x) = \int_{-\infty}^{x} \rho(\xi)\, d\xi\,. \tag{37}$$

Note that the first term on the right side of (36) is the probability of a CLE given that there are no ion hits. The exponential coefficient is the probability of zero hits while $\mathcal{F}(0)$ is the fractional number of FGs with negative-critical-charge losses, which are the only FGs that can produce a CLE when there are no hits. The remainder of the right side of (36) represents FGs

with negative- or positive-critical-charge losses and that received one or more hits to produce a CLE.

An alternate expression for $P(\text{CLE} \mid \Delta Q_C = \Delta q_C)$, applicable only to the FG model used here, is the right side of (28). Using this expression with (35) gives

$$P(CLE) = \exp\left[-H(0)\,\sigma_{sat}\right] \sum_{m,n=0}^{\infty} \frac{1}{m!\,n!} \left[\int_{-\infty}^{\infty} E_{m,n}(\xi)\,\rho(\xi)\,d\xi \right] {\sigma_{S,sat}}^{m}\ {\sigma_{W,sat}}^{n} . \qquad (38)$$

Finally, we consider a pure spectrum. For this case, we can express $P(\text{CLE} \mid \Delta Q_C = \Delta q_C)$ as the right side of (32b) or as the right side of (34b), so that (35) gives

$$P(\text{CLE}) = \exp\left[-H\,\sigma_{sat}\right] \sum_{m,n=0}^{\infty} \frac{\left[H\,\sigma_{S,sat}\right]^{m} \left[H\,\sigma_{W,sat}\right]^{n}}{m!\,n!} \mathcal{F}\left(\left(\frac{m}{a_1} + \frac{n}{a_2} \right) L_T \right) \quad \text{(pure spectrum)} \qquad (39a)$$

$$P(\text{CLE}) = 1 - \exp\left[-H\,\sigma_{sat}\right] \sum_{m,n=0}^{\infty} \frac{\left[H\,\sigma_{S,sat}\right]^{m} \left[H\,\sigma_{W,sat}\right]^{n}}{m!\,n!} \left[1 - \mathcal{F}\left(\left(\frac{m}{a_1} + \frac{n}{a_2} \right) L_T \right) \right]$$

(pure spectrum) . (39b)

Eq. (39a) is less cumbersome than (39b) and also more easily reveals analytical properties of some limiting cases (as seen in the next section). However, it has a disadvantage from the point of view of numerical evaluations because it is not obvious, when the case considered is not a limiting case, which terms need to be included in a sum in order to make a finite sum accurately approximate the double infinite series. A more useful equation from this point of view is (39b).

IX. Limiting Cases for FGs in a Pure Spectrum

The model is a function of two independent variables (fluence and LET) that already contains four fitting parameters (a_1, a_2, $\sigma_{S,sat}$, and $\sigma_{W,sat}$) without counting any parameters that might be contained in the distribution function $\mathcal{F}$. It would be useful to find constraints that allow one or more of these parameters to be calculated in terms of the remaining parameters. Such constraints are available if experimental test data includes LETs large enough to produce "SEU-like" behavior and/or LETs small enough to produce "dose-like" behavior. SEU-like behavior occurs when the LET is large enough for a single, strong interaction to produce a CLE. This can be recognized in experimental data by a straight line with unit slope in a plot of counts versus fluence at the selected LET (this is a sufficient, but not necessary, condition). Dose-like behavior occurs when the LET is small enough so that the number of ion hits required to produce a count is large enough to be approximated by the statistical average number of hits. This leaves FG-to-FG variations as the only source of randomness. Simplifications available for each of these two extremes are given in the two subsections below.

A. SEU-Like

The ultimate extreme of SEU-like behavior occurs when the LET is so large that even one weak interaction can produce a count, but we assume here that this extreme has not been reached. Instead, we assume that a count is produced by one strong interaction. We also assume that the fluence needed to produce a statistically meaningful number of strong interactions is small enough so that the number of weak interactions is unimportant for those few unfortunate FGs that experienced a strong interaction. The accumulated weak interactions being unimportant compared to one strong interaction means that the expected number, denoted $\langle n \rangle$, of weak interactions is small enough to satisfy

$$\frac{1}{a_1} >> \frac{\langle n \rangle}{a_2},$$

so that the dominate terms in the sum on the right side of (39a) are from those values of n satisfying

$$\mathcal{F}\left(\left(\frac{m}{a_1} + \frac{n}{a_2} \right) L_T \right) \approx \mathcal{F}\left(\frac{m}{a_1} L_T \right).$$

Using this approximation for all non-negligible terms on the right side of (39a) gives

$$P(\text{CLE}) \approx \exp\left[- H \sigma_{sat} \right] \sum_{m=0}^{\infty} \frac{\left[H \sigma_{S,sat} \right]^m}{m!} \mathcal{F}\left(\frac{m}{a_1} L_T \right) \sum_{n=0}^{\infty} \frac{\left[H \sigma_{W,sat} \right]^n}{n!} .$$

Recognizing the sum in n as a power series expansion for $\exp[-H\sigma_{W,sat}]$, and using the fact that $\sigma_{sat} = \sigma_{S,sat} + \sigma_{W,sat}$, the above approximation can be written as

$$P(\text{CLE}) \approx \exp\left[-H\,\sigma_{S,sat}\right]\sum_{m=0}^{\infty}\frac{\left[H\,\sigma_{S,sat}\right]^m}{m!}\mathcal{F}\left(\frac{m}{a_1}L_T\right) \qquad (\text{SEU - like}). \tag{40}$$

At this point it is necessary to recognize the distinction between probability and expected numbers. For the classic SEU problem, the expected number of upsets is proportional to fluence and increases without bound as the fluence increases without bound (we are considering the case in which upsets are reset so that multiple upsets are possible). In contrast, a probability cannot exceed 1 and, therefore, is not proportional to fluence. An approximate proportionality is obtained when the fluence is small enough to make the expected number small enough to make the probability approximately equal to the expected number. We, therefore, confine our attention to this small-*H* limit. In this limit, the exponential function in (40) is replaced by 1 and only the first two terms in the sum are retained. The result is

$$P(\text{CLE}) \approx \mathcal{F}(0) + \left[H\,\sigma_{S,sat}\right]\mathcal{F}\left(\frac{L_T}{a_1}\right) \qquad (\text{SEU - like, small } H). \tag{41}$$

The first term on the right side of (41) represents those FGs that were insufficiently charged prior to irradiation. If these can be neglected, only the second term remains. We assume this to be the case so a cross section for a CLE (a function of LET and experimentally defined to be counts divided by fluence for the selected LET) becomes a useful quantity because it is independent of the fluence. This per-bit cross section is denoted here as σ_{CLE} and is defined to be the number of CLE counts (summed over FGs) divided by fluence (for a device cross section) and then divided by the number of FGs in the device (to convert to a per-bit cross section). Recognizing the probability on the left side of (41) as the number of counts divided by the number of FGs in the device, a change in notation writes this approximation as

$$\sigma_{CLE} \approx \sigma_{S,sat}\,\mathcal{F}\left(\frac{L_T}{a_1}\right) \qquad (\text{SEU - like, small } H). \tag{42}$$

B. Dose-Like

We now consider the opposite extreme case of small LET so that the fluence needed to produce a statistically significant number of counts is large enough to make the number of ion hits to a given device region large enough to be approximated by the statistical average number of hits. For this application it is helpful to regard the right side of (39a) as a weighted average of the quantity

$$\mathcal{F}\left(\left(\frac{m}{a_1}+\frac{n}{a_2}\right)L_T\right) \quad (\text{the averaged quantity}) \tag{43}$$

with a normalized (because the sum in *m* and *n* from zero to infinity is 1) weight factor given by

$$\text{weight factor} = \exp\left[-H\,\sigma_{sat}\right]\frac{\left[H\,\sigma_{S,sat}\right]^{m}\left[H\,\sigma_{W,sat}\right]^{n}}{m!\,n!}\,. \tag{44}$$

When H is sufficiently large (the case assumed here), a plot of the weight factor in (44) versus m or n produces a peak at $m \approx H\sigma_{S,sat}$ and $n \approx H\sigma_{W,sat}$, with the weight factor having much smaller values at other values of m or n. Summations using this weight factor are (when H is sufficiently large) analogous to integrals containing Dirac delta functions. The weighted average of the quantity in (43) can then be approximated by the value of this quantity evaluated at $m = H\sigma_{S,sat}$ and $n = H\sigma_{W,sat}$. Using this approximation, (39a) becomes

$$P(\text{CLE}) \approx \mathcal{F}\left(\left(\frac{H\,\sigma_{S,sat}}{a_1}+\frac{H\,\sigma_{W,sat}}{a_2}\right)L_T\right) \qquad (\text{dose-like}),$$

which can also be written as

$$N_{\text{CLE}} \approx N_{bit}\,\mathcal{F}\left(\left(\frac{\sigma_{S,sat}}{a_1}+\frac{\sigma_{W,sat}}{a_2}\right)H\,L_T\right) \qquad (\text{dose-like}), \tag{45}$$

where N_{CLE} is the number of bits in the device that experienced a CLE, and N_{bit} is the total number of bits in the device. If the irradiation is measured by ionizing dose instead of fluence and LET, it is convenient to use

$$H\,L_T = \frac{6.25\times10^{4}\ \text{MeV}}{\text{rad-mg}}\,D\,, \tag{46}$$

where D is the dose in SiO_2 (the LET should also be in SiO_2) and the numerical coefficient is a unit conversion factor where MeV/rad-mg is a designator of the units.

X. An Example

Before considering a specific example of model fitting, some general caveats should be reviewed. The theory in the previous sections used at least two approximations that are in the category of small-perturbation approximations. They are guaranteed to fail if an FG charge loss is sufficiently large. However, if this failure does not occur until the charge loss is enough to be overkill (more than enough to deprogram the FG), the approximations are suitable for predicting the risk of deprogramming. Also, if the fitting parameters in the cross section are somehow known *a priori*, the small-perturbation approximations used here, but applied to conditions outside their scope, are conservative (i.e., they overestimate the risk of deprogramming) when they are not accurate. The problem case is that in which the fitting parameters are selected to fit test data produced by overkill-irradiation exposures. The model would then tend to underestimate the risk of deprogramming in milder radiation environments and this situation should be avoided. Therefore, test data used to evaluate fitting parameters should contain a minimum amount of overkill. Fits should be made only to those data sets in which the number of deprogrammed FGs is much less than the total number of FGs exposed to the irradiation.

An advantage of testing a device with heavy ions at a particle accelerator is that a single ion species and energy can be selected so that all particles that hit the device during a beam run have the same LET. This is also true for protons if direct ionization is the most important effect from protons. However, if proton-induced reaction products have an important role, these reaction products would have to be included as part of the heavy-ion environment, which would be distributed over a range of LETs. Therefore, the same simplification assumed here for heavy ions, that all particles have the same LET, can also be used when interpreting proton test data only if direct ionization can be assumed to be the most important effect from protons.

The device (e.g., a flash memory) is assumed to contain a large enough number of FGs to be treated as a statistical ensemble, in the sense that an experimental measure of the probability of a CLE is the fractional number of FGs that exhibit a CLE. Stated another way, the number of CLEs (called "counts" here) is the probability of a CLE multiplied by the number of FGs in the device. An experimental data set consists of a plot or table of the number of counts versus irradiation fluence, with one plot or table for each of several ion LETs.

The specific example considered here is the data set taken from [3] and reproduced in Fig. 1 (Fig. 2 will be discussed later). The LETs in the Fig. 1 legend were recalculated, via SRIM [9], for SiO_2 and are 5.7 MeV-cm^2/mg for Ar at 25 MeV/amu, 41 MeV-cm^2/mg for Xe at 25 MeV/amu, 43.7 MeV-cm^2/mg for Br at 3.5 MeV/amu, and 72 MeV-cm^2/mg for Ho at 15 MeV/amu. Note that the LET in the legend for Xe (angle) was calculated from the cosine law which does not apply to FGs [11]. The true effective (to compensate for an angular dependence) LET is expected to be only slightly greater than 41. Also, these LETs are incident LETs, which should be adequate for all of the long-range ions. The exceptional case is Br at 3.5 MeV/amu. Tests were performed in air [3] and the ions must also pass through some device material before reaching an FG, so the LET of Br at the FG location will be different than the incident LET. However, even a considerable reduction of energy will cause the LET to change only slightly, making it somewhere between the incident value of 43.7 MeV-cm^2/mg and the Bragg peak value of 44.7 MeV-cm^2/mg.

The first observation from Fig. 1 is that the Ho data, the Br data, the Xe (angle) data, and the Xe (normal incident) data each produce a straight line with unit slope. It will be seen later that these straight lines might not persist indefinitely with increasing fluence, but they clearly apply to the tested fluences. Therefore, over the range of fluences represented by the test data,

we can define CLE cross sections for each of these ions. Dividing counts by fluence and dividing by the number of bits in the device (about 2.21 Gbits) to convert to a per-bit cross section produces Table I. Note that the largest event cross section in Table I is comparable to (perhaps a little larger than to account for track radius) the physical area of the FG (about 0.1μm × 0.1 μm), indicating that a count is produced by a single, strong interaction.

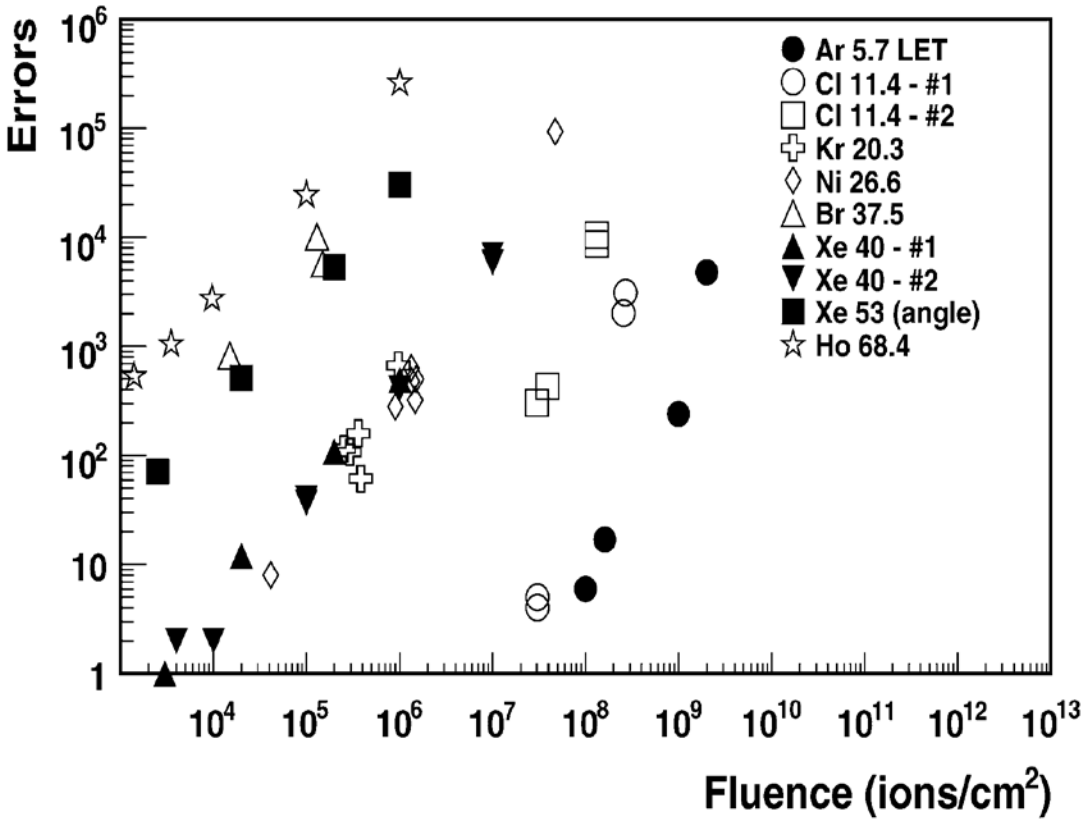

Fig. 1: Counts versus fluence, for each of several LETs, taken from [3]. The LETs in the figure legend were recalculated for SiO_2 and are Ar 5.7, Kr 20, Xe 41, Br 43.7, and Ho 72. Note that the LET in the legend for Xe (angle) was calculated from the cosine law which does not apply to FGs. The true effective LET is expected to be slightly greater than 41.

TABLE I: CROSS SECTIONS AND LETS FOR THE SEU-LIKE DATA IN FIG. 1

Ion	Ho	Br	Xe (angle)	Xe (normal incidence)
L_T (MeV-cm^2/mg)	72	Between 43.7 and 44.7	Effective is slightly greater than 41	41
σ_{CLE} (cm^2 per bit)	1.3×10^{-10}	2.3×10^{-11}	1.2×10^{-11}	2.0×10^{-13}

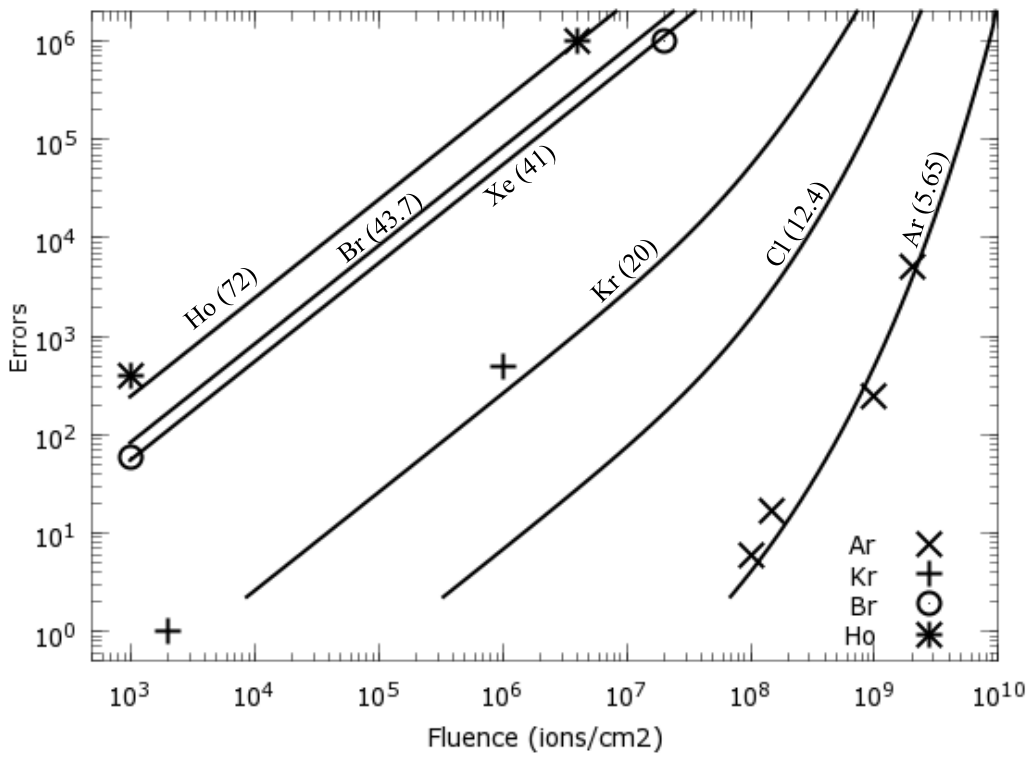

Fig. 2: The curves are fits and the parenthesis in the curve labels are the LETs in SiO_2. The points in this figure are the ones used to determine the fitting parameters. The Ar points are reproductions of data points in Fig. 1. The other points are not, but were selected so that a good fit to these points will also be a good fit to the data points in Fig. 1 for the indicated ion.

TABLE II: FITTING PARAMETERS USED TO CONSTRUCT FIG. 2

b_1 (MeV-cm^2/mg)	b_2 (MeV-cm^2/mg)	$\sigma_{S,sat}$ (cm^2)	$\sigma_{W,sat}$ (cm^2)	k
49.0	3811	1.10×10^{-10}	7.21×10^{-9}	7.643

Fig. 2 is a fit to the Fig. 1 data and the objective of the remainder of this section is to explain how Fig. 2 was constructed and then discuss its implications. The first step is to select the cumulative distribution function that will be used to represent FG-to-FG (a.k.a., bit-to-bit) variations of the critical charge loss. Several choices were tried with the data in Fig. 1. The first one that was tried is a normal distribution. Unfortunately, any choice for the standard deviation that was able to fit the Ar data would predict an unrealistically large number of FGs that were already deprogrammed prior to any irradiation (i.e., had insufficient initial charges). The next set of distributions that were tried were student-t distributions with various numbers of degrees of freedom. Unfortunately, these all produced the same problem as the normal distribution. Specifically, any combination of standard deviation and number of degrees of freedom that was able to fit the Ar data would predict an unrealistically large number of FGs that had insufficient initial charges. This problem can be avoided by using the beta distribution because a characteristic of this distribution is that the random variable is confined to a finite interval. This

confinement is physically reasonable for the critical charge loss if there is no physical mechanism for charging with a reverse polarity, and there is an upper bound to the charging voltage. However, it was discovered that, at least for the data in Fig. 1, the best fit obtainable from the beta distribution is indistinguishable from the best fit obtainable from the Weibull distribution, even though the Weibull distribution has fewer adjustable parameters (here we are counting independent parameters that remain after redundant parameters are combined with a_1 and a_2). The Weibull distribution will be used here so that $\mathcal{F}$ is given by

$$\mathcal{F}(x) = \begin{cases} 1 - \exp\left[-(x/\lambda)^k \right] & \text{if } x \geq 0 \\ 0 \quad \text{if } x < 0 \end{cases}, \tag{47}$$

where k is the shape parameter and λ is the scale parameter. This gives

$$1 - \mathcal{F}\left(\left(\frac{m}{a_1} + \frac{n}{a_2} \right) L_T \right) = \exp\left[-\left(m \frac{L_T}{b_1} + n \frac{L_T}{b_2} \right)^k \right], \tag{48}$$

where b_1 and b_2 are defined by

$$b_1 \equiv a_1 \lambda, \quad b_2 \equiv a_2 \lambda . \tag{49}$$

Substituting (48) into (39b) gives

$$P(\text{CLE}) = 1 - \exp\left[-H \sigma_{sat} \right] \sum_{m,n=0}^{\infty} \frac{\left[H \sigma_{S,sat} \right]^m \left[H \sigma_{W,sat} \right]^n}{m! n!} \exp\left[-\left(m \frac{L_T}{b_1} + n \frac{L_T}{b_2} \right)^k \right] . \tag{50}$$

The final fitting parameters are b_1, b_2, $\sigma_{S,sat}$, $\sigma_{W,sat}$, and k. The physical interpretation of the b-parameters can be understood if we recall that the a-parameters were defined in such a way so that the ion LET divided by a_1 is the charge loss from one strong interaction. Using this fact together with (49) we conclude that the LET divided by b_1 is this charge loss divided by λ. But λ is a characteristic value of the critical-charge loss,[6] i.e., the charge loss needed to produce a CLE. Therefore a small value of b_1 implies that a small LET is enough to make the charge loss exceed the critical-charge loss via a strong interaction. In other words, b_1 is a measure of the sensitivity of the FGs to CLEs via strong interactions, with a smaller value of b_1 implying greater sensitivity. The parameter b_2 has the same interpretation for weak interactions that b_1 has for strong interactions.

Note that the scale parameter λ is not required to be known if b_1 and b_2 replace a_1 and a_2 as fitting parameters but there is a penalty for λ being unknown. The penalty is that if the b-parameters are evaluated by fitting test data produced by a laboratory radiation environment,

[6] If there were no FG-to-FG variations (which is the large-k limit in (47) and produces a step function) λ would be the critical-charge loss. With FG-to-FG variations in the critical-charge loss, λ is the value of the critical-charge loss that is exceeded by only about 37% (which is 1/e converted to percent) of the FG population.

these same parameters can be used to predict the CLE probability in a different (application) radiation environment only if the statistical distribution of critical-charge losses is the same in both environments. In other words, biasing conditions and the amount of charge loss that defines a CLE must be the same in the laboratory as in the application. To make these statements intuitively clear, consider the special case in which all FGs have the same critical-charge loss Δq_C. For this special case, we would have $b_1 = a_1 \Delta q_C$ and $b_2 = a_2 \Delta q_C$. If b_1 (for example) is determined via fits to data under laboratory conditions without any knowledge of Δq_C, then a_1 and Δq_C are individually undermined, it is only the product $a_1 \Delta q_C$ that has been determined. This same product can be assumed when making predictions for an application only if biasing conditions and the definition of a CLE are such that Δq_C is the same under application conditions as it was under laboratory conditions.

We now revisit the data in more detail. Note that the LET of the Xe ions is very different than the LET of the Kr ions (41 for Xe in SiO_2 compared to 20 MeV-cm^2/mg for Kr), but the Xe (normal incident) data in Fig. 1 is essentially the same as the Kr data. The model cannot account for this because it assumes that LET is an adequate description of an ion. Furthermore, the Br LET (43.7 MeV-cm^2/mg in SiO_2) is nearly the same as the Xe LET so the model cannot account for the wide separation between the Xe (normal incident) data and the Br data in Fig. 1. We will, therefore, not attempt to fit the Xe (normal incident) data. The data used to estimate the fitting parameters are from Ho, Br, Kr, and Ar. Using the method in Appendix C for this data set produces the fitting parameters in Table II. With these parameters evaluated, the model can then make predictions for all ions, including those not used to determine the fitting parameters (such as Xe and Cl), and the results are shown in Fig. 2. Note that the model gives a conservative representation of the Xe (normal incident) data, but a fairly good representation of the other ions.

A noticeable characteristic of the curves in Fig. 2 is that those curves that do not resemble straight lines are concave upward. This is also seen in the Ar data points in Fig. 1. There are at least two tendencies for this behavior. The first requires bit-to-bit variations, but does not require weak interactions. For illustration, consider an LET such that some bits can be upset by two (for example) strong interactions, but most require three. At small fluences, only the first population of bits significantly contributes to the counts. However, as the fluence increases so that the probability of three hits increases, the main contribution is now from the second population. A straight-line extrapolation of the small-fluence behavior would properly describe the first population. However, the actual number of counts reflects an increasing contributing bit population and, therefore, increases faster with increasing fluence than this straight-line extrapolation. A second tendency requires weak interactions, but does not require bit-to-bit variations. For illustration, consider an LET such that a CLE requires three (for example) strong interactions when there is no contribution from the weak interactions. At small fluences, there is little help from the weak interactions so the probability of a CLE is the probability of three or more strong interactions. However, as the fluence increases the number of weak interactions increases and reaches a point (at some sufficiently large number) at which only two strong interactions must be added to the weak interactions to produce a CLE. A straight-line extrapolation of the small-fluence behavior would properly describe the case in which there are no weak interactions. However, the actual number of counts reflects the fact that, at some sufficiently large fluence, the weak interactions reduces the number of strong interactions required for a CLE, so the actual number of counts increases faster with increasing fluence than this straight-line extrapolation.

XI. Including a Dose Contribution

A radiation environment containing a mixture of LETs requires some complex calculations and this will be mentioned again in the next section. In particular, a radiation environment that is a sum, or superposition, of two environments cannot be treated by analyzing the two environments independently. However, there is a special case in which adding one radiation environment to another does not add significant complexity to the calculation of P(CLE). This occurs when the environment to be added is dose-like. This means that the fluence is large enough so that the number of hits to an FG is large enough to become deterministic, i.e., it can be approximated by the statistical average and can be described in terms of TID. Here we consider the case in which the radiation environment is a TID contribution added to a heavy-ion contribution. Bagatin *et al*. [10], pointed out that the effective FG charge loss, measured by an FET threshold voltage shift, produced by an ion hit added to TID exposure is less than the sum of charge loss from the ion hit alone (no TID) plus charge loss from TID alone (no ion hit) [10]. The explanation was in terms of the lowering of the electric field in the cells exposed to TID, due to charge loss, which translates into a smaller charge loss from the heavy-ion strike [10]. An approximation that ignores this effect is in the category of a small perturbation approximation discussed in Section II. Such approximations have been used throughout the development of the model. Fortunately, a model that is intended only to be a data fitting tool is not required to precisely agree with all aspects of reality because fitting parameters that produce fits to data are fitting parameters that partially compensate for errors in the physical assumptions. The simple model used here will have to rely on this partial compensation for errors because it does not explicitly account for the above effect.

The number of strong interactions produced by a pure dose-like spectrum is the cross section $\sigma_{S,sat}$ for a strong interaction multiplied by the fluence. Recall from Section VI that a_1 is defined by the condition that the charge loss from one strong interaction from an LET L is L/a_1. Similar considerations apply to weak interactions so the charge loss from a mixed dose-like environment, denoted Δq_D, is given by

$$\Delta q_D = \int_0^\infty \frac{L}{a_1} \sigma_{S,sat}\, h_D(L)\, dL + \int_0^\infty \frac{L}{a_2} \sigma_{W,sat}\, h_D(L)\, dL ,$$

where h_D is the differential in LET fluence for the dose-like environment. The ionizing dose D from the dose-like environment is defined by

$$\mu D = \int_0^\infty L\, h_D(L)\, dL , \tag{51a}$$

where μ is a unit conversion factor given by

$$\mu = \frac{6.25 \times 10^7 \text{ MeV}}{\text{krad - mg}} , \tag{51b}$$

where a krad, like LET, is measured in SiO_2. The charge loss now becomes

$$\Delta q_D = \left(\frac{\sigma_{S,sat}}{a_1} + \frac{\sigma_{W,sat}}{a_2} \right) \mu D \,. \tag{52}$$

A. The General Addition Formula

The simplification provided by the dose-like property of an environmental contribution becomes clear after deriving a more general addition formula. Suppose a radiation environment is represented by a differential fluence $h_{add}(L)$ added to another differential fluence $h(L)$ so the total differential fluence $h_T(L)$ is given by $h_T(L) = h(L) + h_{add}(L)$. Let $P(\Delta Q_T > \Delta q)$ be the probability that the charge loss will exceed Δq when the radiation environment is h_T, $P(\Delta Q > \Delta q)$ is this probability when the environment is h, and $P(\Delta Q_{add} > \Delta q)$ is this probability when the environment is h_{add}. The first probability can be expressed as

$$P(\Delta Q_T > \Delta q) = \int_0^\infty P(\Delta Q_T > \Delta q \mid \Delta Q = \xi) \left[-\frac{d}{d\xi} P(\Delta Q > \xi) \right] d\xi \,,$$

where the square bracket is the probability density for the charge loss from the environment h to be ξ, and the conditional probability $P(\Delta Q_T > \Delta q \mid \Delta Q = \xi)$ is the probability that the charge loss from the environment h_T will exceed Δq given that the charge loss from the environment h is ξ. Given this condition, the charge loss from the environment h_T will exceed Δq if and only if the charge loss from the environment h_{add} exceeds $\Delta q - \xi$ so

$$P(\Delta Q_T > \Delta q \mid \Delta Q = \xi) = P(\Delta Q_{add} > \Delta q - \xi)$$

and the equation for $P(\Delta Q_T > \Delta q)$ becomes

$$P(\Delta Q_T > \Delta q) = \int_0^\infty P(\Delta Q_{add} > \Delta q - \xi) \left[-\frac{d}{d\xi} P(\Delta Q > \xi) \right] d\xi \,. \tag{53}$$

B. The Addition Formula when a Contribution is Dose-Like

A simplification occurs when the added environment h_{add} is the dose-like environment h_D. The added charge loss is deterministic so

$$P(\Delta Q_D > \Delta q) = \begin{cases} 1 & \text{if } \Delta q < \Delta q_D \\ 0 & \text{if } \Delta q > \Delta q_D \end{cases}$$

and combining this with (53) when ΔQ_{add} is ΔQ_D gives

$$P(\Delta Q_T > \Delta q) = \begin{cases} 1 & \text{if } \Delta q < \Delta q_D \\ P(\Delta Q > \Delta q - \Delta q_D) & \text{if } \Delta q > \Delta q_D \end{cases} . \tag{54}$$

Using (23) to rewrite the right side gives

$$P(\Delta Q_T > \Delta q) = \begin{cases} 1 \quad \text{if } \Delta q < \Delta q_D \\ \exp\left[-H(0)\,\sigma_{sat}\right] \sum_{n=1}^{\infty} \frac{1}{n!} G_n(\Delta q - \Delta q_D)\left[H(0)\,\sigma_{sat}\right]^n \quad \text{if } \Delta q > \Delta q_D \end{cases} . \quad (55)$$

Note that the *G*-functions in (55) are constructed from the fluence h, not h_T, via (15a) and (25). When the critical charge loss Δq_C is positive, the probability of a CLE given that the critical charge loss is Δq_C is $P(\Delta Q_T > \Delta q)$ evaluated at $\Delta q = \Delta q_C$. The lower expression in (55) is not used when Δq is negative (because it cannot exceed Δq_D) so it is not necessary to add a unit step function to the sum in the lower expression in (55) as was done in (26). The result is

$$P(\text{CLE} \mid \Delta Q_C = \xi) = \begin{cases} 1 \quad \text{if } \xi < \Delta q_D \\ \exp\left[-H(0)\,\sigma_{sat}\right] \sum_{n=1}^{\infty} \frac{1}{n!} G_n(\xi - \Delta q_D)\left[H(0)\,\sigma_{sat}\right]^n \quad \text{if } \xi > \Delta q_D \end{cases} , \quad (56)$$

so (35) gives

$$P(CLE) = \mathcal{F}(\Delta q_D) + \exp\left[-H(0)\,\sigma_{sat}\right] \sum_{n=1}^{\infty} \frac{1}{n!} \left[\int_{\Delta q_D}^{\infty} G_n(\xi - \Delta q_D)\,\rho(\xi)\,d\xi \right] \left[H(0)\,\sigma_{sat}\right]^n .$$

A change in the integration variable produces an equivalent result given by

$$P(CLE) = \mathcal{F}(\Delta q_D) + \exp\left[-H(0)\,\sigma_{sat}\right] \sum_{n=1}^{\infty} \frac{1}{n!} \left[\int_{0}^{\infty} G_n(\xi)\,\rho(\xi + \Delta q_D)\,d\xi \right] \left[H(0)\,\sigma_{sat}\right]^n , \quad (57)$$

where Δq_D is given by (52). Recall that the *G*-functions are constructed from the fluence h, so the addition of a dose-like environment does not change these functions.

C. Adding a Dose-Like Contribution to a Pure SEU-Like Spectrum

A particular application of (57) is the case in which a dose-like environment is added to a pure spectrum that produces an SEU-like response. This might be able to provide an alternate testing methodology as discussed later. Before discussing an alternate methodology we first explain why an alternate methodology might be desired. This explanation begins with a discussion of the original methodology which produced the data (Fig. 1) for the example in Section X. Recall that very large fluences (10^9/cm^2 or more) were used at the smallest LETs to produce some of the points in Fig. 1. These fluences are much larger than expected from a space radiation environment. For SEE testing, it is typical for test conditions to use fluences much larger than expected from a space environment in order to obtain data having enough statistical significance for reliable risk estimates, but a heavy-ion fluence of 10^9/cm^2 is extreme even from the point of view of standard SEE test procedures. It might be argued that a laboratory fluence should not be required to exceed an application fluence by more orders-of-magnitude than needed to obtain the statistical significance required for a risk estimate. But a counter-argument points out that if an application radiation environment is different than the laboratory environment, a device must be completely characterized in order to use test data to make

predictions for the application environment. For the case of prompt charge loss in FGs (at least for the example in Section X), a very large fluence at the smaller LETs is needed to completely characterize the device. A smaller fluence will either produce no counts or exhibit SEU-like behavior because the only FGs observed are those that require only one hit to produce a CLE. The FGs that require multiple hits to produce a CLE do not become observable in the test data until the fluence is large enough so that a statistically significant number of these FGs receive multiple hits. Though not observable at small fluences, information about these FGs is still needed in order to use laboratory data to predict device response in a different environment, hence the need for very large fluences at the smaller LETs when all testing is done with heavy ions. Appendix D gives a recommendation on how to select LETs and fluences for a complete characterization.

Motivated by a desire to use smaller heavy-ion fluences, small enough to produce SEU-like behavior, an alternate test method might be considered. This method exposes a set of devices to various levels of ionizing dose after programming but before (and without refreshes) performing heavy-ion tests. If the model is valid under these test conditions, it can be used to obtain at least a partial characterization of the device from such test data (as explained later). Unfortunately there is a very serious limitation regarding model applicability to this test method. The model is intended to describe FG charge loss but not TID effects in the sensing circuits.[7] Therefore the model applies only to qualified devices, which are devices having the property that there is some dose level large enough to produce an observable FG charge loss but still small enough to negligibly affect the sensing circuits. In other words, the FGs must be more susceptible to TID than the sensing circuits. Given that a qualified device (e.g., a test structure designed for this purpose) has been found, model validity would be tested by showing that the same model parameters used to fit a complete set of heavy-ion data (the type of data illustrated in Fig. 1 that includes fluences large enough to extend outside the SEU-like behavior) will also produce a fit to the data obtained from the alternate test method. Unfortunately, a qualified device that was tested by both methods has not yet been found in the literature. Data from the alternate test method are given in [10] for an example device but heavy-ion data at fluences large enough to extend beyond the SEU-like behavior are not given. Therefore no example comparisons with data can be given here. Determining which, if any, commercial devices (e.g., flash memories) are qualified devices is a topic for future work, and determining whether model predictions are correct for these devices is also a topic for future work. What is given below is the model prediction that is to be compared to data in future work.

To derive the model prediction of how TID should be expected to influence SEU-like (i.e., small-fluence) heavy-ion test data, it is necessary to add a dose-like environment to a pure spectrum in the model. Recall that the *G*-functions in (57) are constructed from the fluence that is added to the dose contribution, with the former fluence being a pure spectrum in this analysis. The *G*-functions for a pure spectrum were calculated in Appendix B with the result (in Appendix B notation) given by (B9b). This gives

[7] The meaning of a sensing circuit for a NAND flash memory is as follows. A read operation copies a page of data from the memory into a page buffer. Individual bit states are read by assessing the page buffer. The sensing circuit includes all circuit elements that participate in this operation. In addition, the threshold voltage of an FET within the memory is compared to a reference voltage. The sensing circuit also includes the comparator and the circuit that produces this reference voltage.

$$\frac{1}{n!}\left[\int_0^\infty G_n(\xi)\,\rho(\xi+\Delta q_D)\,d\xi\right]\left[H(0)\,\sigma_{sat}\right]^n =$$
$$\sum_{m=0}^{n}\frac{H^n}{m!(n-m)!}(\sigma_{S,sat})^m(\sigma_{W,sat})^{n-m}\left[\mathcal{F}\left(\frac{m}{a_1}L_T+\frac{n\text{-}m}{a_2}L_T+\Delta q_D\right)-\mathcal{F}\left(\Delta q_D\right)\right],$$

where the H on the right side is the heavy-ion test fluence. Combining this with (57) gives

$$P(\text{CLE}) = \mathcal{F}(\Delta q_D) +$$
$$\exp\left[-H\,\sigma_{sat}\right]\sum_{n=1}^{\infty}\sum_{m=0}^{n}\frac{H^n}{m!(n-m)!}(\sigma_{S,sat})^m(\sigma_{W,sat})^{n-m}\left[\mathcal{F}\left(\frac{m}{a_1}L_T+\frac{n\text{-}m}{a_2}L_T+\Delta q_D\right)-\mathcal{F}\left(\Delta q_D\right)\right].$$

The same arguments that converted (39a) into (42) applied to the above equation gives

$$P(\text{CLE}) = \mathcal{F}(\Delta q_D) + H\,\sigma_{S,sat}\left[\mathcal{F}\left(\frac{L_T}{a_1}+\Delta q_D\right)-\mathcal{F}\left(\Delta q_D\right)\right],$$

which can also be written as

$$P(\text{CLE}) = \left(1-H\,\sigma_{S,sat}\right)\mathcal{F}(\Delta q_D) + H\,\sigma_{S,sat}\,\mathcal{F}\left(\frac{L_T}{a_1}+\Delta q_D\right)\quad(\text{SEU - like plus dose}). \tag{58}$$

The terms in (58) have physical interpretations. The expected number of strong interactions in a randomly selected FG from the heavy-ion testing is $H\sigma_{S,sat}$. The quantity $\mathcal{F}(\Delta q_D)$ is the probability that an FG had already produced a CLE, i.e., already failed, from the dose exposure prior to the heavy-ion testing. This quantity is multiplied by $1 - H\sigma_{S,sat}$, instead of 1, in the first term on the right side of (58) so that the first term will include only that subset of already-failed FGs that received no strong interactions during the heavy-ion test. In other words, the first term does not include any FGs that did receive a strong interaction during the heavy-ion test. This is appropriate because all such FGs are included in the second term on the right side of (58). However, a simple approximation can be used. A fluence small enough to produce SEU-like behavior is small enough for the number of FGs that received multiple strong interactions to be negligible compared to the number that received a single strong interaction. This implies that the test fluence is small enough so that the expected number of strong interactions in a randomly selected FG is much less than 1, i.e., $H\sigma_{S,sat} << 1$. The approximation for (58) becomes

$$P(\text{CLE}) \approx \mathcal{F}(\Delta q_D) + H\,\sigma_{S,sat}\,\mathcal{F}\left(\frac{L_T}{a_1}+\Delta q_D\right)\quad(\text{SEU - like plus dose}). \tag{59}$$

The cross section for a charge-loss event, denoted σ_{CLE}, is defined here to be number of additional CLEs (where additional means those above the pure dose contribution, i.e., produced

during the heavy-ion testing) divided by the additional test fluence H (again, additional means the fluence applied after the dose exposure, i.e., applied during the heavy-ion testing). This is $P(CLE) - F(\Delta q_D)$ divided by the test fluence so (59) gives

$$\sigma_{CLE} = \sigma_{S,sat} F\left(\frac{L_T}{a_1} + \Delta q_D\right) \quad \text{(SEU - like plus dose)}.$$

Note that Δq_D is calculated from (52) so the above equation can also be written as

$$\sigma_{CLE} = \sigma_{S,sat} F\left(\frac{L_T}{a_1} + \left(\frac{\sigma_{S,sat}}{a_1} + \frac{\sigma_{W,sat}}{a_2}\right)\mu D\right) \quad \text{(SEU - like plus dose)}.$$

Specializing to the case in which F is the Weibull function in (47), and defining the b-parameters by (49), the above equation now becomes

$$\sigma_{CLE} = \sigma_{S,sat}\left\{1 - \exp\left[-\left(\frac{L_T}{b_1} + \left(\frac{\sigma_{S,sat}}{b_1} + \frac{\sigma_{W,sat}}{b_2}\right)\mu D\right)^k\right]\right\} \quad \text{(SEU - like plus dose)}. \quad (60)$$

Note that the two fitting parameters b_2 and $\sigma_{W,sat}$ appear only in a specific combination, which allows us to reduce the number of fitting parameters. One way to do this is to define ω by

$$\omega \equiv \left(\sigma_{S,sat} + \frac{b_1}{b_2}\sigma_{W,sat}\right)\mu, \quad (61)$$

so that (60) can be written as

$$\sigma_{CLE} = \sigma_{S,sat}\left\{1 - \exp\left[-\left(\frac{L_T + \omega D}{b_1}\right)^k\right]\right\} \quad \text{(SEU - like plus dose)}. \quad (62)$$

The fact that (62) contains only four fitting parameters (which are b_1, ω, $\sigma_{S,sat}$, and k) means that no amount of test data in which (62) applies will be enough to uniquely determine all five of the original fitting parameters (which are b_1, b_2, $\sigma_{S,sat}$, $\sigma_{W,sat}$ and k). However, evaluation of the four fitting parameters contained in (62) via fits to data for which the model applies (recall that model applicability requires the device to be a qualified device) is at least a partial characterization of the device. If the application environment is also an SEU-like (small heavy-ion fluence) contribution added to a dose-like contribution, this partial characterization should be sufficient for risk estimates in the application environment.

For a specific example, consider the example device discussed in Section X. Using the Table II parameters together with (51b) and (61) give $\omega = 0.0127$ MeV-cm^2/mg-krad. Using this with other Table II parameters in (62) produces Fig. 3. It was pointed out in [3] that this example device has a fairly low TID tolerance and cannot be expected to survive at doses greater than

about 40 krads. According to Fig. 3, even 100 krads will have such a small effect that it is unlikely to be discernable from experimental scatter. Therefore, even without data to compare to the model predictions in Fig. 3, we can conclude that the model cannot be used for this application for this example device. Also, although somewhat speculative without data to compare to the curves in Fig. 3, we can predict that if an application environment has a low enough TID level for this example device to be usable in that environment, then TID will also not be a significant contribution to FG charge loss for this example device.

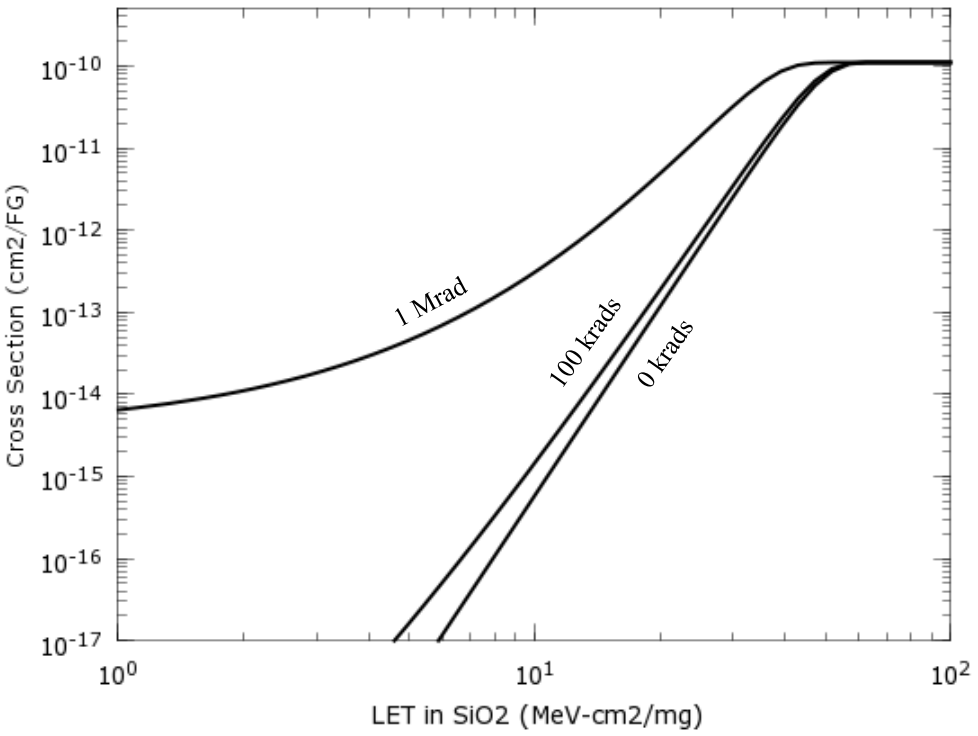

Fig. 3: Model prediction via (62) with Table II parameters.

XII. CLE Probabilities in Space Environments

We now consider a space environment. Such environments are typically better approximated as being isotropic instead of unidirectional, so directional effects requires some discussion. The direction of an ion trajectory relative to the normal to the device plane is important for some kinds of single-event effects involving charge collection at some device node from an ion track (such as SEU in an SRAM) and test data for such cases are typically presented in the cosine-law format. In this format, fluence is measured in the device plane instead of a plane perpendicular to the ion beam (the former fluence is equal to the latter multiplied by the cosine of the incident angle) and the ion LET is reported as an effective LET (which is the actual LET divided by the cosine of the incident angle). The cosine law applies when data points from different incident angles belong to a common cross section (counts divided by fluence) versus LET curve when this plotting format is used. Even for the older device technologies in which feature sizes are large enough for an ion track to be regarded as infinitely thin, the cosine law is still an approximation that breaks down when the incident angle approaches 90 degrees. When a device is so highly scaled so that the geometric dimensions of device structures are comparable to the track diameter, the cosine law fails completely and device susceptibility becomes more isotropic. An isotropic approximation might be more accurate for some track diameters than others, but the assumption used here is that FGs susceptible to charge loss events are physically small enough for susceptibility to be approximately isotropic, i.e., approximately independent of the direction of the ion trajectory. This assumption is consistent with the experimental data presented by Cellere *et al*. [11] showing that an individual cell response does not depend on incident angle. Investigators that want to test this assumption for a particular device of interest should note that the cosine law plotting format is not useful if the goal is to determine whether device susceptibility is approximately isotropic. To make that determination by comparing data taken at different incident angles, fluence should be measured in a plane perpendicular to the beam and LET should be the actual ion LET. It was pointed out in [11] that directional effects do become important if the concern is whether a single ion hit can produce a CLE in multiple FGs because a grazing angle hit can do that. However, it is assumed here that the only concern is the expected number of CLEs in an array of FGs and that a CLE in each of two (for example) FGs produces a count of 2 even if they were both produced by the same ion hit. When using this counting convention, the expected number of counts in an array of FGs is the sum of the expected numbers for each FG in the array (as opposed to counting the ion hits that produced one or more CLEs) so each FG can be considered independently and all directional effects can be ignored. Other motives for using the above counting convention, in the context of SEU, are discussed in [12] and in Appendix B.

A significant complication to address is that space environments contain mixtures of different LETs. The numerical work needed to calculate the probability of a CLE is much more cumbersome for a mixed environment than it was for the pure-spectrum case that was used to fit data in Section X (the routine for a pure spectrum, called `PCLE_PUR.m`, is in the first textbox in Appendix C). In particular, we cannot simply calculate expected numbers of CLEs separately for different environmental components and then add these expected numbers to obtain the expected number for an environment consisting of the sum of these components. We can do this for the extreme case of SEU-like behavior, but in the opposite extreme of dose-like behavior it is the argument to $\mathcal{F}$ on the right side of (45), rather than the N_{CLE} on the left side, that is summed over environmental components. Worse yet, a more general case is somewhere between SEU-like and dose-like so neither simplification applies. To make the situation still worse, a space radiation

environment will be represented by a flux or fluence versus LET table, instead of an analytical function, so all integrals containing fluence must be evaluated numerically. It is therefore not surprising that the required numerical work is much more cumbersome for a mixed environment than for a pure spectrum. A number of approximations designed to streamline the number crunching are used to reduce the numerical work for the mixed environment. Details are in Appendix E, which also includes a numerical routine. Even with these approximations, the routine does not run fast enough to be useful for trail-and-error curve fitting, so the routine in Appendix C is still needed for that, but the routine in Appendix E can be applied to mixed environments while the routine in Appendix C cannot. All of the approximations used for the mixed environment are in the conservative direction, meaning that the error associated with each approximation tends to make the calculated value of P(CLE) larger than would be obtained from an exact calculation. These errors can be made as small as desired by using suitable choices for grid points and the number of terms to include in a sum (details are in Appendix E), but the penalty is a longer computer run time. This will be discussed again later when some specific examples are considered.

The objective of this section is to explain how to use the code in Appendix E, called `PCLE_in_space.m`, and how to construct input files. This code runs in the Octave (a GNU package) platform. The Weibull function is used to represent FG-to-FG variations so the fitting parameters used to fit test data are the ones discussed in Section X and are b_1, b_2, $\sigma_{S,sat}$, $\sigma_{W,sat}$, and k. It is assumed here that these parameters have already been evaluated via fits to test data using the method in Appendix C as illustrated by the example in Section X. The inputs needed by the routine in Appendix E consist of these parameters plus data (including two input files) describing the environment. The output of the routine is the probability, P(CLE), that a randomly selected FG will exhibit a CLE during the fluence exposure defined by the environmental inputs, given that the FG was refreshed (all prior charge loss, if any, has been restored) before the start of the fluence exposure. Therefore, the relevant fluence is the fluence accumulated since the latest refresh. The expected number of CLEs in a collection of FGs, e.g., a flash memory, is this probability multiplied by the number of FGs in the collection. Recall the counting convention that is used here to define expected numbers. Multiple FGs exhibiting a CLE are counted as multiple events regardless of whether they were all produced by the same ion hit or each was produced by a different ion hit.

One of the input files is a two-column table of galactic cosmic ray (GCR) integral flux versus LET. Integral flux means that the flux includes all particles having an LET that exceeds a specified value. This flux table is most likely to be obtained from CREME96 [13]. The units are required to be those used by CREME96. Specifically, LET (first column) is in the units of MeV-cm^2/g and flux (second column) is in the units of 1/m^2-s-sr. Spacecraft shielding and planetary magnetic shielding (if any) are built into the input file. The GCR environment is regarded as constant in time, so flux is converted into fluence by simply multiplying by the number of days of exposure. This number is input via a prompt. The example GCR file, called `GCR_flux.dat`, included in Appendix E represents the GCR environment in interplanetary space (no magnetic shielding) with 100 mils of aluminum shielding. It represents the solar minimum time period (worst case for GCR) because this representation is typically used as an alternative to predicting future levels of solar modulation. Any changes in planetary magnetic shielding and/or spacecraft shielding must be made by using CREME96 to create a replacement for this data file.

The second input file is in the same format as the first, but represents a solar particle event. The CREME96 "worst-week flare" is used because there is a simple conversion from flux to fluence. The fluence is the flux multiplied by 7.5 days and this conversion is built into the code. Other solar particle fluences are treated by expressing them as a multiple or a fraction of the fluence from one CREME96 model flare. This number, identified as a "number of flares," is entered via a prompt. The example file, called `flare_flux.dat`, included in Appendix E represents the model flare in interplanetary space (no magnetic shielding) with 100 mils of aluminum shielding. Any changes in planetary magnetic shielding and/or spacecraft shielding must be made by using CREME96 to create a replacement for this data file.

Protons and/or electrons trapped in a planetary radiation belt (if relevant) are included in "additional dose" that is entered via a prompt. This includes all radiation that is not already included in the GCR or flare files with the assumption that these particles can be treated as dose-like. GCR protons are unlikely to be a concern but flare protons are a concern. We have the option of including them either in the flare input file or at the prompt for additional dose (but not both because this will count the same particles twice). An advantage of the first choice is that these protons will be treated stochastically, whether necessary or not, so we do not have to guess as to whether it is appropriate to treat them as dose-like. In contrast, including them as additional dose instructs the code to treat them as dose-like. One advantage of the latter choice is that the code runs faster because fewer terms are included in a finite sum used to approximate an infinite series. Another advantage is that environmental data provided to flight projects typically include solar-event protons, added to all other significant contributions to dose, in the dose estimates. Such data can be used if protons are not included in the flare data file. The example files, `GCR_flux.dat` and `flare_flux.dat` in Appendix E, do not include protons. It is therefore necessary to include additional dose at the prompt in order to represent solar protons even if all other contributions to ionizing dose can be ignored.

There is a final consideration regarding whether to treat particles as dose-like or including them in an input file. We will have a choice for realistic examples of proton or heavy-ion environments (electrons will be treated as dose-like), but not for academic examples in which the expected number of particle hits to an FG (which is $H(0)\sigma_{sat}$ in the equations or `c1` in the Appendix E code) is several hundred or more. Such a large fluence input via a data file will either produce an unacceptably long run time, or cause the code to crash with an Octave-generated error message stating that a convergence condition was not satisfied. The solution to this problem, if the problem is encountered, is to remove the most abundant particles from the data file and include them in the dose-like calculation. Fortunately, the same examples that require a dose-like calculation, because of large numbers of hits, are the examples for which a dose-like calculation is most accurate.

We now consider two test cases to verify that the code, `PCLE_in_space.m` in Appendix E, is working properly on the user's computer, and to get an idea of what to expect from the code. Both test cases consider a pure spectrum so that results from this code can be compared to the more accurate results obtained from the code `PCLE_PUR.m` in Appendix C. The latter code is more accurate when it applies (i.e., when the environment is a pure spectrum) because simplifications implied by a pure spectrum make conservative approximations unnecessary. Also note that the two codes are executed differently in the Octave command window because the latter is a function file. To run `PCLE_PUR.m` we first assign values (e.g., values used in the specific examples given below) in the Octave command window to `b1`, `b2`, `s1` (abbreviated notation for $\sigma_{S,sat}$), `s2` (abbreviated notation for $\sigma_{W,sat}$), `k`, `L` (abbreviated

notation for L_T), and the fluence `H` and then enter in the Octave command window the command `PCLE_PUR(b1,b2,s1,s2,k,L,H)`. In contrast, `PCLE_in_space.m` is a routine that accepts inputs from prompts and from at least one of two input files, as illustrated by the examples.

To make the first example more specific, suppose the FG parameters are those in Table II and the ion LET is 12.4 MeV-cm^2/mg, which produced the Cl curve in Fig. 2. Consider, for example, the point on the curve produced by a fluence `H` equal to 10^6/cm^2. Using these inputs with `PCLE_PUR` produces the estimate P(CLE) = 3.0567×10^{-9}. In order to give the same input information to `PCLE_in_space.m`, we have to compensate for unit conversions. This is done by constructing the `GCR_flux.dat` file to contain two lines which are

```
1.010E+002,  9.21E+003
1.240E+004,  9.21E+003
```

The code interprets these lines to mean that all particles have an LET greater than or equal to 101 MeV-cm^2/g (or 0.101MeV-cm^2/mg) because this LET is the first entry and the first entry is interpreted by the code to include all particles of interest. The code also interprets these lines to mean that the environment contains no particles with an LET greater than 1.24×10^4 MeV-cm^2/g (or 12.4 MeV-cm^2/mg) because this LET is the last entry and the code interprets the last entry to be the largest LET in the environment. For this example, the integral flux is the same on both lines, which is interpreted by the code to mean that there are no particles with LET between the listed values. Therefore, for this example, the interpretation of the code is that all particles have an LET equal to the largest listed value which is 12.4 MeV-cm^2/mg. Note that the smaller listed LET could be changed to some other number, as long as it is less than the larger listed LET, without affecting this interpretation. However, this change would affect grid-point construction done by the code and could change some calculated numbers so the discussions below assume the specific numbers listed above. The integral flux in the second column is the selected fluence (10^6/cm^2 for this example) divided by 108.6 to compensate for unit conversions when entering 1 at the prompt asking for the number of days of the GCR environment. The complete input to `PCLE_in_space.m` for this example consists of the above two lines in the file `GCR_flux.dat`, any valid entry in the file `flare_flux.dat` (which is not used for this example, but some file, such as the example in Appendix E, is needed so the code will not crash while trying to read the file), and inputs to the prompts. The inputs to the prompts are the numbers in Table II together with 1-day of GCR, zero-flares, and zero additional dose. The output of the code should be `PCLE` (abbreviated notation for P(CLE)) = 3.9818×10^{-9}, which is close to, but greater than the more accurate estimate (from `PCLE_PUR`) of 3.0567×10^{-9}.

The next example is the same as the first except that the fluence is increased by two orders of magnitude. The only changes made from the first example are to use `H` = 10^8/cm^2 (instead of 10^6) before running `PCLE_PUR`, and then increasing the flux in the file `GCR_flux.dat` by two orders of magnitude so the two lines now become

```
1.010E+002,  9.21E+005
1.240E+004,  9.21E+005
```

The agreement between PCLE_PUR and PCLE_in_space is not as good for this example, with the former giving the more accurate estimate of $P(\text{CLE}) = 6.8746\times10^{-7}$, and the latter giving the more conservative estimate of 13.617×10^{-7}. There is a factor-of-2 disagreement. Nearly all of this error is in the PCLE_in_space code and could be improved by using a finer grid-point spacing and/or using interpolations instead of upper bounds (see Appendix E). But a finer grid-point spacing creates a longer run time (too long), and substituting interpolations for upper bounds invalidates the earlier claim that all approximations are conservative. Another option, the one used here, is to accept this error in order to have a code with an acceptable run time and that guarantees conservatism. Users that give accuracy a higher priority than the guarantee of conservatism can modify the code (Appendix E gives suggestions on this), but discussions given here refer to the code as it is presented here. To put this factor-of-2 disagreement in perspective, it should be noted that the example considered is a point on the Cl curve in Fig. 2 where the curve is steep enough for calculations to be very sensitive to small errors. An over estimate by a factor of 2 might seem more acceptable when viewed this way.

The previous examples considered laboratory environments. The next example considers a space-radiation environment. The code in Appendix E is the only one that can be used for this application, so predictions cannot be tested for accuracy by comparison to predictions from the code in Appendix C, but we can rely on the fact that any errors in the calculations will be in the conservative direction. For this example, a flash memory will be on a three-year mission in interplanetary space (no planetary magnetic protection, but also no radiation belt particles to encounter) without any refreshes during that time, so the relevant radiation environment consists of all radiation sources encountered during those three years. The time period has a possibility of encountering a solar-particle event and environmental experts have informed us that we should be prepared for something as severe as one occurrence of the CREME96 model flare at a 1 AU distance from the Sun. Using conservatism to compensate for the uncertainty of predicting future levels of solar modulation of the GCR environment, we assume the worst-case (solar minimum) conditions for the GCR environment even though we must be prepared for possible solar activity. The spacecraft has not yet been built, but the present plans do not include heavy mass shielding around the flash memory so we will base our estimate (subject to change when more information becomes available) on the default assumption of 100 mils of aluminum shielding provided by the spacecraft. The two input files, GCR_flux.dat and flare_flux.dat, in Appendix E apply to the stated conditions. Note that the LETs in these tables refer to Si when the LETs required for the calculations should refer to SiO_2. However, this error is insignificant compared to the error from the assumption that the encountered space environment will be equal to some model prediction, so the input files in Appendix E are good enough for this example.

Another concern is that these files do not include solar protons, so solar protons must be included in a dose-like calculation. We assume, for this example, that environmental experts have informed us to be prepared for a radiation dose (from three-years of possible solar activity) of 1 krad when the shielding is 100 mils of aluminum. Again, the difference between dose in Si and dose in SiO_2 is insignificant compared to the error from the assumption that the encountered space environment will be equal to some model prediction, so the material that the dose refers to is not important here. We will take the dose to be 1 krad. The inputs to PCLE_in_space for this example consist of the data files GCR_flux.dat and flare_flux.dat in Appendix E, the device parameters in Table II, 1095 days (three years) of GCR, 1 model flare, and an additional dose of 1 krad. The returned result should be $\text{PCLE} = 6.6775\times10^{-10}$. In other words, a flash memory with 2.21×10^{9} (for example) FGs characterized by the inputs assumed here can be

expected to experience a charge-loss event in 1 FG during the space operation. It is interesting to consider how this prediction would be changed by omitting the solar protons. The inputs are the same as above except that the additional dose is now zero. The returned result should be `PCLE` = 6.6542×10^{-10}, almost the same as the above result of 6.6775×10^{-10}, indicating that the solar protons were not important for this example. However, one example is not enough to reach general conclusions, so we should not interpret this observation to mean that solar protons can always be ignored when estimating the probability of a charge-loss event.

Appendix A: Several Properties of Convolutions

Let f be any sectionally continuous function satisfying

$$f(x) \geq 0 \quad \text{for all } x > 0, \qquad \int_0^\infty f(\xi)\, d\xi = 1 \tag{A1}$$

and let G be given by

$$G(x) \equiv \int_x^\infty f(\xi)\, d\xi \quad \text{for all } x \geq 0\,, \tag{A2}$$

so G is a decreasing function that satisfies

$$f(x) = -\frac{d}{d\,x} G(x) \quad \text{for all } x > 0 \tag{A3}$$

and

$$0 \leq G(x) \leq 1 \quad \text{for all } x \geq 0, \qquad G(0) = 1, \qquad \lim_{x \to \infty} G(x) = 0\,. \tag{A4}$$

Now let G_A be any decreasing continuous function that satisfies

$$0 \leq G_A(x) \leq 1 \quad \text{for all } x \geq 0, \qquad G_A(0) = 1 \tag{A5}$$

and let G_B be defined by the integral equation

$$G_B(x) = G(x) + \int_0^x f(\xi)\, G_A(x - \xi)\, d\xi\,. \tag{A6}$$

The goal is to derive properties of G_B implied by given properties of G_A.

For the first example, suppose it is given that, in addition to (A5), G_A also satisfies

$$\lim_{x \to \infty} G_A(x) = 0 \quad \text{(for the present example)}\,. \tag{A7}$$

The goal is to show that G_B also has this limit. To prove this assertion, select any $\varepsilon > 0$. Existence of the integral in (A1) implies that there exists an $x_1(\varepsilon)$ satisfying

$$0 \leq \int_{x_1(\varepsilon)}^\infty f(\xi)\, d\xi < \frac{1}{3}\varepsilon\,. \tag{A8}$$

Also, the limit in (A4) implies that there exists an $x_2(\varepsilon)$ satisfying

$$0 \leq G(x) < \frac{1}{3}\varepsilon \quad \text{for all } x > x_2(\varepsilon)\,. \tag{A9}$$

Similarly, when (A7) applies, there exists an $x_3(\varepsilon)$ satisfying

$$0 \le G_A(x) < \frac{1}{3}\varepsilon \quad \text{for all } x > x_3(\varepsilon) \quad \text{(for the present example)}. \tag{A10}$$

Now let $x_4(\varepsilon)$ be given by

$$x_4(\varepsilon) = \max\{x_2(\varepsilon), x_1(\varepsilon) + x_3(\varepsilon)\}$$

and select any number x that is greater than $x_4(\varepsilon)$. Since $x > x_2(\varepsilon)$ we have

$$0 \le G(x) < \frac{1}{3}\varepsilon .$$

Also, $x > x_1(\varepsilon)$ and G_A satisfies (A5), so

$$0 \le \int_{x_1(\varepsilon)}^{x} f(\xi) G_A(x-\xi)\, d\xi \le \int_{x_1(\varepsilon)}^{x} f(\xi)\, d\xi \le \int_{x_1(\varepsilon)}^{\infty} f(\xi)\, d\xi < \frac{1}{3}\varepsilon .$$

Also, $x > x_1(\varepsilon) + x_3(\varepsilon)$, so for any ξ between zero and $x_1(\varepsilon)$ we have $x - \xi > x_3(\varepsilon)$, so (A10) applies and gives

$$0 \le \int_{0}^{x_1(\varepsilon)} f(\xi) G_A(x-\xi)\, d\xi \le \frac{1}{3}\varepsilon \int_{0}^{x_1(\varepsilon)} f(\xi)\, d\xi \le \frac{1}{3}\varepsilon \int_{0}^{\infty} f(\xi)\, d\xi = \frac{1}{3}\varepsilon .$$

Adding the three inequalities above gives

$$0 \le G(x) + \int_{x_1(\varepsilon)}^{x} f(\xi) G_A(x-\xi)\, d\xi + \int_{0}^{x_1(\varepsilon)} f(\xi) G_A(x-\xi)\, d\xi < \frac{1}{3}\varepsilon + \frac{1}{3}\varepsilon + \frac{1}{3}\varepsilon$$

or

$$0 \le G(x) + \int_{0}^{x} f(\xi) G_A(x-\xi)\, d\xi < \varepsilon .$$

In other words, for any $\varepsilon > 0$ we can find an $x_4(\varepsilon)$ such that the right side of (A6) is between zero and ε for any x > $x_4(\varepsilon)$. This proves that

$$\text{if } \lim_{x\to\infty} G_A(x) = 0 \quad \text{then } \lim_{x\to\infty} G_B(x) = 0 . \tag{A11}$$

Using (A11) in a proof by mathematical induction verifies (16c) in the main text.

Appendix B: Derivation of (28)

To shorten the notation we write σ_1 instead of $\sigma_{S,sat}$, σ_2 instead of $\sigma_{W,sat}$, σ (which is $\sigma_1+\sigma_2$) instead of σ_{sat}, and H_0 instead of $H(0)$. The recurrence formula (14) can be written in this notation as

$$(H_0\sigma)^{n+1} G_{n+1}(x) = \int_0^\infty \left[H_0\sigma\, f(\xi)\right]\left[(H_0\sigma)^n G_n(x-\xi)\right] d\xi \quad \text{for } n = 1, 2, \ldots\ , \tag{B1}$$

while (25) becomes

$$H_0\sigma\, G_1(x) = H(a_1\, x)\sigma_1 + H(a_2\, x)\sigma_2 \tag{B2}$$

$$H_0\sigma\, f(x) = a_1\, h(a_1\, x)\sigma_1 + a_2\, h(a_2\, x)\sigma_2\,. \tag{B3}$$

It is easy to show from (27a)-(27h) that the C's and D's satisfy recurrence relations that can be written in the present notation as

$$\int_0^\infty \left[H_0\sigma\, f(\xi)\right] C_{m,n}(x-\xi)\, d\xi = \sigma_1\, C_{m+1,n}(x) + \sigma_2\, C_{m,n+1}(x) \quad \text{for } m = 0,1,\ldots \text{ and } n = 0,1,\ldots$$

$$\int_0^\infty \left[H_0\sigma\, f(\xi)\right] D_{m,n}(x-\xi)\, d\xi = \sigma_1\, D_{m+1,n}(x) + \sigma_2\, D_{m,n+1}(x) \quad \text{for } m = 0,1,\ldots \text{ and } n = 0,1,\ldots$$

A result that will be useful later is obtained by combining the above recurrence formulas with (27j)-(27L) to obtain

$$\int_0^\infty \left[H_0\sigma\, f(\xi)\right] E_{m,n-m}(x-\xi)\, d\xi =$$

$$\sigma_1\left[\frac{m}{n} C_{m,n-m}(x) + \frac{n-m}{n} D_{m+1,n-m-1}(x)\right] +$$

$$\sigma_2\left[\frac{m}{n} C_{m-1,n-m+1}(x) + \frac{n-m}{n} D_{m,n-m}(x)\right] \quad \text{for } n = 1,2,\ldots \text{ and } m = 0,1,..,n\,. \tag{B4}$$

Note that any C's or D's with a negative index in (B4) (e.g., the second term in the first square bracket on the right side when $m = n$) is multiplied by zero so it is not necessary to extend the definitions of the C's and D's to include negative indices. A recurrence formula can be derived for the sum that appears in the curly bracket below by using (B4) to obtain

$$\int_0^\infty \left[H_0\sigma\, f(\xi)\right]\left\{\sum_{m=0}^{n} \frac{n!}{m!(n-m)!} {\sigma_1}^m {\sigma_2}^{n-m} E_{m,n-m}(x-\xi)\right\} d\xi =$$

$$\sum_{m=0}^{n}\frac{n!}{m!(n-m)!}{\sigma_1}^{m+1}{\sigma_2}^{n-m}\left[\frac{m}{n}C_{m,n-m}(x)+\frac{n-m}{n}D_{m+1,n-m-1}(x)\right]+$$

$$\sum_{m=0}^{n}\frac{n!}{m!(n-m)!}{\sigma_1}^{m}{\sigma_2}^{n-m+1}\left[\frac{m}{n}C_{m-1,n-m+1}(x)+\frac{n-m}{n}D_{m,n-m}(x)\right] \quad \text{for } n=1,2,...$$

Changing the summation index in the first sum on the right, and separating the last term from the first sum and the first term from the second sum, and combining the sums that remain gives

$$\int_0^\infty [H_0\sigma f(\xi)]\left\{\sum_{m=0}^{n}\frac{n!}{m!(n-m)!}{\sigma_1}^{m}{\sigma_2}^{n-m}E_{m,n-m}(x-\xi)\right\}d\xi = {\sigma_1}^{n+1}C_{n,0}(x)+{\sigma_2}^{n+1}D_{0,n}(x)+$$
$$\sum_{m=1}^{n}\frac{n!}{m!(n-m+1)!}{\sigma_1}^{m}{\sigma_2}^{n-m+1}\left[m\,C_{m-1,n-m+1}(x)+(n-m+1)\,D_{m,n-m}(x)\right] \quad \text{for } n=1,2,...$$

We now use (27j)-(27L) to write this as

$$\int_0^\infty [H_0\sigma f(\xi)]\left\{\sum_{m=0}^{n}\frac{n!}{m!(n-m)!}{\sigma_1}^{m}{\sigma_2}^{n-m}E_{m,n-m}(x-\xi)\right\}d\xi =$$

$${\sigma_1}^{n+1}E_{n+1,0}(x)+{\sigma_2}^{n+1}E_{0,n+1}(x)+\sum_{m=1}^{n}\frac{(n+1)!}{m!(n+1-m)!}{\sigma_1}^{m}{\sigma_2}^{n+1-m}E_{m,n+1-m}(x) \quad \text{for } n=1,2,...$$

or

$$\left\{\sum_{m=0}^{n+1}\frac{(n+1)!}{m!(n+1-m)!}{\sigma_1}^{m}{\sigma_2}^{n+1-m}E_{m,n+1-m}(x)\right\}=$$
$$\int_0^\infty [H_0\sigma f(\xi)]\left\{\sum_{m=0}^{n}\frac{n!}{m!(n-m)!}{\sigma_1}^{m}{\sigma_2}^{n-m}E_{m,n-m}(x-\xi)\right\}d\xi \quad \text{for } n=1,2,... \qquad \text{(B5)}$$

Regarding the curly brackets in (B5) as functions of n, we can interpret (B5) as a recurrence formula for the curly bracket.

To prove (28), we first relate the curly bracket in (B5) to the G_n function. This is done by noting from (B5) that the curly bracket satisfies the same recurrence formula that is given by (B1) for $(H_0\sigma)^nG_n$. Furthermore, the curly bracket at $n = 1$ is $(H_0\sigma)G_1$. This can be shown by using (27j) and (27k) to express the curly bracket at $n = 1$ in terms of $C_{0,0}$ and $D_{0,0}$, then use (27a) and (27e) to express this in terms of H, and finally use (25a) to complete the proof. We, therefore, conclude that the curly bracket is $(H_0\sigma)^nG_n$, i.e.,

$$(H_0\sigma)^n\,G_n(x)=\sum_{m=0}^{n}\frac{n!}{m!(n-m)!}{\sigma_1}^{m}{\sigma_2}^{n-m}E_{m,n-m}(x) \quad \text{for } n=1,2,.... \qquad \text{(B6)}$$

The next step in the proof of (28) uses (27i) and (B6) to write (26) in the present notation as

$$e^{H_0\sigma}P(CLE) = E_{0,0}(\Delta q_C) + \sum_{n=1}^{\infty}\sum_{m=0}^{n}\frac{1}{m!(n-m)!}{\sigma_1}^m{\sigma_2}^{n-m}E_{m,n-m}(\Delta q_C)\ .$$

The first term on the right will be included in the double sum by including an $n = 0$ term in the outer sum so the above becomes

$$P(CLE) = e^{-H_0\sigma}\sum_{n=0}^{\infty}\sum_{m=0}^{n}\frac{1}{m!(n-m)!}{\sigma_1}^m{\sigma_2}^{n-m}E_{m,n-m}(\Delta q_C)\ . \qquad \text{(B7)}$$

This is one way to express $P(CLE)$ in terms of the E-functions when Δq_C is given but an alternate expression is obtained by combining (B7) with the summation identity

$$\sum_{n=0}^{\infty}\sum_{m=0}^{\infty}A_{m,n} = \sum_{n=0}^{\infty}\sum_{m=0}^{n}A_{m,n-m}$$

to obtain

$$P(CLE) = e^{-H_0\sigma}\sum_{n=0}^{\infty}\sum_{m=0}^{\infty}\frac{1}{m!\ n!}{\sigma_1}^m{\sigma_2}^{n}E_{m,n}(\Delta q_C)\ . \qquad \text{(B8)}$$

Converting back to the original notation produces (28).

The G-functions produced by a pure spectrum are easily derived from (B6). Using $h(\xi) = H_0\,\delta(\xi - L_T)$ (where δ is the Dirac δ-function) and $H(\xi) = H_0\ U(L_T - \xi)$ with (27) gives

$$E_{m,n}(x) = {H_0}^{m+n}\,U\left(\frac{m\,L_T}{a_1} + \frac{n\,L_T}{a_2} - x\right) \quad \text{(pure spectrum)} \qquad \text{(B9a)}$$

so (B6) gives

$$G_n(x) = \sum_{m=0}^{n}\frac{n!}{m!(n-m)!}\left(\frac{\sigma_1}{\sigma}\right)^m\left(\frac{\sigma_2}{\sigma}\right)^{n-m}U\left(\frac{m\,L_T}{a_1} + \frac{(n-m)\,L_T}{a_2} - x\right) \quad \text{(pure spectrum)}\ . \qquad \text{(B9b)}$$

Appendix C: A Routine for Fitting (50) to Data

A routine for calculating P(CLE) via (50) that runs in the Octave (a GNU package) platform is in the textbox below. The contents can be typed into a file named "PCLE_PUR.m" (the PUR indicates a pure spectrum). This is a function file so the file name must be as stated unless the function name is changed consistently. The Weibull function is used to represent bit-to-bit variations in the critical charge loss.

PCLE_PUR.m

```
function z=PCLE_PUR(b1,b2,s1,s2,k,L,F);
  y1=s1.*F;
  y2=s2.*F;
  y=y1+y2;
  SUM_N=0;
  coefn=1;
    for n=0:100;
    SUM_M=0;
    coefm=1;
    for m=0:100;
        argue=(((m./b1)+(n./b2)).*L).^k;
        SUM_M=SUM_M+coefm.*exp(-argue);
        coefm=y1.*coefm./(m+1);
        end
    SUM_N=SUM_N+coefn.*SUM_M;
    coefn=y2.*coefn./(n+1);
    end
z1=SUM_N;
z=1-exp(-y).*z1;
for i=1:length(z);
  if (z(i)<1E-9)
  z(i)=0;
  endif
end
endfunction
```

This function has seven arguments. The first five, in order, are the fitting parameters denoted b_1-bar, b_2-bar, $\sigma_{S,sat}$, $\sigma_{W,sat}$, and k in (50). The sixth argument is the LET denoted L_T in (50), and the last argument is the fluence denoted H in (50). This function will accept an array (a vector) for the fluence so that plots and/or tables of P(CLE) versus fluence can be constructed without requiring a loop that reassigns single values to the fluence. The double infinite series in (50) is approximated by a finite double sum. The version shown here uses 100 terms in each sum, but the user can change these numbers by editing the code. The goal is to obtain adequate numerical accuracy without producing excessive CPU time (fitting routines make many calls to this function so CPU time becomes an issue). An unfortunate property of (50) is that any set of inputs that produce a very small value of P(CLE) are inputs such that the right side of (50) is the difference between nearly-equal numbers, so numerical precision becomes an issue. Because of the approximation discussed above, calculated values of P(CLE) that are less than 10^{-9} are changed to zero in the routine, so a returned value of zero is a flag that the actual value is less than 10^{-9}.

Many software products provide tools for finding best fits to data but we assume here that the only tools available to the user are those in the Octave package which is publically available at no cost. Two steps are used to find the best fit. The first finds a rough estimate of the fitting parameters by performing a global search, via random number generators, for the fitting parameters that minimize the error between the fit and data. This is done with two files. The file below defines the error between the fit and data and is a function file so the file name must be "PCLE_ERR_CRS.m" (the CRS indicates a coarse fit) unless the function name is changed consistently. It defines the error between a fit and data by calculating square errors at each data point and summing over data points. The error is a relative, or percent, error as opposed to an absolute error so the logarithm of the fit is compared to the logarithm of the data. Note that PCLE_PUR returns a value of zero when the calculating probability is less than 10^{-9}, so 1 is added to the arguments of the logarithms in PCLE_ERR_CRS to avoid undefined calculations. The numbers in the version of the code shown here are unique to the data in Fig. 1, but can be changed for other data sets by editing the code.

PCLE_ERR_CRS.m

```
function ERR=PCLE_ERR_CRS(x);
b1=x(1);
b2=x(2);
s1=x(3);
s2=x(4);
k=x(5);
E(1)=(log10(1+2.21e9*PCLE_PUR(b1,b2,s1,s2,k,72,1e3))-2.6)^2;
E(2)=(log10(1+2.21e9*PCLE_PUR(b1,b2,s1,s2,k,72,4e6))-6)^2;
E(3)=(log10(1+2.21e9*PCLE_PUR(b1,b2,s1,s2,k,43.7,2e7))-6)^2;
E(4)=(log10(1+2.21e9*PCLE_PUR(b1,b2,s1,s2,k,43.7,1e3))-1.78)^2;
E(5)=(log10(1+2.21e9*PCLE_PUR(b1,b2,s1,s2,k,20,2e3))-0)^2;
E(6)=(log10(1+2.21e9*PCLE_PUR(b1,b2,s1,s2,k,20,1e6))-2.7)^2;
E(7)=(log10(1+2.21e9*PCLE_PUR(b1,b2,s1,s2,k,5.7,1e8))-0.78)^2;
E(8)=(log10(1+2.21e9*PCLE_PUR(b1,b2,s1,s2,k,5.7,1.5e8))-1.23)^2;
E(9)=(log10(1+2.21e9*PCLE_PUR(b1,b2,s1,s2,k,5.7,1e9))-2.4)^2;
E(10)=(log10(1+2.21e9*PCLE_PUR(b1,b2,s1,s2,k,5.7,2e9))-3.7)^2;
ERR=sum(E);
endfunction
```

The second code used in the first step is called "PCLE_bestfit_CRS.m" and is shown in the text box below. It selects fitting parameters at random in a search for parameters that produce the smallest error returned by PCLE_ERR_CRS. The numbers assigned to xf(1), … ,xf(5) are arbitrary guesses for b_1-bar, b_2-bar, $\sigma_{S,sat}$, $\sigma_{W,sat}$, and k. If the code finds a better set of fitting parameters (i.e., that produce a smaller error), it will output those parameters. Each set of fitting parameters that are better than all previously found sets are output. The version of the code shown here uses (42) instead of a random number generator to assign values to x(3) (which is $\sigma_{S,sat}$) because the Ho data are known to be SEU-like. If this information was not available, this assignment statement would be deactivated and the random number assignment would be activated. Also, the version of the code shown selects random numbers from relatively narrow intervals because iterations were already performed and indicated that the optimum parameters will be in these intervals. A more general procedure starts with relatively wide intervals and

performs several hundred searches (the version of the code shown here performs 300 searches) for the optimum fitting parameters. This can be repeated (each run of the same code produces a new set of results because random number generators are used) as many times as needed to obtain some rough idea of what the optimum parameters are. This information is then used to reduce the intervals that the random numbers are selected from, and the runs are repeated using the smaller intervals. Continuing this procedure with progressively smaller intervals produces estimates for the fitting parameters that are used as the initial guess for the second step.

PCLE_bestfit_CRS.m

```
xf(1)=54.9;
xf(2)=2531;
xf(3)=1.3e-10;
xf(4)=1.519e-8;
xf(5)=7.313;
Errf=PCLE_ERR_CRS(xf);
disp(' ')
printf('Err= %f', Errf)
disp(' ')
printf('b1= %f b2= %f s1= %e s2= %e',xf(1),xf(2),xf(3),xf(4))
disp(' ')
printf('k= %f',xf(5))
disp(' ')
for i=1:300
x(1)=unifrnd(50,70);
x(2)=unifrnd(2200,2600);
%x(3)=unifrnd(1.3e-10,2.5e-10);
x(4)=unifrnd(1.3e-8,1.7e-8);
x(5)=unifrnd(5,8);
x(3)=1.3e-10/(1-exp(-(72/x(1))^x(5)));
Err=PCLE_ERR_CRS(x);
if (Err<Errf)
  Errf=Err;
  xf=x;
  disp(' ')
  printf('Err= %f', Errf)
  disp(' ')
  printf('b1= %f b2= %f s1= %e s2= %e',xf(1),xf(2),xf(3),xf(4))
  disp(' ')
  printf('k= %f',xf(5))
  disp(' ')
endif
end
```

The second step provides the fine tuning by using a gradient-based search for a local minimum in the error measure. The first textbox below is the function that is called and the

second textbox is the calling routine that searches for the best fit. The FIN in the file names indicates fine tuning.

PCLE_ERR_FIN.m

```
function ERR=PCLE_ERR_FIN(x);
b1=100*x(1);
b2=1000*x(2);
s1=1E-10*x(3);
s2=1E-8*x(4);
k=x(5);
E(1)=(log10(1+2.21e9*PCLE_PUR(b1,b2,s1,s2,k,72,1e3))-2.6)^2;
E(2)=(log10(1+2.21e9*PCLE_PUR(b1,b2,s1,s2,k,72,4e6))-6)^2;
E(3)=(log10(1+2.21e9*PCLE_PUR(b1,b2,s1,s2,k,43.7,2e7))-6)^2;
E(4)=(log10(1+2.21e9*PCLE_PUR(b1,b2,s1,s2,k,43.7,1e3))-1.78)^2;
E(5)=(log10(1+2.21e9*PCLE_PUR(b1,b2,s1,s2,k,20,2e3))-0)^2;
E(6)=(log10(1+2.21e9*PCLE_PUR(b1,b2,s1,s2,k,20,1e6))-2.7)^2;
E(7)=(log10(1+2.21e9*PCLE_PUR(b1,b2,s1,s2,k,5.7,1e8))-0.78)^2;
E(8)=(log10(1+2.21e9*PCLE_PUR(b1,b2,s1,s2,k,5.7,1.5e8))-1.23)^2;
E(9)=(log10(1+2.21e9*PCLE_PUR(b1,b2,s1,s2,k,5.7,1e9))-2.4)^2;
E(10)=(log10(1+2.21e9*PCLE_PUR(b1,b2,s1,s2,k,5.7,2e9))-3.7)^2;
ERR=sum(E);
endfunction
```

PCLE_bestfit_FIN.m

```
f=@(x) PCLE_ERR_FIN(x);
% The function f above requires scaled parameters with scale factors selected
% to make the minimization routine run better by making the function
% arguments closer to having equal orders of magnitude. The required scaling is
% x(1)=b1/100
% x(2)=b2/1000
% x(3)=s1*1E10
% x(4)=s2*1E8
% x(5)=k
% The initial guess with this scaling is x0. Lower and upper bounds
% are lb and ub.
x0=[0.5312,2.504,1.3,1.318,7.6124];
lb=[0.20,1,1,0.1,1];
ub=[2,6,4,10,100];
[xf,obj,info,iter,nf,lambda]=sqp (x0,f,[],[],lb,ub,100,1e-12);
Err=obj
b1=100*xf(1)
b2=1000*xf(2)
s1=1E-10*xf(3)
s2=1E-8*xf(4)
k=xf(5)
```

Appendix D: Selecting LETs and Fluences for a Complete Characterization

Suppose a device (e.g., a flash memory) containing a collection of FGs was tested with heavy ions using fluences small enough to produce SEU-like behavior. Such data do not provide a complete characterization of the device. A complete characterization requires larger fluences at the smaller LETs as needed to produce a statistically significant deviation from SEU-like behavior. However, before performing such additional tests, we should first look for a more quantitative description of "smaller LET" and "larger fluence." The goal of this discussion is to use data obtained from the small-fluence tests to estimate the LETs and fluences that should be suitable for the additional, large-fluence, testing. The analysis given here is simplified by considering only strong interactions. The justification for this simplification is that the inclusion of weak interactions can only produce a further deviation from SEU-like behavior. Therefore, if test conditions (LET and fluence) are such that strong interactions alone are enough for a deviation from SEU-like behavior, such a deviation can be expected to occur.

We begin by selecting some test fluence, denoted H_T, and test LET, denoted L_T, and determine the condition that these parameters should satisfy in order to obtain a complete characterization of the collection of FGs. If the required condition is not satisfied by a particular selection of L_T and H_T, it is necessary to make another selection. Let N_{total} denote the total number of FGs in the collection and let $\sigma_{CLE}(L)$ denote the per-bit cross section obtained from the small-fluence (SEU-like) test data as a function of LET L. This per-bit cross section is obtained by dividing the number of counts first by fluence, to obtain a cross section for the collection of FGs, and then by N_{total} to convert this cross section to a per-bit cross section. Let N_{counts} denote the number of counts from the collection of FGs produced by the large-fluence test when the fluence is H_T and the LET is L_T. The fluence is large enough for the device behavior to be outside the SEU-like regime if the quantity $N_{counts}/(H_T N_{total})$ is measurably larger than $\sigma_{CLE}(L)$, where measurably larger means that the difference between the quantities is large enough to be distinguishable from experimental error. Therefore the fluence must be large enough to satisfy

$$\frac{N_{counts}}{H_T\, N_{total}} - \sigma_{CLE}(L_T) > \text{experimental error} \qquad \text{(required)}, \tag{D1}$$

where the error on the right side includes scatter in the data associated with counting statistics. The goal now is to predict whether the required condition (D1) will or will not be satisfied by a particular choice of the parameters H_T and L_T.

The first step towards the above goal divides the FGs in the collection into groups and uses the SEU-like (small-fluence) cross section data to estimate the number of FGs in each group. The first group consists of those FGs that require only one strong interaction at an LET L_T to become deprogrammed. The number of FGs in this group, denoted N_1, is estimated by noting that the small-fluence cross section for the collection of FGs, which is $N_{total}\, \sigma_{CLE}(L)$ when the LET is L, is the sum of FG cross sections at LET L, summed over all FGs in the collection. At an LET of L_T, only the FGs in the first group contribute to the cross section because multiple hits can be ignored in the small-fluence data. Each of these FGs has a cross section of $\sigma_{S,sat}$, and there are N_1 of these FGs, so the sum of FG cross sections summed over FGs in the first group is $N_1\sigma_{S,sat}$. This gives

$$N_{total}\, \sigma_{CLE}(L_T) = N_1\, \sigma_{S,sat}\,.$$

The second group consists of those FGs that will become deprogrammed by two strong interactions, but not by one strong interaction, at an LET of L_T. An FG is in this group if, and only if, a single strong interaction produced by an LET of $2L_T$ will deprogram the FG, but a single strong interaction at an LET of L_T will not. The number of FGs in this group, denoted N_2, is estimated by noting that the FGs that contribute to the small-fluence cross section for the collection of FGs at an LET of $2L_T$ consists of those in the first group plus those in the second group. This gives

$$N_{total}\,\sigma_{CLE}(2L_T) = N_1\,\sigma_{S,sat} + N_2\,\sigma_{S,sat}\,.$$

Continuing with this group designation, the n^{th} group consists of those FGs that will become deprogrammed by n strong interactions, but not by $n - 1$ strong interactions, at an LET of L_T. An FG is in this group if, and only if, a single strong interaction produced by an LET of nL_T will deprogram the FG, but a single strong interaction at an LET of $(n - 1)L_T$ will not. Let N_n denote the number of FGs in this group. An obvious extension of the derivation of the above equation gives

$$N_{total}\,\sigma_{CLE}(n\,L_T) = \sigma_{S,sat}\sum_{k=1}^{n} N_k \qquad \text{for } n = 1, 2, \ldots . \tag{D2a}$$

Replacing n with $n - 1$ in (D2a) and subtracting the resulting equation from (D2a) allows us to solve for N_n with the result

$$N_n = N_{total}\,\frac{\sigma_{CLE}\left(n\,L_T\right) - \sigma_{CLE}\left((n-1)\,L_T\right)}{\sigma_{S,sat}} \quad \text{for } n = 1, 2, \ldots , \tag{D2b}$$

where we use the convention that $\sigma_{CLE}(0) = 0$, so that (D2b) will also apply when $n = 1$. There is a maximum value, call it $n_{\max}$, of the group designator having the property that the group numbered $n_{\max}$ contains a nonzero number of FGs, i.e., $N_n > 0$ when $n = n_{\max}$, but $N_n = 0$ when $n > n_{\max}$. This number is determined by the condition that the total number of FGs is N_{total}, which gives

$$\sum_{k=1}^{n_{\max}} N_k = N_{total}\,. \tag{D3a}$$

Furthermore, all groups with larger designations contain zero FGs, so

$$\sum_{k=1}^{n} N_k = N_{total} \qquad \text{if } n \geq n_{\max}\,. \tag{D3b}$$

The value of $n_{\max}$, as well as $\sigma_{S,sat}$, can be recognized by the saturation of the small-fluence cross section data. This is seen by combining (D3) with (D2a) to get

$$\sigma_{CLE}(n_{\max} L_T) = \sigma_{S,sat} \tag{D4a}$$

$$\sigma_{CLE}(n L_T) = \sigma_{S,sat} \qquad \text{if } n \geq n_{\max} . \tag{D4b}$$

We conclude from (D4) that the cross section $\sigma_{S,sat}$ can be estimated from the small-fluence cross section data as the saturation value (large LET limit) of $\sigma_{CLE}(L)$. Furthermore, $n_{\max}L_T$ is the smallest integer multiple of L_T that produces the saturation value.

Having divided the collection of FGs into groups, we can now express N_{counts} as a sum of terms given by

$$N_{counts} = \sum_{n=1}^{n_{\max}} N_{counts,n} , \tag{D5}$$

where $N_{counts,n}$ is the number of deprogrammed FGs from the n^{th} group of FGs and produced by a fluence H_T of LET L_T. It is assumed that these numbers of counts are large enough for the ensemble interpretation of a probability to be used with these numbers. Specifically, $N_{counts,n}$ is taken to be equal to the number of FGs in the n^{th} group multiplied by the probability that a randomly selected FG from this group will become deprogrammed. This probability is the probability that an FG will undergo n or more strong interactions from the fluence H_T. Using the Poisson distribution for this probability gives

$$N_{counts,n} = N_n \left\{1 - \mathcal{P}_{oisson}(n-1, H_T \sigma_{S,sat})\right\}, \tag{D6}$$

where $\mathcal{P}_{oisson}$ is the cumulative Poisson distribution function defined by (E4) in Appendix E. Substituting (D6) and (D2b) into (D5) gives

$$N_{counts} = \frac{N_{total}}{\sigma_{S,sat}} \sum_{n=1}^{n_{\max}} \left\{\sigma_{CLE}(n L_T) - \sigma_{CLE}((n-1) L_T)\right\}\left\{1 - \mathcal{P}_{oisson}(n-1, H_T \sigma_{S,sat})\right\}.$$

A summation analog of an integration by parts, using (D4a) and $\sigma_{CLE}(0) = 0$, allows this to be rewritten as

$$\frac{N_{counts}}{N_{total}} = \left\{1 - \mathcal{P}_{oisson}(n_{\max} - 1, H_T \sigma_{S,sat})\right\} + e^{-H_T \sigma_{S,sat}} \sum_{n=1}^{n_{\max}-1} \frac{\sigma_{CLE}(n L_T)}{\sigma_{S,sat}} \frac{(H_T \sigma_{S,sat})^n}{n!} . \tag{D7a}$$

It is possible to write (D7a) in a more compact form, but the penalty is to replace a finite sum with an infinite series. This is done by using

$$1-\mathcal{P}_{oisson}(n_{\max}-1, H_T\,\sigma_{S,sat}) = 1-e^{-H_T\,\sigma_{S,sat}}\sum_{n=0}^{n_{\max}-1}\frac{(H_T\,\sigma_{S,sat})^n}{n!}$$

$$= e^{-H_T\,\sigma_{S,sat}}\left(e^{H_T\,\sigma_{S,sat}} - \sum_{n=0}^{n_{\max}-1}\frac{(H_T\,\sigma_{S,sat})^n}{n!}\right) = e^{-H_T\,\sigma_{S,sat}}\sum_{n=n_{\max}}^{\infty}\frac{(H_T\,\sigma_{S,sat})^n}{n!}$$

where the last equality was obtained by replacing the exponential function in the large parenthesis by a series expansion. Combining this with (D4b) gives

$$1-\mathcal{P}_{oisson}(n_{\max}-1, H_T\,\sigma_{S,sat}) = e^{-H_T\,\sigma_{S,sat}}\sum_{n=n_{\max}}^{\infty}\frac{\sigma_{CLE}(n\,L_T)}{\sigma_{S,sat}}\,\frac{(H_T\,\sigma_{S,sat})^n}{n!},$$

so (D7a) can be rewritten as

$$\frac{N_{counts}}{N_{total}} = e^{-H_T\,\sigma_{S,sat}}\sum_{n=1}^{\infty}\frac{\sigma_{CLE}(n\,L_T)}{\sigma_{S,sat}}\,\frac{(H_T\,\sigma_{S,sat})^n}{n!}$$

or

$$\frac{N_{counts}}{H_T\,N_{total}} = e^{-H_T\,\sigma_{S,sat}}\sum_{n=1}^{\infty}\sigma_{CLE}(n\,L_T)\,\frac{(H_T\,\sigma_{S,sat})^{n-1}}{n!}. \qquad \text{(D7b)}$$

The right side is a sum of positive terms and is greater than the sum of the first two terms, so

$$\frac{N_{counts}}{H_T\,N_{total}} > e^{-H_T\,\sigma_{S,sat}}\left[\sigma_{CLE}(L_T)+\frac{1}{2}(H_T\,\sigma_{S,sat})\sigma_{CLE}(2L_T)\right]. \qquad \text{(D8)}$$

The required equations have been derived, so we now consider an example to illustrate how the equations are used to answer the question of whether a given choice of L_T and H_T will satisfy (D1). The best choice for L_T is the LET that produces the largest value for the ratio $\sigma_{CLE}(2L)/\sigma_{CLE}(L)$. Suppose, for this example, that we can find an L_T satisfying

$$\frac{\sigma_{CLE}(2L_T)}{\sigma_{CLE}(L_T)} \geq 100 \qquad \text{(example)}. \qquad \text{(D9a)}$$

For the example curve labelled "0 krads" in Fig. 3, the condition (D9a) is satisfied for any LET in the plotted range up to 20 MeV-cm^2/mg. We also use the example device represented in Fig. 3 to provide a value for $\sigma_{S,sat}$, which is 10^{-10} cm^2. Finally, there are practical considerations (beam time) for not wanting to use a fluence larger than 10^9/cm^2, but we are willing to go that high with the fluence. Therefore, the remaining inputs for this example are

$$\sigma_{S,sat} = 10^{-10}\,\mathrm{cm}^2, \quad H_T = 10^9/\mathrm{cm}^2 \qquad \text{(example)}. \tag{D9b}$$

Substituting (D9) into (D8), we find that $N_{counts}/(H_T N_{total})$ is greater than $5.4\sigma_{CLE}(L_T)$ for this example, which gives

$$\frac{N_{counts}}{H_T\, N_{total}} - \sigma_{CLE}(L_T) > 4.4\,\sigma_{CLE}(L_T) \qquad \text{(example)}. \tag{D10}$$

Given that the experimental error is small enough so that $\sigma_{CLE}(L_T)$ could be measured, i.e., $\sigma_{CLE}(L_T)$ is greater than the measurement error, we conclude from (D10) that the left side is also greater than the measurement error, so the requirement (D1) is satisfied. The example device is the same device represented in Figs. 1 and 2, and the conclusion given here for this example is that a fluence of $10^9/\mathrm{cm}^2$ should be enough to produce an experimentally observable deviation from SEU-like behavior for any of the tested ions up to an LET of 20 MeV-cm^2/mg. This deviation is seen in the test data (Fig. 1) only for Ar because that is the only ion tested at such large fluences, but we can predict that this deviation would also become observable in the Kr data if larger test fluences were used. This agrees with the model prediction in Fig. 2 (derived from fits to the Fig. 1 data) showing some curvature in the Kr curve at the larger fluences.

Appendix E: A Routine for Calculating *P*(CLE) in Space Environments

To calculate *P*(CLE) in space environments we start with (57) which is repeated below:

$$P(\text{CLE}) = \mathcal{F}(\Delta q_D) + \exp\left[-H(0)\,\sigma_{sat}\right]\sum_{n=1}^{\infty}\frac{1}{n!}\left[\int_0^{\infty} G_n(\xi)\,\rho(\xi+\Delta q_D)\,d\xi\right]\left[H(0)\,\sigma_{sat}\right]^n. \quad \text{(E1)}$$

We also consider the case in which the Weibull function (47) describes FG-to-FG variations in the critical charge loss, so

$$\mathcal{F}(x) = \mathcal{W}_{\lambda,k}(x) \equiv \begin{cases} 1-\exp\left[-(x/\lambda)^k\right] & \text{if } x > 0 \\ 0 & \text{if } x \le 0 \end{cases} \quad \text{(E2a)}$$

$$\rho(x) = \frac{d}{d\,x}\mathcal{W}_{\lambda,k}(x) = \begin{cases} \dfrac{k}{\lambda}\left(\dfrac{x}{\lambda}\right)^{k-1}\exp\left[-(x/\lambda)^k\right] & \text{if } x > 0 \\ 0 & \text{if } x \le 0 \end{cases}. \quad \text{(E2b)}$$

Properties implied by these equations that will be useful later are

$$\mathcal{F}(\lambda\,x) = \mathcal{W}_{1,k}(x), \qquad \lambda\,\rho(\lambda\,x) = \frac{d}{d\,x}\mathcal{W}_{1,k}(x). \quad \text{(E2c)}$$

The infinite series in (E1) can be replaced by a finite sum using a conservative approximation. This is obtained by using (16a) with the fact that ρ is a normalized density to conclude that

$$\int_0^{\infty} G_n(\xi)\,\rho(\xi+\Delta q_D)\,d\xi \le \int_0^{\infty}\rho(\xi+\Delta q_D)\,d\xi = \int_{\Delta q_D}^{\infty}\rho(\xi)\,d\xi \le \int_0^{\infty}\rho(\xi)\,d\xi = 1.$$

Using this with (E1) gives

$$P(\text{CLE}) \le \mathcal{F}(\Delta q_D) + \left\{\exp\left[-H(0)\,\sigma_{sat}\right]\sum_{n=1}^{N}\frac{1}{n!}\left[\int_0^{\infty} G_n(\xi)\,\rho(\xi+\Delta q_D)\,d\xi\right]\left[H(0)\,\sigma_{sat}\right]^n\right\} + \left\{1-\mathcal{P}_{oisson}(N, H(0)\,\sigma_{sat})\right\} \quad \text{for } N = 1, 2, \ldots, \quad \text{(E3)}$$

where $\mathcal{P}_{oisson}$ is the cumulative Poisson distribution function defined by

$$\mathcal{P}_{oisson}(N,\lambda) \equiv e^{-\lambda}\sum_{n=0}^{N}\frac{\lambda^n}{n!}. \quad \text{(E4)}$$

Note that $P(\text{CLE}) - \mathcal{F}(\Delta q_D)$ is less than or equal to the sum of the two curly brackets on the right side of (E3), but greater than or equal to the first curly bracket. Therefore, the error produced by using the right side of (E3) as an approximation for the left side, which is a conservative approximation, is no larger than the second curly bracket. By letting N be large enough to make the second curly bracket equal to 10^{-12} (for example), the error produced by using the right side of (E3) as an approximation for the left side is no greater than 10^{-12}.

To shorten the notation, define the c-coefficients by

$$c_n \equiv \frac{1}{n!}\left[H(0)\,\sigma_{sat}\right]^n \quad \text{for } n = 1, 2, \ldots \,. \tag{E5}$$

They can be calculated from the recurrence formula

$$c_1 = H(0)\,\sigma_{sat}, \qquad c_{n+1} = \frac{c_1}{n+1}\; c_n \quad \text{for } n = 1, 2, \ldots \,. \tag{E6}$$

Using this notation, (E3) can be written as

$$P(\text{CLE}) \le \mathcal{F}(\Delta q_D) + \left\{ e^{-c_1} \sum_{n=1}^{N} c_n \left[\int_0^\infty G_n(\xi)\,\rho(\xi + \Delta q_D)\,d\xi \right] \right\} + \left\{1 - \mathcal{P}_{oisson}(N, c_1)\right\}. \tag{E7}$$

Calculation of Δq_D via (52) requires the a-parameters to be known. Also, calculation of the G-functions requires the a-parameters to be known because the recurrence formula (15a) implicitly contains these parameters via (25b). Replacements for these quantities that can be calculated when the b-parameters (recall that $b_1 \equiv \lambda a_1$ and $b_2 \equiv \lambda a_2$) are known, instead of the a-parameters, are $\Delta q_D'$ and the T-functions defined by

$$\Delta q_D' \equiv \frac{1}{\lambda}\Delta q_D = \left(\frac{\sigma_{S,sat}}{b_1} + \frac{\sigma_{W,sat}}{b_2} \right) \mu D \tag{E8a}$$

$$T_n(x) \equiv G_n(\lambda x) \quad \text{for } n = 1, 2, \ldots, \tag{E8b}$$

where μ is given by (51b). The T-functions are calculated by combining (E8b) with (15a) and (25b) and changing integration variables to produce the recurrence formula

$$T_{n+1}(x) = T_1(x) + \int_0^x \left[\frac{b_1\, h(b_1\,\xi)}{H(0)}\,\frac{\sigma_{S,sat}}{\sigma_{sat}} + \frac{b_2\, h(b_2\,\xi)}{H(0)}\,\frac{\sigma_{W,sat}}{\sigma_{sat}} \right] T_n(x - \xi)\,d\xi \quad \text{for } n = 1, 2, \ldots \,. \tag{E9}$$

To get the T-function sequence started, we combine (E8a) with (25a) to get

$$T_1(x) = \frac{H(b_1\, x)\sigma_{S,sat} + H(b_2\, x)\sigma_{W,sat}}{H(0)\,\sigma_{sat}}. \qquad \text{(E10)}$$

The next step expresses (E7) in terms of $\Delta q_D'$ and the T-functions by using (E2c) and (E8) together with a change of integration variable to get

$$P(CLE) \le \mathcal{W}_{1,k}(\Delta q_D') + e^{-c_1} \sum_{n=1}^{N} \left[c_n \int_0^{\infty} T_n(\xi) \frac{d}{d\,\xi} \mathcal{W}_{1,k}(\xi + \Delta q_D')\, d\xi \right] + 1 - \mathcal{P}_{oisson}(N, c_1). \qquad \text{(E11)}$$

The infinite upper integration limits on the right side of (E11) can be replaced by finite limits. One possible approach utilizes the fact that the maximum LET of any ion is less than some upper bound (the upper bound is slightly greater than 100 MeV-cm^2/mg), which implies that the integral fluence $H(L)$ is zero when L is greater than this finite upper bound. This fact can be used to conclude that $T_1(x)$ given by (E10) is zero when x is greater than some finite upper bound. Unfortunately, the same upper bound for x to produce a nonzero value does not apply to $T_2(x)$ or $T_3(x)$, etc. This can be seen by considering any x satisfying the condition that $T_1(x) > 0$. It can be shown from (E9) that this implies that $T_2(2x) > 0$. Therefore, while it is true that for each n there is a finite domain of x at which $T_n(x) > 0$, this domain becomes larger with increasing n. This dependence on n is a complication that must be considered when constructing a numerical routine that takes advantage of the fact that the maximum LET of any ion is less than some upper bound.

An alternate approach, used here, replaces the infinite upper integration limit on the right side of (E11) with a finite limit (the same limit for all n) by using a conservative approximation having the property that an upper bound for the error in this approximation can be predicted and controlled. Let $x_{\max}$ denote the maximum argument for which $T_n(x)$ will be numerically evaluated. Note from (16f) and (E8) that $T_n(\xi) \le T_n(x_{\max})$ when $\xi > x_{\max}$. This inequality together with the fact that the derivative of $\mathcal{W}_{1,k}$ is positive gives

$$\int_0^{\infty} T_n(\xi) \frac{d}{d\,\xi} \mathcal{W}_{1,k}(\xi + \Delta q_D')\, d\xi = \int_0^{x_{\max}} T_n(\xi) \frac{d}{d\,\xi} \mathcal{W}_{1,k}(\xi + \Delta q_D')\, d\xi +$$

$$\int_{x_{\max}}^{\infty} T_n(\xi) \frac{d}{d\,\xi} \mathcal{W}_{1,k}(\xi + \Delta q_D')\, d\xi \le \int_0^{x_{\max}} T_n(\xi) \frac{d}{d\,\xi} \mathcal{W}_{1,k}(\xi + \Delta q_D')\, d\xi +$$

$$T_n(x_{\max}) \int_{x_{\max}}^{\infty} \frac{d}{d\,\xi} \mathcal{W}_{1,k}(\xi + \Delta q_D')\, d\xi$$

or

$$\int_0^{\infty} T_n(\xi) \frac{d}{d\,\xi} \mathcal{W}_{1,k}(\xi + \Delta q_D')\, d\xi \le \int_0^{x_{\max}} T_n(\xi) \frac{d}{d\,\xi} \mathcal{W}_{1,k}(\xi + \Delta q_D')\, d\xi +$$

$$T_n(x_{\max})\, e^{-(x_{\max} + \Delta q_D')^k}. \qquad \text{(E12)}$$

The conservative approximation that will be used here uses the right side of (E12) as an approximation for the left side. It is conservative because the right side of (E12) is greater than, when not equal to, the left side. For the purpose of obtaining a worst-case estimate of the error in this approximation, we consider another inequality (not intended to provide an accurate approximation) which is

$$\int_0^{\infty} T_n(\xi)\frac{d}{d\xi}\mathcal{W}_{1,k}(\xi+\Delta q_D')\,d\xi \geq \int_0^{x_{\max}} T_n(\xi)\frac{d}{d\xi}\mathcal{W}_{1,k}(\xi+\Delta q_D')\,d\xi \geq$$

$$T_n(x_{\max})\int_0^{x_{\max}} \frac{d}{d\xi}\mathcal{W}_{1,k}(\xi+\Delta q_D')\,d\xi$$

or

$$\int_0^{\infty} T_n(\xi)\frac{d}{d\xi}\mathcal{W}_{1,k}(\xi+\Delta q_D')\,d\xi \geq T_n(x_{\max})\left[e^{-(\Delta q_D')^k} - e^{-(x_{\max}+\Delta q_D')^k}\right]. \qquad \text{(E13)}$$

The right side of (E12) exceeds the left side by an amount that is not more than the term on the far right of (E12). If $T_n(x_{\max}) = 0$, there is no error. If $T_n(x_{\max}) > 0$, a worst-case estimate of the relative error, or fractional error, is the term on the far right side of (E12) divided by the right side of (E13); i.e.,

$$\text{relative error} \leq \frac{e^{-(x_{\max}+\Delta q_D')^k}}{e^{-(\Delta q_D')^k} - e^{-(x_{\max}+\Delta q_D')^k}} . \qquad \text{(E14)}$$

For example, if $x_{\max}$ is selected to satisfy

$$x_{\max} = \left[(\Delta q_D')^k + 9.22\right]^{1/k} - \Delta q_D' \qquad \text{(example)} ,$$

the relative error produced by using the right side of (E12) as an approximation for the left side will not exceed 0.0001.

The integral on the right side of (E12) must be evaluated numerically and, again, we use a conservative approximation. The accuracy of the approximation is controlled by the choice of grid points. Select a set of grid points denoted $x_1, \ldots, x_M$, with $M \geq 2$, which satisfy

$$x_1 = 0, \qquad x_M = x_{\max}, \qquad x_{m-1} < x_m \quad \text{for each } m = 2, 3, ..., M . \qquad \text{(E15)}$$

To shorten the notation, we define

$$T_{n,m} \equiv T_n(x_m) \quad \text{for each } m = 1, ..., M \text{ and each } n = 1, 2, ..., N . \qquad \text{(E16)}$$

The fact that T_n is a decreasing function and the derivative in (E12) is positive implies

$$\int_0^{x_{\max}} T_n(\xi)\frac{d}{d\,\xi}\mathcal{W}_{1,k}(\xi+\Delta q_D')\,d\xi = \sum_{m=2}^{M}\int_{x_{m-1}}^{x_m} T_n(\xi)\frac{d}{d\,\xi}\mathcal{W}_{1,k}(\xi+\Delta q_D')\,d\xi$$

$$\leq \sum_{m=2}^{M} T_{n,m-1}\int_{x_{m-1}}^{x_m}\frac{d}{d\,\xi}\mathcal{W}_{1,k}(\xi+\Delta q_D')\,d\xi$$

or

$$\int_0^{x_{\max}} T_n(\xi)\frac{d}{d\,\xi}\mathcal{W}_{1,k}(\xi+\Delta q_D')\,d\xi \leq \sum_{m=2}^{M} T_{n,m-1}\left[e^{-(x_{m-1}+\Delta q_D')^k} - e^{-(x_m+\Delta q_D')^k}\right]. \quad \text{(E17)}$$

Combining this with (E12) gives

$$\int_0^{\infty} T_n(\xi)\frac{d}{d\,\xi}\mathcal{W}_{1,k}(\xi+\Delta q_D')\,d\xi \leq \sum_{m=2}^{M} T_{n,m-1}\left[e^{-(x_{m-1}+\Delta q_D')^k} - e^{-(x_m+\Delta q_D')^k}\right] +$$

$$T_{n,M}\,e^{-(x_M+\Delta q_D')^k}\ . \quad \text{(E18)}$$

An upper bound for P(CLE), which also serves as an approximation for P(CLE) after the $T_{n,j}$ array has been calculated, is obtained by combining (E18) with (E11) to get

$$P(\text{CLE}) \leq \mathcal{W}_{1,k}(\Delta q_D') + 1 - \mathcal{P}_{oisson}(N, c_1) +$$

$$e^{-c_1}\sum_{n=1}^{N} c_n\left\{\sum_{m=2}^{M} T_{n,m-1}\left[e^{-(x_{m-1}+\Delta q_D')^k} - e^{-(x_m+\Delta q_D')^k}\right] + T_{n,M}\,e^{-(x_M+\Delta q_D')^k}\right\}. \quad \text{(E19)}$$

In order to use the right side of (E19) as a conservative estimate of the left side, the T-array must be calculated. Again, a conservative approximation is used. The fact that T_n is a decreasing function and the square bracket in (E9) is positive implies

$$T_{n+1}(x_m) = T_1(x_m) + \int_0^{x_m}\left[\frac{b_1\,h(b_1\,\xi)}{H(0)}\frac{\sigma_{S,sat}}{\sigma_{sat}} + \frac{b_2\,h(b_2\,\xi)}{H(0)}\frac{\sigma_{W,sat}}{\sigma_{sat}}\right]T_n(x_m-\xi)\,d\xi$$

$$= T_1(x_m) + \sum_{j=2}^{m}\int_{x_{j-1}}^{x_j}\left[\frac{b_1\,h(b_1\,\xi)}{H(0)}\frac{\sigma_{S,sat}}{\sigma_{sat}} + \frac{b_2\,h(b_2\,\xi)}{H(0)}\frac{\sigma_{W,sat}}{\sigma_{sat}}\right]T_n(x_m-\xi)\,d\xi$$

$$\leq T_1(x_m) + \sum_{j=2}^{m} T_n(x_m-x_j)\int_{x_{j-1}}^{x_j}\left[\frac{b_1\,h(b_1\,\xi)}{H(0)}\frac{\sigma_{S,sat}}{\sigma_{sat}} + \frac{b_2\,h(b_2\,\xi)}{H(0)}\frac{\sigma_{W,sat}}{\sigma_{sat}}\right]d\xi\ ,$$

which applies for each n = 1, 2, …, N and each m = 2, 3, …, M. Changing the integration variable and using the fact that the differential fluence $h(L)$ is the negative of the L derivative of the integral fluence $H(L)$ gives

$$\int_{x_{j-1}}^{x_j} \left[\frac{b_1 \, h(b_1 \, \xi)}{H(0)} \frac{\sigma_{S,sat}}{\sigma_{sat}} \right] d\xi = \frac{H(b_1 \, x_{j-1}) - H(b_1 \, x_j)}{H(0)} \frac{\sigma_{S,sat}}{\sigma_{sat}}$$

with a similar equation for the integral containing b_2 so the above recurrence formula for the T-array becomes

$$T_{n+1,m} \le T_{1,m} + \sum_{j=2}^{m} T_n(x_m - x_j) \left\{ \frac{H(b_1 \, x_{j-1}) - H(b_1 \, x_j)}{H(0)} \frac{\sigma_{S,sat}}{\sigma_{sat}} + \frac{H(b_2 \, x_{j-1}) - H(b_2 \, x_j)}{H(0)} \frac{\sigma_{W,sat}}{\sigma_{sat}} \right\} \quad \text{for } n = 1, 2, ..., N-1 \text{ and } m = 2, 3, ..., M \, . \qquad \text{(E20)}$$

Note that (E20) is used only when $m \ge 2$, but it is not needed when $m = 1$ because the convention of taking x_1 to be zero and the definition $T_{n,m} \equiv T_n(x_m)$ gives $T_{n,1} = T_n(0)$, so (E8b) and (16b) give

$$T_{n,1} = 1 \quad \text{for each } n = 1, 2, ..., N \, . \qquad \text{(E21a)}$$

Another equation that will be useful later is obtained from (E10) and is

$$T_{1,m} = \frac{H(b_1 \, x_m)}{H(0)} \frac{\sigma_{S,sat}}{\sigma_{sat}} + \frac{H(b_2 \, x_m)}{H(0)} \frac{\sigma_{W,sat}}{\sigma_{sat}} \quad \text{for } m = 1, 2, ..., M \, . \qquad \text{(E21b)}$$

Now consider the argument to T_n on the right side of (E20), which is $x_m - x_j$ with $2 \le m \le M$ and $2 \le j \le m$. The argument is bracketed by $0 \le x_m - x_j \le x_M - x_2$ so $x_1 \le x_m - x_j < x_M$. Therefore, there is a pair of adjacent grid points having the property that the left (smaller) point is less than or equal to $x_m - x_j$ and the right point is greater than $x_m - x_j$. Stated another way, there is an integer $m'(m, j)$, a function of m and j, satisfying

$$x_{m'(m,j)} \le x_m - x_j < x_{m'(m,j)+1} \, . \qquad \text{(E21c)}$$

Because $T_n(x)$ is decreasing in x, $T_n(x_m - x_j)$ is less than or equal to the left grid point value. This gives

$$T_n(x_m - x_j) \le T_n\left(x_{m'(m,j)}\right) = T_{n,m'(m,j)} \, . \qquad \text{(E21d)}$$

It should be noted that the most effective way to improve the accuracy of the calculations is to use an interpolation, instead of the right side of (E21d), to obtain an estimate of the left side. However, doing so would invalidate the claim that all approximations are conservative. Readers that would like to give numerical accuracy a higher priority than guaranteed conservatism can modify the routine as pointed out later in the discussion under **Block 6**. Here, we will honor the claim that all approximations are conservative by using (E21d) with (E20) to get

$$T_{n+1,m} \le T_{1,m} + \sum_{j=2}^{m} T_{n,m'(m,j)} \left\{ \frac{H(b_1 x_{j-1}) - H(b_1 x_j)}{H(0)} \frac{\sigma_{S,sat}}{\sigma_{sat}} + \frac{H(b_2 x_{j-1}) - H(b_2 x_j)}{H(0)} \frac{\sigma_{W,sat}}{\sigma_{sat}} \right\} \quad \text{for } n = 1, 2, ..., N-1 \text{ and } m = 2, 3, ..., M \,. \tag{E21e}$$

A conservative approximation uses the right side of (E21e) as an estimate of the left side.

There still remains the issue of selecting the grid points $x_1, \ldots, x_M$. Flux or fluence data for typical space environments are such that the greatest resolution is needed at the smaller LETs, and this can be accomplished by a uniform spacing of the positive grid points (which are $x_2, \ldots, x_M$) on a logarithmic scale. The smallest positive grid point, x_2, should be small enough so that calculated fluences include all of the particles represented in the flux input files (tabulations of flux versus LET). The input files will represent heavy ions and possibly protons. For protons we have the option of including them in a separate dose-like calculation or including them in a flux input file so they may or may not be included in an input file. It is assumed that electrons will be included in a separate dose-like calculation and not included in a flux input file. Let $L_{\min}$ denote the smallest LET found in the flux input files, unless this value is less than 0.0017 MeV-cm^2/mg, in which case we let $L_{\min}$ = 0.0017 MeV-cm^2/mg. The reason for this cutoff is that the LET of protons in SiO_2 is greater than or equal to 0.0017 MeV-cm^2/mg for any proton energy greater than some fraction of a keV, so smaller LETs are irrelevant. Selecting x_2 in such a way so that calculations for both strong interactions and weak interactions include all particles with LET greater than or equal to $L_{\min}$ can be accomplished by selecting x_2 to satisfy $b_1 x_2 \le L_{\min}$ and $b_2 x_2 \le L_{\min}$. This condition will be satisfied, with a little margin, by using

$$x_2 = \frac{L_{\min}}{b_1 + b_2} \,.$$

Recall that we also have $x_M = x_{\max}$, so we must also select a value for $x_{\max}$. The right side of (E14) can be made to be equal to about 0.0001 (for example) by using

$$x_{\max} = \left[(\Delta q_D')^k + 9.22 \right]^{1/k} - \Delta q_D' \,. \tag{E22a}$$

After selecting an $M \ge 3$, a complete set of grid points can be calculated from (E22a) together with

$$x_1 = 0, \qquad x_2 = \frac{L_{\min}}{b_1 + b_2} \tag{E22b}$$

$$x_{m+1} = r\, x_m \quad \text{for } m = 2, 3, ..., M-1 \,, \tag{E22c}$$

where the ratio r is given by

$$r = \left(\frac{x_{\max}}{x_2} \right)^{\frac{1}{M-2}} . \qquad \text{(E22d)}$$

For the example represented by Table II, we have $b_1 + b_2 = 3860$ MeV-cm^2/mg, $k = 7.643$, and $D = 0$ (so $\Delta q_D{}' = 0$ which produces the largest $x_{\max}$), so (E22a) gives $x_{\max} = 1.34$. If protons are included in either one of the input files, we will have $L_{\min} = 0.0017$ MeV-cm^2/mg and (22b) gives $x_2 = 4.40\times10^{-7}$ for this example. The two quantities, x_2 and $x_{\max}$, differ by more than six orders of magnitude for this example. But if we let $M = 250$ (for example), there will be more than thirty grid points per decade. The ratio r of adjacent positive grid points, given by (E22d), will be about 1.062. This is a fairly fine spacing of grid points on a logarithmic scale, but a finer spacing, if desired, can be obtained by using a larger value for M.

A routine for calculating P(CLE) in space environments, that runs in the Octave (a GNU package) platform, is called `PCLE_in_space.m` in the textbox below. The steps are partitioned into blocks that are explained as follows:

Block 1 first sets the ratio r between adjacent positive grid points to produce forty grid points per decade. This can be changed, if desired, by editing the code. Then Block 1 initializes vectors and matrices to be scalers with a value of zero. This is done because prior executions of Octave might have created larger vectors or matrices having the same names and only some matrix elements will be overwritten by the current execution with other obsolete matrix elements still in memory. The initialization ensures that the dimensions of vectors and matrices will correspond to the current assignments. Then Block 1 reads input data and files. The files are assumed to be in the CREME96 format so LET is in the units of MeV-cm^2/g and flux is in the units of 1/m2-s-sr. Immediately after reading a file as a two-column matrix, the columns are separated into two vectors with units changed so LET is in MeV-cm^2/mg and flux is in 1/cm^2-day, and some additional data points are inserted to control the way that an interpolation routine will extrapolate outside the data range.

Block 2 constructs flux functions representing the input files (with units converted) via interpolation/extrapolation. Extrapolations below the smallest tabulated LET produce the same flux assigned to the smallest tabulated LET. Extrapolations above the largest tabulated LET produce zero flux. Then the flux functions are used to construct a total fluence function of LET.

Block 3 assigns the integer N a value that makes the second curly bracket on the right side of (E3) less than 10^{-12} and constructs the coefficients $c_1, \ldots, c_N$.

Block 4 calculates $\Delta q_D{}'$, denoted QD in the code, from (E8a) and then calculates x_{max} from (E22a).

Block 5 constructs the grid points. It first finds the smallest nonzero LET value listed in the input files (the LET values in the input files are required to be in increasing order but it is possible for the first entry to be zero). If the entered number of flares is zero, the minimum LET, denoted $L_{\min}$, is reset to be the smallest nonzero value in the GCR file. If the entered number of days of GCR is zero, the minimum LET is reset to be the smallest nonzero value in the flare file. Then $L_{\min}$ is reset again to 0.0017 MeV-cm^2/mg if it was less than that. Then x_1 and x_2 are calculated from D(22b). This value of x_2 is compared to $x_{\max}$ to ensure that the grid points are in increasing order. If x_2 is not less than $x_{\max}$ it is reset to the value $x_{\max}/r$. The remaining grid points are calculated from (E22c) with the same steps also assigning a value to M. Since r was selected to produce a specified grid point spacing instead of selected to satisfy $x_M = x_{\max}$, x_M will be

slightly greater than $x_{\max}$. The grid point x_M is given the role of an updated $x_{\max}$ in later calculations.

Block 6 constructs the T-array by first constructing $H1$- and $H2$-arrays to shorten the notation in (E21). Then the T-array is constructed from (E21) with (E21e) interpreted as an equality. Note that `mp` in the code is the $m'(m, j)$ satisfying (E21c). As pointed out in the discussion under (E21d), readers that would like to give numerical accuracy a higher priority than guaranteed conservatism can modify the steps in this block by using an interpolation, instead of the right side of (E21d), to obtain an estimate of the left side. However, doing so would invalidate the claim that all approximations are conservative.

Block 7 estimates $P(CLE)$ by treating (E19) as an equality. The inner loop constructs an inner sum, denoted `inSUM` in the code, which is the curly bracket on the right side of (E19). The outer loop constructs an outer sum, denoted `outSUM` in the code, which is denoted the sum in n on the right side of (E19). The last step combines all of the terms on the right side of (E19).

PCLE_in_space.m (Page 1)

```
% ****BLOCK 1
r=10^0.025;
Data1=0;
Ldata1=0;
fluxdata1=0;
Data2=0;
Ldata2=0;
fluxdata2=0;
c=0;
x=0;
H1=0;
H2=0;
T=0;
%
Data1=dlmread("GCR_flux.dat");
Ldata1=[0;Data1(:,1)/1000];
fluxdata1=[108.6*Data1(1,2);108.6*Data1(:,2)];
Ndata1=length(Ldata1);
Ldata1(Ndata1+1)=Ldata1(Ndata1);
fluxdata1(Ndata1+1)=0;
Ldata1(Ndata1+2)=2*Ldata1(Ndata1);
fluxdata1(Ndata1+2)=0;
%
Data2=dlmread("flare_flux.dat");
Ldata2=[0;Data2(:,1)/1000];
fluxdata2=[108.6*Data2(1,2);108.6*Data2(:,2)];
Ndata2=length(Ldata2);
Ldata2(Ndata2+1)=Ldata2(Ndata2);
fluxdata2(Ndata2+1)=0;
Ldata2(Ndata2+2)=2*Ldata2(Ndata2);
fluxdata2(Ndata2+2)=0;
%
NGCR=input("Enter number of days of GCR flux  ");
Nflare=input("Enter number of flares  ");
b1=input("Enter b1 in MeV-cm2/mg  ");
b2=input("Enter b2 in MeV-cm2/mg  ");
sig1=input("Enter the crosssection for strong interactions in cm2  ");
sig2=input("Enter the crosssection for weak interactions in cm2  ");
k=input("Enter the Weibull k parameter (must be > 0)  ");
D=input("Enter additional dose in krads in SiO2 (must be >= 0) ");
sig=sig1+sig2;
%
```

PCLE_in_space.m (page 2)

```
%****BLOCK 2
flux1=@(L) interp1(Ldata1,fluxdata1,L,"extrap");
flux2=@(L) interp1(Ldata2,fluxdata2,L,"extrap");
H=@(L) NGCR*flux1(L)+7.5*Nflare*flux2(L);
H0=H(0);
%
%**** BLOCK 3
c1=H0*sig;
N=1;
do
  N++;
  until ((1-poisscdf(N,c1))<=1e-12)
  finalN=N
%
c(1)=c1;
for i=1:N-1
  c(i+1)=c1*c(i)/(i+1);
  end
%
%**** BLOCK 4
QD=6.25e7*((sig1/b1)+(sig2/b2))*D;
xmax=(9.22+QD^k)^(1/k)-QD;
%
%**** BLOCK 5
Lmin1=Ldata1(2);
if (Lmin1<=0)
  Lmin1=Ldata1(3);
  endif
Lmin2=Ldata2(2);
if (Lmin2<=0)
  Lmin2=Ldata2(3);
  endif
Lmin=Lmin1;
if (Lmin>Lmin2)
  Lmin=Lmin2;
  endif
if (NGCR<=0)
  Lmin=Lmin2;
  endif
if (Nflare<=0)
  Lmin=Lmin1;
  endif
if (Lmin<0.0017)
  Lmin=0.0017;
  endif
x(1)=0;
x(2)=Lmin/(b1+b2);
if (x(2)>=xmax)
  x(2)=xmax/r;
  endif
%
```

PCLE_in_space.m (page 3)

```
M=2;
do
  M++;
  x(M)=r*x(M-1);
  until (x(M)>=xmax)
  finalM=M
%
% ****BLOCK 6
for m=1:M
  H1(m)=H(b1*x(m))*sig1/c1;
  H2(m)=H(b2*x(m))*sig2/c1;
  T(1,m)=H1(m)+H2(m);
  end
%
for n=1:N
  T(n,1)=1;
  end
%
for n=1:N-1
  for m=2:M
    T(n+1,m)=T(1,m);
    for j=2:m
      mp=lookup(x,x(m)-x(j));
      T(n+1,m)=T(n+1,m)+T(n,mp)*(H1(j-1)-H1(j)+H2(j-1)-H2(j));
      end
    end
  end
  %
  %****BLOCK 7
  outSUM=0;
  for n=1:N
    EM=exp(-(x(M)+QD)^k);
    inSUM=T(n,M)*EM;
    for m=2:M
      Em=exp(-(x(m-1)+QD)^k)-exp(-(x(m)+QD)^k);
      inSUM=inSUM+T(n,m-1)*Em;
      end
    outSUM=outSUM+c(n)*inSUM;
    end
  PCLE=2-exp(-QD^k)-poisscdf(N,c1)+exp(-c1)*outSUM
```

Two example input data files are in the text boxes below. These are abbreviations of CREME96 output files, abbreviated by including only one out of three data points to reduce the file length. This abbreviation is not essential and the complete CREME96 output files (but with headers deleted) can be used if desired. The first file, called `GCR_flux.dat`, is a table of LET (first column) versus galactic cosmic ray (GCR) flux (second column). The units are those used in CREME96 output files so LET is in MeV-cm^2/g (instead of the more customary MeV-cm^2/mg) and flux is in 1/m^2-s-sr. This example data file represents the GCR environment in interplanetary space (no planetary magnetic shielding) during a solar minimum time period (the worst-case time period for GCR) with 100 mils of aluminum spacecraft shielding. Any

changes in planetary magnetic shielding and/or spacecraft shielding must be made by using CREME96 to create a replacement for this data file. Protons are not included so the smallest LET listed in the table is 101 MeV-cm^2/g (or 0.101 MeV-cm^2/mg). The second file, called `fare_flux.dat`, is a table of LET versus flux in the same format and in the same units used for the first file, but the flux now refers to the worst-week solar flare model used in CREME96. As with the GCR example, this applies to interplanetary space (no planetary magnetic shielding) at 1 AU distance from the Sun and with 100 mils of aluminum spacecraft shielding. Any changes in planetary magnetic shielding and/or spacecraft shielding must be made by using CREME96 to create a replacement for this data file. Protons are not included in this file, so the smallest LET listed in the table is 101 MeV-cm^2/g (or 0.101 MeV-cm^2/mg), but solar protons cannot be ignored and must therefore be included in a dose-like calculation.

GCR_flux.dat (page 1)

1.010E+002,	2.047E+001
1.046E+002,	2.011E+001
1.083E+002,	1.827E+001
1.121E+002,	1.685E+001
1.161E+002,	1.588E+001
1.202E+002,	1.511E+001
1.245E+002,	1.446E+001
1.289E+002,	1.389E+001
1.335E+002,	1.339E+001
1.382E+002,	1.290E+001
1.431E+002,	1.247E+001
1.481E+002,	1.209E+001
1.534E+002,	1.173E+001
1.588E+002,	1.141E+001
1.644E+002,	1.111E+001
1.703E+002,	1.056E+001
1.763E+002,	1.014E+001
1.825E+002,	9.789E+000
1.890E+002,	9.486E+000
1.957E+002,	9.213E+000
2.026E+002,	8.948E+000
2.098E+002,	8.661E+000
2.172E+002,	8.425E+000
2.249E+002,	8.213E+000
2.329E+002,	8.019E+000
2.411E+002,	7.744E+000
2.496E+002,	7.197E+000
2.585E+002,	6.873E+000
2.676E+002,	6.611E+000
2.771E+002,	6.385E+000
2.869E+002,	6.130E+000
2.971E+002,	5.905E+000
3.076E+002,	5.717E+000
3.185E+002,	5.548E+000
3.297E+002,	5.282E+000
3.414E+002,	4.891E+000
3.535E+002,	4.640E+000
3.660E+002,	4.437E+000
3.790E+002,	4.254E+000
3.924E+002,	4.086E+000
4.063E+002,	3.940E+000
4.207E+002,	3.807E+000
4.356E+002,	3.644E+000
4.510E+002,	3.496E+000
4.669E+002,	3.375E+000
4.835E+002,	3.265E+000
5.006E+002,	3.151E+000
5.183E+002,	3.054E+000
5.367E+002,	2.966E+000
5.557E+002,	2.861E+000
5.753E+002,	2.772E+000
5.957E+002,	2.693E+000
6.168E+002,	2.607E+000
6.386E+002,	2.529E+000
6.612E+002,	2.462E+000
6.847E+002,	2.359E+000
7.089E+002,	2.273E+000
7.340E+002,	2.203E+000
7.600E+002,	2.133E+000
7.869E+002,	2.073E+000
8.147E+002,	2.019E+000
8.436E+002,	1.939E+000
8.734E+002,	1.881E+000
9.044E+002,	1.822E+000
9.364E+002,	1.767E+000
9.695E+002,	1.721E+000
1.004E+003,	1.646E+000

GCR_flux.dat (page 2)

1.039E+003,	1.594E+000
1.076E+003,	1.532E+000
1.114E+003,	1.480E+000
1.154E+003,	1.331E+000
1.195E+003,	1.117E+000
1.237E+003,	9.923E-001
1.281E+003,	8.961E-001
1.326E+003,	8.174E-001
1.373E+003,	7.381E-001
1.421E+003,	6.746E-001
1.472E+003,	6.198E-001
1.524E+003,	5.710E-001
1.578E+003,	5.271E-001
1.634E+003,	4.883E-001
1.692E+003,	4.528E-001
1.752E+003,	4.198E-001
1.814E+003,	3.895E-001
1.878E+003,	3.616E-001
1.944E+003,	3.359E-001
2.013E+003,	3.121E-001
2.084E+003,	2.896E-001
2.158E+003,	2.693E-001
2.234E+003,	2.500E-001
2.314E+003,	2.322E-001
2.395E+003,	2.157E-001
2.480E+003,	2.004E-001
2.568E+003,	1.861E-001
2.659E+003,	1.728E-001
2.753E+003,	1.603E-001
2.851E+003,	1.488E-001
2.951E+003,	1.381E-001
3.056E+003,	1.280E-001
3.164E+003,	1.187E-001
3.276E+003,	1.102E-001
3.392E+003,	1.021E-001
3.512E+003,	9.463E-002
3.637E+003,	8.766E-002
3.765E+003,	8.126E-002
3.899E+003,	7.520E-002
4.037E+003,	6.957E-002
4.180E+003,	6.446E-002
4.328E+003,	5.957E-002
4.481E+003,	5.515E-002
4.640E+003,	5.094E-002
4.804E+003,	4.704E-002
4.974E+003,	4.347E-002
5.150E+003,	4.002E-002
5.332E+003,	3.696E-002
5.521E+003,	3.415E-002
5.716E+003,	3.151E-002
5.919E+003,	2.908E-002
6.128E+003,	2.679E-002
6.345E+003,	2.468E-002
6.570E+003,	2.278E-002
6.802E+003,	2.097E-002
7.043E+003,	1.931E-002
7.293E+003,	1.761E-002
7.551E+003,	1.627E-002
7.818E+003,	1.503E-002
8.095E+003,	1.390E-002
8.382E+003,	1.283E-002
8.678E+003,	1.185E-002
8.985E+003,	1.094E-002
9.304E+003,	1.007E-002
9.633E+003,	9.251E-003
9.974E+003,	8.520E-003
1.033E+004,	7.838E-003

GCR_flux.dat (page 3)

1.069E+004,	7.204E-003
1.107E+004,	6.608E-003
1.146E+004,	6.043E-003
1.187E+004,	5.480E-003
1.229E+004,	5.007E-003
1.272E+004,	4.574E-003
1.318E+004,	4.155E-003
1.364E+004,	3.787E-003
1.412E+004,	3.423E-003
1.462E+004,	3.095E-003
1.514E+004,	2.821E-003
1.568E+004,	2.567E-003
1.623E+004,	2.328E-003
1.681E+004,	2.101E-003
1.740E+004,	1.897E-003
1.802E+004,	1.706E-003
1.866E+004,	1.528E-003
1.932E+004,	1.360E-003
2.000E+004,	1.202E-003
2.071E+004,	1.053E-003
2.144E+004,	9.061E-004
2.220E+004,	7.836E-004
2.299E+004,	6.659E-004
2.380E+004,	5.482E-004
2.464E+004,	4.430E-004
2.552E+004,	3.438E-004
2.642E+004,	2.450E-004
2.735E+004,	1.467E-004
2.832E+004,	1.432E-005
2.933E+004,	9.475E-006
3.036E+004,	2.330E-006
3.144E+004,	1.200E-006
3.255E+004,	9.016E-007
3.370E+004,	7.442E-007
3.490E+004,	6.317E-007
3.613E+004,	5.555E-007
3.741E+004,	4.876E-007
3.874E+004,	4.346E-007
4.011E+004,	3.854E-007
4.153E+004,	3.415E-007
4.300E+004,	3.037E-007
4.452E+004,	2.704E-007
4.610E+004,	2.416E-007
4.773E+004,	2.158E-007
4.942E+004,	1.917E-007
5.117E+004,	1.689E-007
5.298E+004,	1.486E-007
5.485E+004,	1.298E-007
5.680E+004,	1.122E-007
5.881E+004,	9.607E-008
6.089E+004,	8.199E-008
6.304E+004,	6.845E-008
6.528E+004,	5.825E-008
6.759E+004,	4.901E-008
6.998E+004,	4.050E-008
7.246E+004,	3.291E-008
7.502E+004,	2.610E-008
7.768E+004,	2.039E-008
8.043E+004,	1.516E-008
8.328E+004,	1.034E-008
8.622E+004,	5.631E-009
8.928E+004,	2.475E-009
9.244E+004,	3.964E-010
9.571E+004,	2.650E-010
9.910E+004,	1.604E-010
1.026E+005,	2.339E-011

flare_flux.dat (page 1)

```
1.010E+002,  1.802E+004
1.046E+002,  1.721E+004
1.083E+002,  1.644E+004
1.121E+002,  1.568E+004
1.161E+002,  1.491E+004
1.202E+002,  1.418E+004
1.245E+002,  1.346E+004
1.289E+002,  1.277E+004
1.335E+002,  1.209E+004
1.382E+002,  1.143E+004
1.431E+002,  1.081E+004
1.481E+002,  1.021E+004
1.534E+002,  9.633E+003
1.588E+002,  9.070E+003
1.644E+002,  8.542E+003
1.703E+002,  8.040E+003
1.763E+002,  7.561E+003
1.825E+002,  7.105E+003
1.890E+002,  6.663E+003
1.957E+002,  6.253E+003
2.026E+002,  5.865E+003
2.098E+002,  5.499E+003
2.172E+002,  5.144E+003
2.249E+002,  4.818E+003
2.329E+002,  4.511E+003
2.411E+002,  4.215E+003
2.496E+002,  3.944E+003
2.585E+002,  3.689E+003
2.676E+002,  3.444E+003
2.771E+002,  3.220E+003
2.869E+002,  3.010E+003
2.971E+002,  2.808E+003
3.076E+002,  2.625E+003
3.185E+002,  2.452E+003
3.297E+002,  2.288E+003
3.414E+002,  2.139E+003
3.535E+002,  1.994E+003
3.660E+002,  1.865E+003
3.790E+002,  1.738E+003
3.924E+002,  1.626E+003
4.063E+002,  1.516E+003
4.207E+002,  1.416E+003
4.356E+002,  1.323E+003
4.510E+002,  1.234E+003
4.669E+002,  1.154E+003
4.835E+002,  1.077E+003
5.006E+002,  1.005E+003
5.183E+002,  9.379E+002
5.367E+002,  8.775E+002
5.557E+002,  8.200E+002
5.753E+002,  7.655E+002
5.957E+002,  7.147E+002
6.168E+002,  6.673E+002
6.386E+002,  6.231E+002
6.612E+002,  5.819E+002
6.847E+002,  5.431E+002
7.089E+002,  5.054E+002
7.340E+002,  4.714E+002
7.600E+002,  4.399E+002
7.869E+002,  4.095E+002
8.147E+002,  3.822E+002
8.436E+002,  3.555E+002
8.734E+002,  3.309E+002
9.044E+002,  3.080E+002
9.364E+002,  2.864E+002
9.695E+002,  2.659E+002
1.004E+003,  2.468E+002
```

flare_flux.dat (page 2)

```
1.039E+003,  2.290E+002
1.076E+003,  2.120E+002
1.114E+003,  1.962E+002
1.154E+003,  1.812E+002
1.195E+003,  1.671E+002
1.237E+003,  1.539E+002
1.281E+003,  1.413E+002
1.326E+003,  1.294E+002
1.373E+003,  1.179E+002
1.421E+003,  1.069E+002
1.472E+003,  9.589E+001
1.524E+003,  8.407E+001
1.578E+003,  6.570E+001
1.634E+003,  6.287E+001
1.692E+003,  6.010E+001
1.752E+003,  5.741E+001
1.814E+003,  5.485E+001
1.878E+003,  5.234E+001
1.944E+003,  4.994E+001
2.013E+003,  4.764E+001
2.084E+003,  4.540E+001
2.158E+003,  4.327E+001
2.234E+003,  4.119E+001
2.314E+003,  3.922E+001
2.395E+003,  3.731E+001
2.480E+003,  3.547E+001
2.568E+003,  3.374E+001
2.659E+003,  3.204E+001
2.753E+003,  3.044E+001
2.851E+003,  2.889E+001
2.951E+003,  2.742E+001
3.056E+003,  2.602E+001
3.164E+003,  2.466E+001
3.276E+003,  2.338E+001
3.392E+003,  2.213E+001
3.512E+003,  2.096E+001
3.637E+003,  1.983E+001
3.765E+003,  1.875E+001
3.899E+003,  1.773E+001
4.037E+003,  1.673E+001
4.180E+003,  1.581E+001
4.328E+003,  1.489E+001
4.481E+003,  1.403E+001
4.640E+003,  1.318E+001
4.804E+003,  1.236E+001
4.974E+003,  1.157E+001
5.150E+003,  1.074E+001
5.332E+003,  1.009E+001
5.521E+003,  9.465E+000
5.716E+003,  8.859E+000
5.919E+003,  8.278E+000
6.128E+003,  7.703E+000
6.345E+003,  7.159E+000
6.570E+003,  6.661E+000
6.802E+003,  6.162E+000
7.043E+003,  5.661E+000
7.293E+003,  5.037E+000
7.551E+003,  4.686E+000
7.818E+003,  4.378E+000
8.095E+003,  4.087E+000
8.382E+003,  3.806E+000
8.678E+003,  3.542E+000
8.985E+003,  3.287E+000
9.304E+003,  3.035E+000
9.633E+003,  2.776E+000
9.974E+003,  2.573E+000
1.033E+004,  2.380E+000
```

flare_flux.dat (page 3)

```
1.069E+004,  2.196E+000
1.107E+004,  2.021E+000
1.146E+004,  1.850E+000
1.187E+004,  1.670E+000
1.229E+004,  1.525E+000
1.272E+004,  1.393E+000
1.318E+004,  1.263E+000
1.364E+004,  1.142E+000
1.412E+004,  1.012E+000
1.462E+004,  9.011E-001
1.514E+004,  8.247E-001
1.568E+004,  7.527E-001
1.623E+004,  6.824E-001
1.681E+004,  6.123E-001
1.740E+004,  5.577E-001
1.802E+004,  5.061E-001
1.866E+004,  4.580E-001
1.932E+004,  4.121E-001
2.000E+004,  3.686E-001
2.071E+004,  3.269E-001
2.144E+004,  2.852E-001
2.220E+004,  2.512E-001
2.299E+004,  2.189E-001
2.380E+004,  1.874E-001
2.464E+004,  1.569E-001
2.552E+004,  1.263E-001
2.642E+004,  9.471E-002
2.735E+004,  5.912E-002
2.832E+004,  3.901E-003
2.933E+004,  2.120E-003
3.036E+004,  4.108E-004
3.144E+004,  1.624E-004
3.255E+004,  1.039E-004
3.370E+004,  7.796E-005
3.490E+004,  6.081E-005
3.613E+004,  5.054E-005
3.741E+004,  3.986E-005
3.874E+004,  3.356E-005
4.011E+004,  2.732E-005
4.153E+004,  2.320E-005
4.300E+004,  2.001E-005
4.452E+004,  1.748E-005
4.610E+004,  1.556E-005
4.773E+004,  1.386E-005
4.942E+004,  1.227E-005
5.117E+004,  1.077E-005
5.298E+004,  9.346E-006
5.485E+004,  7.943E-006
5.680E+004,  6.542E-006
5.881E+004,  5.210E-006
6.089E+004,  4.187E-006
6.304E+004,  3.447E-006
6.528E+004,  2.986E-006
6.759E+004,  2.596E-006
6.998E+004,  2.259E-006
7.246E+004,  1.930E-006
7.502E+004,  1.626E-006
7.768E+004,  1.350E-006
8.043E+004,  1.082E-006
8.328E+004,  8.085E-007
8.622E+004,  4.945E-007
8.928E+004,  2.471E-007
9.244E+004,  2.000E-008
9.571E+004,  1.082E-008
1.026E+005,  0.000E+000
```

Appendix F: Symbols, Acronyms, and Definitions

Symbols

mostly in order of appearance
(See Acronyms and Definitions for additional explanations)

L, L_T	A value of LET. The subscript emphasizes that L_T is the LET used for a heavy-ion test. Without the subscript, it is more generic and might refer to a natural space environment.
δq, δQ	The upper case is the charge loss from a single ion hit as a statistical random variable. The lower case is a value of this random variable.
$S(L,\delta q)$	A set of points associated with a selected FG. It is the set of points in the device plane having the property that a normal-incident ion hit at any of these points, by an ion having LET L, produces a charge loss that exceeds δq in the selected FG. Each FG in a collection of FGs has its own set of these points.
$\sigma(L,\delta q)$	The area of the set $S(L,\delta q)$. It is the cross section associated with a selected FG for a normal-incident ion having LET L to produce a charge loss that exceeds δq in the selected FG.
σ_{sat}	Called the saturation cross section, this is the limit of $\sigma(L,\delta q)$ as $\delta q \rightarrow 0$.
$H(L)$, $h(L)$	$H(L)$ is the irradiation fluence consisting of all ions having an LET greater than L, while $h(L)$ is the negative of the L derivative of $H(L)$.
Δq, ΔQ	The upper case is the charge loss accumulated over all ion hits as a statistical random variable. The lower case is a value of this random variable.
$P(*)$, $P(*\|*)$	The first function is a generic probability function and its argument is any set of outcomes or any designation of a set of outcomes. For example, the probability that ΔQ exceeds Δq can be denoted $P(\Delta Q > \Delta q)$. The second function is a generic conditional probability function and has two arguments. The first is any set of outcomes or any designation of a set of outcomes. The second argument is a given condition. For example, the probability that ΔQ exceeds Δq, given that there were n ion hits, can be written as $P(\Delta Q > \Delta q \mid \#\text{ hits} = n)$ or more compactly as $P(\Delta Q > \Delta q \mid n)$ when the text explains the meaning of the more compact notation. In particular, P(CLE) is the probability of a charge-loss event and the goal of this work is to calculate this probability for a given radiation environment.
f, G_1, G_n	These functions are defined by (15) for the general case and by (25) and (15a) for the FG charge-loss model used here. The only role of the function f is to construct the G-functions. The significance of the G-functions is their roles in (36) and (57).
Δq_C, ΔQ_C	The upper case is the critical charge loss as a statistical random variable. The lower case is a value of this random variable.
$\sigma_{S,sat}$, $\sigma_{W,sat}$, σ_{sat}	The first two are the normal-incident saturation cross sections for a selected FG for strong interactions and weak interactions, respectively. The sum of these is σ_{sat}.
a_1, a_2	Defined by the condition that the charge loss from one strong interaction is LET divided by a_1, and the charge loss from one weak interaction is LET divided by a_2.
$U(x)$	Unit step function defined by $U(x) = 1$ when $x > 0$ and $U(x) = 0$ when $x \leq 0$.
$C_{m,n}$, $D_{m,n}$, $E_{m,n}$	Unlike the G-functions that can be defined in a more general context, the C-, D-, and E-functions are definable only in the context of the FG charge-loss model used here. In this context, they are defined by (27). The only purpose of the C- and D-

	functions is to construct the *E*-functions. The significance of the *E*-functions is their role in (28), which reduces to (34) when the environment is a pure spectrum.
σ_{CLE}	Cross section, per FG, for a CLE under SEU-like conditions. It is experimentally defined for a large collection of FGs exposed to a fluence small enough to produce SEU-like behavior. The cross section is the number of CLE counts divided by fluence and then divided again by the number of FGs in the collection.
D, Δq_D	D is the dose in SiO_2 and can be calculated by (46). Δq_D is the FG charge loss produced by this dose and can be calculated from (52).
ρ, $\mathcal{F}$, k, λ	The first two are the probability density function and cumulative distribution function, respectively, for the critical charge loss. These functions refer to an arbitrary distribution in (36) through (45), but refer to the Weibull distribution with shape parameter k and scale parameter λ in (47) and all later equations.
b_1, b_2	The b-parameters are defined by (49). The physical significance of b_1 is that it is a measure of the sensitivity of FGs to CLEs via strong interactions, with a smaller value of b_1 implying greater sensitivity. The parameter b_2 has the same interpretation for weak interactions that b_1 has for strong interactions.

Acronyms

in alphabetical order
(See Definitions for additional explanations)

CLE	Charge loss event.
FET	Field-effect transistor.
FG	Floating gate.
LET	Linear energy transfer.
SEE	Single-event effect.
SEU	Single-event upset.
TID	Total ionizing dose.

Definitions

in alphabetical order
(See Acronyms for additional explanations)

Actual charge loss	See "Prompt charge loss."
Charge loss	See "Prompt charge loss."
Charge loss event	A user-defined event characterized by the charge stored in an FG crossing some threshold value via prompt charge loss. A frequently cited example is the deprogramming of an initially programmed (charged) FG in a flash memory.
Critical charge loss	The charge loss needed to produce a user-defined charge loss event. A frequently-cited example is the charge loss needed to deprogram an initially programmed (charged) FG in a flash memory.
Dose-like	An FG, or a collection of FGs, exhibits dose-like behavior when the number of ion hits needed to produce a CLE is large enough to be approximately deterministic, i.e., can be approximated by the statistical average. This can occur only when the LET is small enough so that a large number of hits are needed for a CLE. The model prediction applicable to dose-like behavior is (45). (See, also, "SEU-like.")
Effective charge loss	See "Prompt charge loss."
Prompt charge loss	The loss of FG charge that occurs immediately after a hit from an ionizing particle. An actual FG charge loss is from a direct hit to the FG (a strong interaction). An effective charge loss is any combination of actual charge loss and charge trapping in a nearby oxide (a weak interaction) that has the same effect on a charge-sensing circuit as an actual charge loss.
Pure spectrum	An ion radiation environment is a pure spectrum when all ions have the same LET. This is a typical laboratory environment used for heavy-ion testing.
SEU-like	A collection of FGs exhibits SEU-like behavior when nearly all FGs that underwent a CLE received only one ion hit. This can be recognized in test data by the number of CLE counts being proportional to fluence. Given that the LET is large enough so that counts can be produced by single hits, this behavior can still only occur when the fluence is sufficiently small, so this behavior is also known as "small-fluence" behavior. The model prediction applicable to SEU-like behavior is (42) when there is no added dose, and by (62) when there is added dose. (See, also, "Dose-like.")
Small fluence	See "SEU-like."
Strong interaction	Occurs when an ion strikes an FG and the effective charge loss is an actual FG charge loss.
Weak interaction	Occurs when an ion strikes a nearby oxide resulting in charge trapping in the oxide that has the same effect on a charge-sensing circuit as an actual FG charge loss.

REFERENCES

[1] A. Scarpa, A. Paccagnella, F. Montera, G. Ghibaudo, G. Pananakakis, G. Ghidini, and P. G. Fuochi, "Ionizing radiation induced leakage current on ultra-thin gate oxides," *IEEE Trans. Nucl. Sci.*, vol. 44, no. 6, pp. 1818-1825, Dec. 1997.

[2] G. Cellere, A. Paccagnella, A. Visconti, M. Bonanomi, and A. Candelon, "Transient conductive path induced by a single ion in 10 nm SiO2 layers," *IEEE Trans. Nucl. Sci.*, vol. 51, no. 6, pp. 3304-3311, Dec. 2004.

[3] S. M. Guertin, D. N. Nguyen, and J. D. Patterson, "Microdose induced data loss on floating gate memories," *IEEE Trans. Nucl. Sci.*, vol. 53, no. 6, pp. 3518-3524, Dec. 2006.

[4] T.P. Ma and P.V. Dressendorfer (editors), *Ionizing Radiation Effects in MOS Devices and Circuits*, John Wiley & Sons, p. 102, 1989.

[5] L. D. Edmonds, "An elementary derivation of confidence intervals and outlier probability," (online at: https://rgdoi.net/10.13140/RG.2.1.2715.1524)

[6] G. Cellere, A. Paccagnella, A. Visconti, and M. Bonanomi, "Secondary effects of single ions on floating gate memory cells," *IEEE Trans. Nucl. Sci.*, vol. 53, no. 6, pp. 3291-3297, Dec. 2006.

[7] E.L. Petersen, J. C. Pickel, J. H. Adams Jr., and E. C. Smith, "Rate predictions for single event effects – A critique," *IEEE Trans. Nucl. Sci.*, vol. 39, pp. 1577-1599, Dec. 1992.

[8] N. C. Hooten, L. D. Edmonds, W. G. Bennett, J. R. Ahlbin, N. A. Dodds, R. A. Reed, R. D. Schrimpf, and R. A. Weller, "The significance of high-level carrier generation conditions for charge collection in irradiated devices," *IEEE Trans. Nucl. Sci.*, vol. 59, no. 6, pp. 2710-2721, Dec. 2012.

[9] SRIM (online: http://www.srim.org/SRIM/SRIMLEGL.htm).

[10] M. Bagatin, S. Gerardin, A. Paccagnella, G. Cellere, A. Visconti, and M. Bonanomi, "Increase in the heavy-ion upset cross section of floating gate cells previously exposed to TID," *IEEE Trans. Nucl. Sci.*, vol. 57, no. 6, pp. 3407-3413, Dec. 2010.

[11] G. Cellere, A. Paccagnella, A. Visconti, M. Bonanomi, R. Harboe-Sorensen, and A. Virtanen, "Angular dependence of heavy ion effects in floating gate memory arrays," *IEEE Trans. Nucl. Sci.*, vol. 54, no. 6, pp. 2371-2378, Dec. 2007.

[12] L. D. Edmonds and F. Irom, "Extension of a proton SEU cross section model to include 14 MeV neutrons," *IEEE Trans. Nucl. Sci.*, vol. 55, no. 1, pp. 649-655, Feb. 2008.

[13] The original CREME96 website is no longer available but environmental models identified as CREME96 models are still industry standards and can be found at other websites such as (https://creme.isde.vanderbilt.edu/) or (https://www.spenvis.oma.be/intro.php).